

**ANALYTICAL MODEL OF OPEN CIRCUIT
VOLTAGE OF A SCHOTTKY BARRIER SOLAR CELL
FOR ALL LEVELS OF INJECTION**

by

TANVIR AHMED

A Thesis submitted to the Department of Electrical and Electronic Engineering in Partial
Fulfillment of the requirement for the degree

of

MASTER OF SCIENCE IN ELECTRICAL AND ELECTRONIC ENGINEERING

DEPARTMENT OF ELECTRICAL AND ELECTRONIC ENGINEERING
BANGLADESH UNIVERSITY OF ENGINEERING AND TECHNOLOGY (BUET)

APRIL 2015

The thesis titled, “**Analytical Model of Open Circuit Voltage of A Schottky Barrier Solar Cell For All Levels of Injection**” submitted by Tanvir Ahmed, Roll no.-p0413062256, Session April 2013 has been accepted as satisfactory in partial fulfillment of the requirements for the degree of **Master of Science in Electrical and Electronic Engineering** on April 15, 2015.

BOARD OF EXAMINERS

- | | |
|---|--------------------------|
| 1.
Dr. M. M. Shahidul Hassan
Professor, Department of EEE, BUET. | Chairman
(Supervisor) |
| 2.
Dr. Taifur Ahmed Chowdhury
Professor & Head, Department of EEE, BUET. | Member
(Ex-officio) |
| 3.
Dr. Md. Ziaur Rahman Khan
Professor, Department of EEE, BUET | Member |
| 4.
Dr. Farseem Mannan Mohammedy
Associate Professor, Department of EEE, BUET | Member |
| 5.
Prof. Dr. M. Rezwana Khan
Vice Chancellor, United International University. | Member
(External) |

DECLARATION

It is hereby declared that this thesis or any part of it has not been submitted elsewhere for the award of any degree or diploma.

Signature of the candidate

(Tanvir Ahmed)

DEDICATION

To My Parents

TABLE OF CONTENTS

Title	I
Certification of thesis approval	II
Declaration	III
Dedication	IV
Table of contents	V
List of tables	IX
List of figures	X
List of symbols	XII
Acknowledgements	XIV
Abstract	XV
1 INTRODUCTION	1
1.1 Introduction	1
1.2 Schottky Barrier Diode (SBD)	1
1.2.1 Structure of SBD	2
1.3 Solar Cell	4
1.3.1 Operating Principle of Solar Cell	5
1.3.2 Efficiency and fill factor of Solar Cell	7
1.3.3 Open Circuit Voltage	8
1.3.4 Advantage of Schottky Barrier in Solar Cell	8
1.4 Literature Review	9
1.5 Objective of the work	11
1.6 Scope of the work	11
1.7 Conclusion	12
2 MATHEMATICAL DERIVATIONS	13
2.1 Introduction	13
2.2 Mathematical modeling of open circuit voltage for all levels of injection	14
2.2.1 Open circuit potential in depletion region($0 \leq X \leq W$)	16
2.2.2 Open circuit potential in neutral region($W \leq X \leq L$)	18
2.2.3 Open Circuit Voltage in SB Solar Cell	20
2.2.4 Mathematical expression of Open Circuit Voltage (V_{OC}) for the special case of High level injection	20
2.2.5 Mathematical expression of Open Circuit Voltage (V_{OC}) for the special case of Low level injection	21

2.2.6	Summary of mathematical expressions of open circuit voltage of SB Solar cell for different levels of injections	22
2.2.7	Determination of excess minority carrier concentrations in depletion and neutral region	23
2.2.8	Evaluation of unknown constants C_1, C_2, C_3 & C_4 Using proper boundary conditions	25
2.3	Mathematical expression of Open Circuit Voltage	27
2.4	Conclusions	29
3	RESULTS AND DISCUSSIONS	30
3.1	Introduction	30
3.2	Open Circuit Voltage as a function of doping concentrations for various metal-semiconductor combinations of SB Solar Cell	30
3.2.1	Effect of Doping concentrations on Open Circuit Voltage for all levels of injection (metal- n Si Semiconductor)	31
3.2.2	Effect of Doping concentrations on Open Circuit Voltage for low level of injection(metal-n Si Semiconductor)	32
3.2.3	Effect of Doping concentrations on Open Circuit Voltage for high level of injection(metal-n Si Semiconductor)	33
3.2.4	Effect of Doping concentrations on Open Circuit Voltage for all levels of injection(metal-n GaAs Semiconductor)	34
3.2.5	Effect of Doping concentrations on Open Circuit Voltage for low level of injection(n-GaAs Semiconductor)	35
3.2.6	Effect of Doping concentrations on Open Circuit Voltage for high level of injection(n-GaAs Semiconductor)	36
3.3	Effect of metal work function at the metal-semiconductor interface on Open circuit voltage for different levels of injections	37
3.3.1	Effect of metal work function at the metal-n-Si semiconductor interface on Open circuit voltage for different levels of injections	37
3.3.2	Effect of metal work function at the metal-n-GaAs semiconductor interface on Open circuit voltage for different levels of injections	38

3.4 Effect of surface recombination velocity on Open circuit voltage for SB Solar Cell	40
3.4.1 Effect of surface recombination velocity on Open circuit voltage for metal-n Si combinations considering all levels of injection	40
3.4.2 Effect of surface recombination velocity on Open circuit voltage for metal-n Si combinations considering low level of injection	41
3.4.3 Effect of surface recombination velocity on Open circuit voltage for metal-n Si combinations considering high level of injection	42
3.5 Effect of the semiconductor thickness on Open circuit voltage	43
3.5.1 Effect of the semiconductor thickness on Open circuit voltage considering all levels of injections for metal n-Si semiconductor SB Solar Cell	43
3.5.2 Effect of the semiconductor thickness on Open circuit voltage considering low level of injection for metal n-Si semiconductor SB Solar Cell	44
3.5.3 Effect of the semiconductor thickness on Open circuit voltage considering high level of injection for metal n-Si semiconductor SB Solar Cell	45
3.5.4 Comparison of low level and high level of injection by studying the effect of thickness on Open circuit voltage for metal-n Si SB Solar cell	46
3.5.5 Effect of the semiconductor thickness on Open circuit voltage considering all levels of injections for metal n-GaAs semiconductor SB Solar Cell	47
3.5.6 Effect of the semiconductor thickness on Open circuit voltage considering low level of injection for metal n-GaAs semiconductor SB Solar Cell	48
3.5.7 Effect of the semiconductor thickness on Open circuit voltage considering high level of injection for metal n-GaAs semiconductor SB Solar Cell	49
3.5.8 Comparison of low level and high level of injection by studying the effect of thickness on Open circuit voltage for metal-n GaAs SB Solar cell	50
3.6 Variation of Open circuit voltage with metal work functions for various doping concentrations (N_d) under different levels of injection	51
3.6.1 Variation of Open circuit voltage with metal work functions for various doping concentrations (N_d) under all levels of injection of metal-n Si SB Solar Cell	51
3.6.2 Variation of Open circuit voltage with metal work functions for various doping concentrations (N_d) under low level of injection of metal-n Si SB Solar Cell	52
3.6.3 Variation of Open circuit voltage with metal work functions for various doping concentrations (N_d) under high level of injection of metal-n Si SB Solar Cell	53
3.7 Variation of Open circuit voltage with thickness of semiconductor for various doping concentrations (N_d)	55
3.7.1 Variation of Open circuit voltage with thickness of semiconductor for various doping concentrations (N_d) for all levels of injection	55
3.7.2 Variation of Open circuit voltage with thickness of semiconductor for various doping concentrations (N_d) for low level of injection	56

3.7.3	Variation of Open circuit voltage with thickness of semiconductor for various doping concentrations (N_d) for high level of injection	57
3.8	Open circuit voltage as a function of Semiconductor layer thickness for various ranges of effective surface recombination velocity	58
3.8.1	Open circuit voltage as a function of Semiconductor layer thickness for various ranges of effective surface recombination velocity under all levels of injection	58
3.8.2	Open circuit voltage as a function of Semiconductor layer thickness for various ranges of effective surface recombination velocity under low level of injection	59
3.8.3	Open circuit voltage as a function of Semiconductor layer thickness for various ranges of effective surface recombination velocity under high level of injection	60
3.9	Comparison of Open circuit voltage as a function of doping concentrations for all, low and high level of injections for a metal- n Si and metal-n GaAs SB Solar Cell	61
3.10	Conclusions	64
4	CONCLUSION	65
4.1	Summary	65
4.2	Future Course of research work	66
	REFERENCES	67

LIST OF TABLES

Table 2.1	Summary of mathematical expressions of Open Circuit Voltage of SB Solar cell under different levels of injection	22
Table 3.1	Work function of different metals	30

LIST OF FIGURES

Figure 1.1	a) Energy-band diagram of a metal and semiconductor before contact	3
	b) Ideal energy-band diagram of a metal-n-semiconductor junction for $\phi_m > \phi_s$	3
Figure 1.2	a) Under reverse bias	4
	b) Under forward bias	4
Figure 1.3	Principle of operation of Solar Cell	6
Figure 1.4	Different plots from Literature Review	10-11
Figure 2.1	One dimensional structure of SB Solar Cell	14
Figure 2.2	Energy Band Diagram of a Metal/n-type Semiconductor Schottky Barrier Solar Cell	14
Figure 2.3	Variation of surface potential with excess hole carrier concentration	18
Figure 2.4	Variation of Excess hole carrier concentration with length of the semiconductor	19
Figure 3.1	Variation of Open Circuit Voltage with doping concentration for different metal-n Si combinations for all levels of injection	31
Figure 3.2	Variation of Open Circuit Voltage with doping concentration for different metal-n Si combinations for low level of injection	32
Figure 3.3	Variation of Open Circuit Voltage with doping concentration for different metal-n Si combinations for high level of injection	33
Figure 3.4	Variation of Open Circuit Voltage with doping concentration for different metal-n GaAs combinations for all levels of injection	34
Figure 3.5	Variation of Open Circuit Voltage with doping concentration for different metal-n GaAs combinations for low level of injection	35
Figure 3.6	Variation of Open Circuit Voltage with doping concentration for different metal-n GaAs combinations for high level of injection	36
Figure 3.7	Effect of different levels of injections on Open circuit voltage for various metal work functions for different metal-n Si SB Solar Cell	38
Figure 3.8	Effect of different levels of injections on Open circuit voltage for various metal work functions for different metal-n GaAs SB Solar Cell	39
Figure 3.9	Open circuit voltage characteristics with variation of effective surface recombination velocity for all levels of injections for metal-n Si Solar cell	40
Figure 3.10	Open circuit voltage characteristics with variation of effective surface recombination velocity for low level of injection for metal-n Si Solar cell	41
Figure 3.11	Open circuit voltage characteristics with variation of effective surface recombination velocity for high level of injection for metal-n Si Solar cell	42
Figure 3.12	Effect of semiconductor thickness on Open circuit voltage for all level of injection for different metal-n Si Solar cell	43
Figure 3.13	Effect of semiconductor thickness on Open circuit voltage for low level of injection for different metal-n Si Solar cell	44
Figure 3.14	Effect of semiconductor thickness on Open circuit voltage for high level of injection for different metal-n Si Solar cell	45

Figure 3.15	Comparison of Open circuit voltage variation on Semiconductor thickness for both low level and high level injection	46
Figure 3.16	Effect of semiconductor thickness on Open circuit voltage for all levels of injections for different metal-n GaAs Solar cell	47
Figure 3.17	Effect of semiconductor thickness on Open circuit voltage for low level injection for different metal-n GaAs Solar cell	48
Figure 3.18	Effect of semiconductor thickness on Open circuit voltage for high level injection for different metal-n GaAs Solar cell	49
Figure 3.19	Open circuit voltage variation on Semiconductor thickness for both low level and high level injection for metal-n GaAs SB Solar Cell	50
Figure 3.20	Variation of Open circuit voltage with metal work functions for various doping concentrations for different metal-n Si SB Solar cells for all levels of injection	51
Figure 3.21	Variation of Open circuit voltage with metal work functions for various doping concentrations for different metal-n Si SB Solar cells for low level of injections	53
Figure 3.22	Variation of Open circuit voltage with metal work functions for various doping concentrations for different metal-n Si SB Solar cells for high level of injections	54
Figure 3.23	Open circuit voltage as a function of Si semiconductor thickness for various doping concentrations under all levels of injection	55
Figure 3.24	Open circuit voltage as a function of Si semiconductor thickness for various doping concentrations under low level of injection	56
Figure 3.25	Open circuit voltage as a function of Si semiconductor thickness for various doping concentrations under high level of injection	57
Figure 3.26	Variation of open circuit voltage as a function of semiconductor thickness for different values of effective surface recombination velocity under all levels of injection	59
Figure 3.27	Variation of open circuit voltage as a function of semiconductor thickness for different values of effective surface recombination velocity under low level of injection	60
Figure 3.28	Variation of open circuit voltage as a function of semiconductor thickness for different values of effective surface recombination velocity under high level of injection	61
Figure 3.29	Comparison of Open circuit voltage for different levels of injection as a function of doping concentrations for metal-n Si SB Solar Cell	62
Figure 3.30	Comparison of Open circuit voltage for different levels of injection as a function of doping concentrations for metal-n GaAs SB Solar Cell	63

List of Symbols

J_n	Total drift and diffusion electron current density (Acm^{-2})
J_p	Total drift and diffusion hole current density (Acm^{-2})
J_T	Total current density(Acm^{-2})
F_N	Quasi Fermi potential for electron current density(Vcm^{-2})
F_p	Quasi Fermi potential for hole current density(Vcm^{-2})
E	Electric field (Vcm^{-1})
q	Electron charge (C)
n	Electron concentration in n region (cm^{-3})
p	Hole concentration in n region (cm^{-3})
μ_n	Electron mobility ($cm^2V^{-1}S^{-1}$)
μ_p	Hole mobility ($cm^2V^{-1}S^{-1}$)
D_n	Diffusion coefficient of electron (cm^2s^{-1})
D_p	Diffusion coefficient of hole (cm^2s^{-1})
K	Boltzman's Constant ($JK^{-1}molecule^{-1}$)
T	Temperature(K)
V_t	Thermal Voltage (V)
E_b	Electric field due to donor densities (eV)
E_g	Electric field due to generation of electron-hole pairs (eV)
n_0	Thermal equilibrium electron concentration (cm^{-3})
p_0	Thermal equilibrium hole concentration (cm^{-3})
Δn	Excess electron concentration (cm^{-3})
Δp	Excess hole concentration (cm^{-3})
τ_n	Majority carrier electron life time (s)
τ_p	Minority carrier hole life time (s)
$G(x)$	Generation rate for holes(cm^3s^{-1})
W	Length of depletion region (cm)
Φ_s	Surface potential (V)
ϵ_s	Dielectric permittivity of semiconductor (Fcm^{-2})
L	Length of the semiconductor thickness (cm)
n_i	Intrinsic carrier concentration (cm^{-3})
N_d	External doping concentration (cm^{-3})
V_{oc}	Open circuit voltage (V)
$V_{oc(low)}$	Open circuit voltage (V) for low level injection
$V_{oc(high)}$	Open circuit voltage (V) for high level injection
$\Delta p(0)$	Excess hole density at point zero (cm^{-3})
$\Delta p(W)$	Excess hole density at depletion region (cm^{-3})
$\Delta p(L)$	Excess hole density at end of the semiconductor (cm^{-3})
$R(\lambda)$	Reflection coefficient
$\alpha(\lambda)$	Absorbance of thin metallic layer(cm^{-1})
$f(\lambda)$	Probability of photon producing electron-hole pair
Φ'	Flux of photons striking the interface($cm^{-2}s^{-1}$)

λ	Wavelength of the incident light(m)
L_p	Diffusion length for holes (cm)
L_n	Diffusion length for electrons(cm)
S_p	Effective surface recombination velocity (cm s^{-1})

ACKNOWLEDGEMENTS

I am highly pleased to express my sincere and profound gratitude to my M.Sc thesis Supervisor Dr. M. M. Shahidul Hassan, Professor, Department of Electrical and Electronic Engineering, Bangladesh University of Engineering and Technology (BUET) for providing me the opportunity to conduct my Masters research on Schottky Barrier Solar Cell. His helpful suggestion, continuous support and supervision inspired me throughout the process of the work.

I am grateful to my parents, friends and well wishers for their co-operation and support throughout the entire cycle of the work.

Finally I am grateful to Almighty Allah for giving strength and courage to complete M.Sc thesis work.

ABSTRACT

Today's research works surrounding Solar cells revolve around finding out different ways to improve efficiency. Open Circuit Voltage is now considered as an important parameter in determining efficiency of Solar Cell. In this work, analytical modeling of open circuit voltage (V_{OC}) is performed for Schottky Barrier (SB) Solar Cell and mathematical expression for V_{OC} is derived for all levels of injection of carriers. No analytical work for finding open circuit voltage of SB solar cell for all levels of injection has been done previously. Some of the works attribute to analytical modeling of open circuit voltage of SB Solar Cell for special cases of low and high level of injection. This work is valid for all levels of injection and it has tracked down the previous results for low and high level of injection by applying necessary assumptions. Mathematical expressions obtained after applying necessary assumptions are then compared with previous mathematical modeling of low and high level of injection. Mathematical expression of V_{OC} for low and high level of injection is found same to those obtained by works done previously. For finding out this mathematical representation of open circuit voltage second order differential equation is required to be solved to obtain excess minority carrier hole concentration in depletion and neutral region of a n-type SB Solar Cell. Proper boundary conditions are applied in evaluating constants of the solution of the differential equation. Effect of doping concentration, Metal work function, effective surface recombination velocity at the n-n+ interface and thickness of semiconductor on V_{OC} has been studied. Variation of V_{OC} with doping concentration and metal work function has been explained. Both Si and GaAs are considered as semiconductors and different metals are used. Comparison of V_{OC} for different levels of injection as function of doping concentration has been performed. With the increase of doping concentration and metal work functions V_{OC} increases for different levels of injection. For changing level of injection from low to all level it has been found that V_{OC} increases by around 0.1 volt for a certain metal and while changing level of injection from all level to high level around 0.1 volt increase of V_{OC} occurs for a certain metal. While changing doping level from 10^{14} to 10^{17} range, V_{OC} increases about 0.1-0.25 volt for various metal combinations. Using GaAs instead of Si means increase of about 0.2 volt in V_{OC} . Increase of metal work function indicates increase in V_{OC} . The variation of V_{OC} is less prominent among various levels of injection while using n-GaAs instead of n-Si as semiconductor. Increase of effective surface recombination velocity S_{eff} and thickness of the semiconductor L does not imply significant change in V_{OC} . With increase of S_{eff} , V_{OC} decreases slightly for all level and low level of injection. With increase of L , V_{OC} remains almost constant under all level and low level of injection. High level of injection indicates slight increase of V_{OC} with S_{eff} and L . In the end comparisons of low level and high level of injection has been performed while using current analytic model with the previous result obtained for low and high level of injection.

CHAPTER 1

INTRODUCTION

1.1 Introduction

Open circuit voltage is a very important parameter that determines several other performance parameters of Solar cell. One of the major concerns of research in today's world revolves around to find the way to increase the efficiency of Solar Cell. Efficiency and fill factor of Solar cell are very important aspects of research works regarding Solar Cell and Open Circuit voltage is the main concern in this case. To carefully understand the impact of Open Circuit Voltage on the efficiency of Solar Cells lots of works have been done using Si, GaAs and different combinations of materials to improve the efficiency of Solar Cell.

Improving the efficiency of solar cell using various kinds of materials and fabrication techniques are worked over a long time [1-4]. A great amount of research efforts on Schottky barrier solar cells have been done to understand the effects of various factors to improve efficiency [5-7]. To improve the short circuit current density is one of the ways to improve the efficiency of the solar cells. But it has been much easier to concentrate on open circuit voltage (V_{oc}) of the cell to improve the efficiency of the device [8-10].

In this work Analytical modeling of Open Circuit Voltage of Schottky barrier (SB) Solar Cell is performed for different levels of injections.

In this chapter, basic operating principles of Schottky Barrier Diode (SBD) and Solar Cell will be discussed. Literature survey will be carried out on relevant research works made on SB Solar Cell in the past to improve its efficiency and different characteristics.

1.2 Schottky Barrier Diode (SBD)

Research works based on metal semiconductor rectifying systems started by hand of Braun. In 1874, he first noted the dependence of the total resistance of a point contact on the polarity of the applied voltage and on the detailed surface conditions using mercury metal contacted with copper and iron sulfide semiconductors. Practical implementation of point contact rectifier started in 1904. In 1931, based on the band theory of solids, transport theory of semiconductor was developed by Wilson. This theory proved to be pivotal in case of research works related to metal semiconductor contacts. The first theory that predicted the correct direction of rectification of the metal–semiconductor junction was given by Nevill Mott in 1939. A major breakthrough was done by contribution of Walter H.Schottky who gave

suggestions that potential barriers could arise from stable space charges present in the semiconductor. That was the starting concept for a Schottky barrier diode. These models were further enhanced by Hans Bethe in 1942 to become the thermionic-emission model which accurately describes the electrical behavior. Because of their importance in direct current and microwave applications and as intricate parts of other semiconductor devices, metal-semiconductor contacts have been studied extensively. They have been used as photo detectors, solar cells, rectifiers, as the gate electrode of the MESFET, etc. they have also got different kinds of voltage clamping applications. Most importantly, the metal contact on heavily doped semiconductor forms an ohmic contact that is required for every semiconductor device in order to pass current in and out of the device. Many of the literatures are trying continuously in their search for other applications in various fields with Schottky barrier diode.

1.2.1 Structure of SBD

The ideal energy-band diagram for a particular metal and n-type semiconductor before making contact is shown in Figure 1.1(a). Here the vacuum level is the reference level. Also in figure 1.1(a), ϕ_m is the metal work function, ϕ_s is the semiconductor work function, and χ is the electron affinity. Work function is the necessary energy to remove an electron from Fermi level to vacuum. Electron affinity is the difference between minima of conduction band and vacuum level. Here for $\phi_m > \phi_s$, the ideal thermal-equilibrium metal-semiconductor energy-band diagram is shown in Figure 1.1(b). Before contact, the Fermi level in the semiconductor was above that of the metal. In order for the Fermi level to become a constant through the system in thermal equilibrium, electrons from the semiconductor side flow to the lower energy states in the metal. Positively charged donor atoms remain in the semiconductor, creating a space charge region.

Here ϕ_{B0} is the ideal barrier height of the semiconductor contact, the potential barrier seen by electrons in the metal trying to move into the semiconductor. This barrier is known as the Schottky barrier and is given by

$$\phi_{B0} = \phi_m - \chi \quad (1.1)$$

On the semiconductor side, V_{bi} is the built-in potential barrier seen by electrons in the conduction band trying to move into the metal. This is given by

$$V_{bi} = \phi_{B0} - \phi_n \quad (1.2)$$

Here V_{bi} is a slight function of the semiconductor doping.

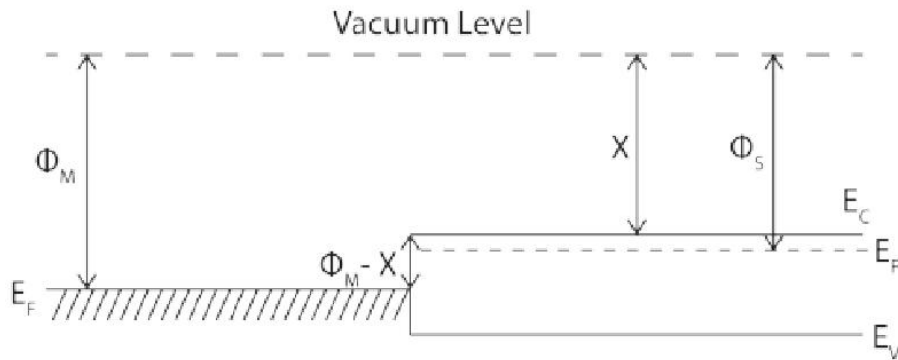


Figure 1.1. (a) Energy-band diagram of a metal and semiconductor before contact;

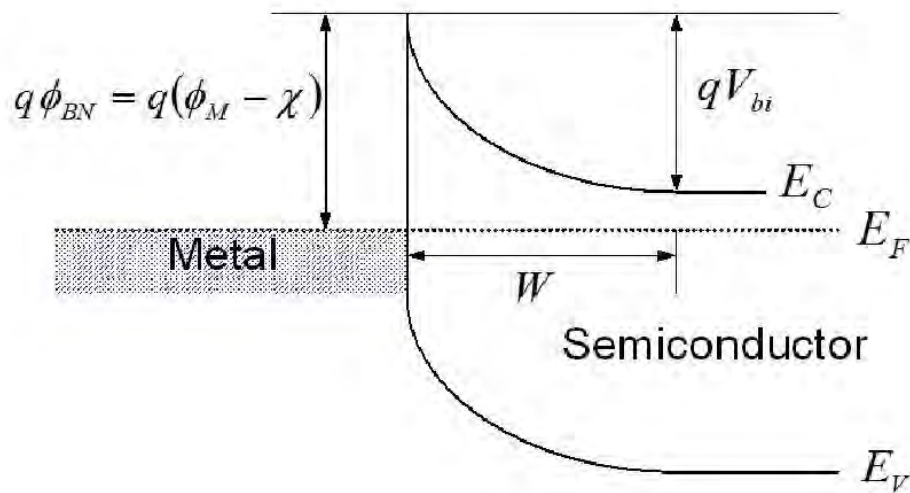


Figure 1.1. (b) Ideal energy-band diagram of a metal-n-semiconductor junction for $\phi_m > \phi_s$

Now if we apply a positive voltage to the semiconductor with respect to the metal, the semiconductor-to-metal barrier height increases, while ϕ_{B0} remains constant in this idealized case. This bias condition is the reverse bias. If a positive voltage is applied to the metal with respect to the semiconductor, the semiconductor-to-metal barrier V_{bi} is reduced while ϕ_{B0} again remains essentially constant. In this situation, electrons can more easily flow from the semiconductor into the metal since the barrier has been reduced. This bias condition is the forward bias. The energy-band diagrams for the reverse and forward bias are shown in Figure 1.2, where V_R is the magnitude of the reverse-bias voltage and V_0 is the magnitude of the forward-bias voltage.

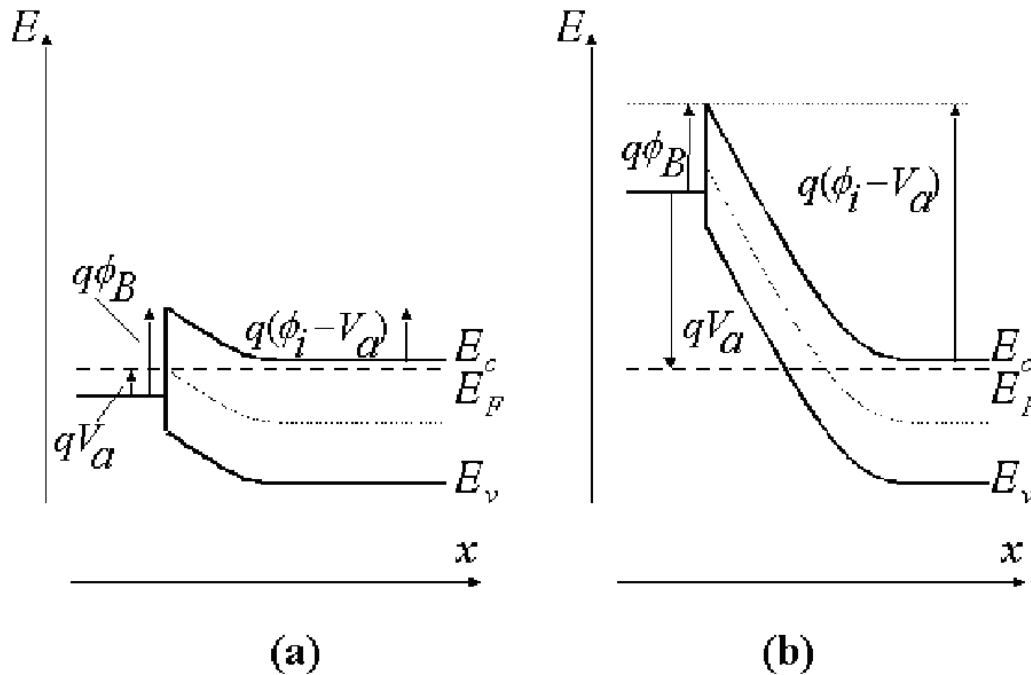


Figure 1.2. a) Under reverse bias b) Under forward bias

In forward bias, the barrier seen by the electrons in the semiconductor is reduced, so majority carrier electrons flow more easily from the semiconductor into the metal. The forward-bias current is in the direction from metal to semiconductor; it is an exponential function of the forward-bias voltage V_0 .

1.3 Solar Cell

A solar cell, or photovoltaic cell, is an electrical device that converts the energy of light directly into electricity by the photovoltaic effect. It is a form of photoelectric cell, defined as a device whose electrical characteristics, such as current, voltage, or resistance, vary when exposed to light. Solar cells are the building blocks of photovoltaic modules, otherwise known as solar panels. Solar cells are described as being photovoltaic irrespective of whether the source is sunlight or an artificial light. They are used as a photo detector (for example infrared detectors), detecting light or other electromagnetic radiation near the visible range, or measuring light intensity.

The Photovoltaic effect was experimentally demonstrated first by French physicist Edmond Becquerel Willoughby Smith first described the "Effect of Light on Selenium during the passage of an Electric Current" in a 20 February 1873 issue of Nature. In 1883 Charles

Fritts built the first solid state photovoltaic cell by coating the semiconductor selenium with a thin layer of gold to form the junctions; the device was only around 1% efficient.

In 1888 Russian physicist Aleksandr Stoletov built the first cell based on the outer photoelectric effect discovered by Heinrich Hertz in 1887.

Albert Einstein explained the underlying mechanism of light instigated carrier excitation—the photoelectric effect—in 1905, for which he received the Nobel Prize in Physics in 1921. Russell Ohl patented the modern junction semiconductor solar cell in 1946 while working on the series of advances that would lead to the transistor.

The first practical photovoltaic cell was publicly demonstrated on 25 April 1954 at Bell Laboratories. The inventors were Daryl Chapin, Calvin Souther Fuller and Gerald Pearson.

Solar cells gained prominence when they were proposed as an addition to the 1958 Vanguard I satellite. By adding cells to the outside of the body, the mission time could be extended with no major changes to the spacecraft or its power systems. In 1959 the United States launched Explorer 6, featuring large wing-shaped solar arrays, which became a common feature in satellites. These arrays consisted of 9600 Hoffman solar cells.

Improvements were gradual over the next two decades. The only significant use was in space applications where they offered the best power-to-weight ratio.

1.3.1 Operating principle of Solar Cell

The working principle of all today solar cells is essentially the same. It is based on the photovoltaic effect. In general, the photovoltaic effect means the generation of a potential difference at the junction of two different materials in response to visible or other radiation. The basic processes behind the photovoltaic effect are:

- a. Generation of the charge carriers due to the absorptions of photons in the materials that form a junction
- b. Subsequent separation of the photo-generated charge carriers in the junction
- c. Collection of the photo-generated charge carriers at the terminals of the junction.

In general, a solar cell structure consists of an absorber layer, in which the photons of incident radiation are efficiently absorbed resulting in the creation of electron-hole pairs. In order to separate the photo-generated electrons and holes from each other, the so-called “semi permeable membranes” are attached to the both sides of the absorber. The important requirement for the semi-permeable membranes is that they selectively allow only one type of charge carrier to pass through. An important issue for designing an efficient solar cell is that the electrons and holes generated in the absorber layer reach the membranes. This

requires that the thickness of the absorber layer is smaller than the diffusion lengths of the charge carriers.

In the figure 1.3, simplified schematic diagram of Solar cell is shown. Here we have considered a p-n junction with a very narrow and more heavily doped n region. The illumination is through the n side. The depletion region (space charge layer) extends primarily into the p side. There is a built in field E_0 in the depletion layer. The electrodes attached to the n side must allow illumination to enter the device. A thin reflection coating on the surface reduces reflections and allows more lights to enter the device.

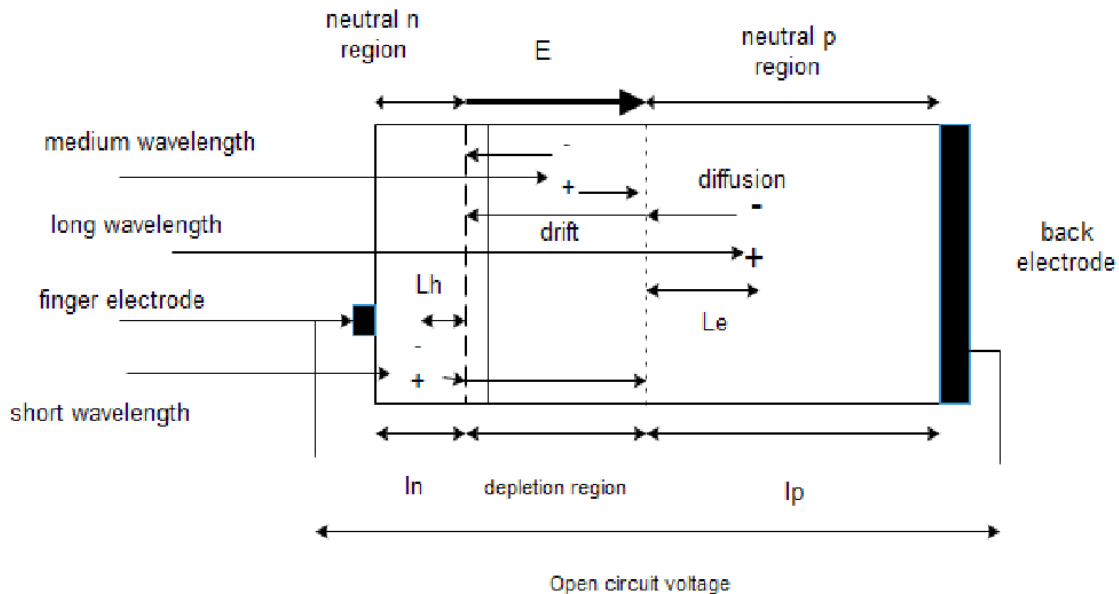


Figure 1.3. Principle of operation of Solar Cell

As the n side is very narrow most of the photons are absorbed within the depletion region and within the neutral p side and photo generate electron-hole pairs in these regions. EHPs photo generated in the depletion region are immediately separated by the built in field E_0 which drifts them apart. The electron drifts and reaches the neutral n side whereupon it makes the region negative by an amount of charge $-e$. Similarly the hole drifts and reaches the neutral p side and thereby makes the side positive. As a result, open circuit voltage develops between the terminals of the device with the p side positive with respect to n side.

The EHPs photo generated by long wavelength photons that are absorbed in the neutral p side can only diffuse in this region as there is no electric field. If the recombination lifetime of the electron is τ_e , it diffuses a mean length L_e given by $L_e = \sqrt{2D_e\tau_e}$ where D_e is its diffusion coefficient in the p side. Those electrons within a distance L_e to the depletion region can readily diffuse and reach this region whereupon they become drifted by E_0 to the n side. Consequently only those EHPs photo generated within the minority carrier diffusion length L_e to the depletion layer can contribute to photovoltaic effect. Once an electron diffuses to the

depletion region it is swept over to the n side by electric field to give an additional negative charge there. Holes left behind in the p side contribute a net positive charge to this region. Those photo generated EHPs further away from depletion region than L_e are lost by recombination. It is therefore important to have the minority carrier diffusion length as long as possible. Similarly holes photo generated within a diffusion length L_h can reach the depletion layer and become swept across to the p side. The photo generation of EHPs that contribute to the photovoltaic effect therefore occurs in a volume covering L_h+W+L_e . If the terminals of the device are shorted then the excess electron in the n side can flow through the external circuit to neutralize the excess holes in the p side. This current due to flow of photo generated carriers is called the photocurrent.

Under a steady state operation there can be no net current through an open circuit solar cell. This means the photocurrent inside the device due to the flow of photo generated carriers must be exactly balanced by a flow of carriers in the opposite direction. EHPs photo generated by energetic photons absorbed in the n side near the surface region or outside the diffusion length L_h to the depletion layer are lost by recombination as the lifetime in the n side is generally very short (due to heavy doping). The n side is therefore made very thin. The length l_n of the n side may be shorter than the hole diffusion length L_h . The EHPs photo generated very near the surface of the n side however disappear by recombination due to various surface effects acting as recombination centers.

At long wavelengths the absorption coefficient is small and the absorption depth is greater. To capture these long wavelength photons we therefore need a thick p side and at the same time a long minority carrier diffusion length.

1.3.2 Efficiency and fill factor of Solar Cell

Solar cell efficiency is the ratio of the electrical output of a solar cell to the incident energy in the form of sunlight. The energy conversion efficiency (η) of a solar cell is the percentage of the solar energy to which the cell is exposed that is converted into electrical energy. This is calculated by dividing a cell's power output (in watts) at its maximum power point (P_m) by the input light (E , in W/m^2) and the surface area of the solar cell (A_c in m^2).

$$\eta = \frac{P_m}{E \times A_c}$$

Another defining term in the overall behavior of a solar cell is the fill factor (FF). This is the available power at the maximum power point (P_m) divided by the open circuit voltage (V_{oc}) and the short circuit current (I_{sc}):

$$FF = \frac{P_m}{V_{oc} \times I_{sc}}$$

The fill factor is directly affected by the values of the cell's series and shunt resistances. Increasing the shunt resistance (R_{sh}) and decreasing the series resistance (R_s) lead to a higher fill factor, thus resulting in greater efficiency, and bringing the cell's output power closer to its theoretical maximum.

So fill factor plays a major role in increasing the efficiency of solar cell and in this case Open Circuit Voltage and Short circuit current are very important parameters.

1.3.3 Open Circuit Voltage

The open-circuit voltage is the voltage at which no current flows through the external circuit. It is the maximum voltage that a solar cell can deliver. The V_{oc} corresponds to the forward bias voltage, at which the dark current compensates the photo-current. The V_{oc} depends on the photo-generated current density and can be calculated assuming that the net current is zero.

V_{oc} depends on the saturation current of the solar cell and the photo-generated current. While J_{ph} typically has a small variation, the key effect is the saturation current, since this may vary by orders of magnitude. The saturation current density, J_0 , depends on the recombination in the solar cell. Therefore, V_{oc} is a measure of the amount of recombination in the device. Laboratory crystalline silicon solar cells have a V_{oc} of up to 720 mV under the standard AM1.5 conditions, while commercial solar cells typically have V_{oc} above 600 mV.

1.3.4 Advantage of Schottky barrier in Solar Cell

The advantages of Schottky barriers in Solar cell include

1. Low-temperature processing because no high-temperature diffusion or annealing is required;
2. Adaptability to polycrystalline and thin-film solar cells;
3. High radiation resistance due to high electrical field near the surface;
4. High current output and good spectral response, because the presence of a depletion region right at the semiconductor surface can substantially reduce the effects of low lifetime and high recombination velocity near the surface.

1.4 Literature Review

At first in the year of 1958 new developments in Silicon photovoltaic devices are attributed by Prince and Wolf [11] for both low and low level lights. Later on it has been tried to increase the efficiency of the Solar cells by numerous researchers like Bortfeld, Gobart, Lamorte and Mciver[12]. Their work revolves around high efficiency GaAs Solar Cell. Till then, different methods are tried to increase the efficiency of Solar cells upto the recent works by Marti, Cuadra and Luque[13].

Schottky Barrier Solar Cell concept has arisen by the work of Anderson and Delahoy [14, 15] who have worked on the concept of using Schottky junctions for Solar energy conversion. They have also worked on Schottky barrier height modification. Efficiency calculation for thin film Schottky barrier Solar cell has been shown in the work of Lanza and Hovel[16]. Recent works on Schottky barrier Solar cells include works of Corpus, De Souza and Hamelmann [17] which concentrates on design of Schottky contacts for optimum performance of thin film Solar cells. Light induced degradation in different cell structures has also been studied by Liu, Lee and Collins [18]. Device performance and current transport mechanisms were studied in the works of Ji and Anderson [19].

Use of open circuit voltage for determining barrier height to study the effect on illumination and fill factor has been studied in work of Panayotatos, Card [20]. The residual oxide layer was minimized and theoretical analysis has been matched with experimental results. Open circuit voltage characteristics of Schottky barrier Solar cell has been studied in the works of Peckerer, Lin and Kocher [21]. Their work exhibited ways to control the Schottky barrier height and its effect on open circuit voltage of Schottky barrier Solar Cell to increase the efficiency and tried to reach the efficiency level of the commercially available Solar Cells. Later on effect of dislocations on the open circuit voltage of GaAs Solar cells has been studied by Zolper and Barnett [22]. Gong, Posthuma, Dross [23] have worked on comparison of n type and p type Si based Solar Cell for low level of illumination. Later on Wolf [24] worked on high level of injections to study the effect on SB solar cells. Effect of content, thickness and defect density on the performance of p-i-n InGaN single homojunction and heterojunction solar cells has been studied by Cai, Wang, Chen, Liang, Liu and Zhang[25].

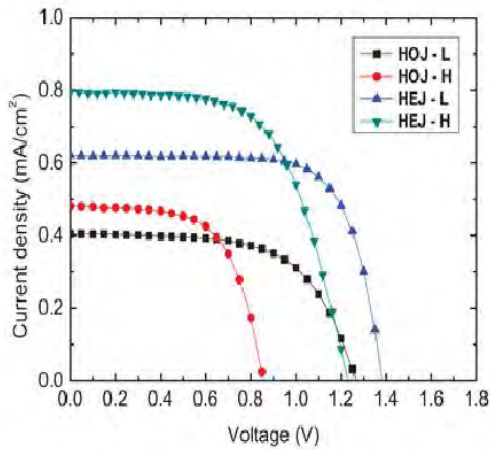


Fig 1.4.1. variation of current density with voltage (ref. [25])

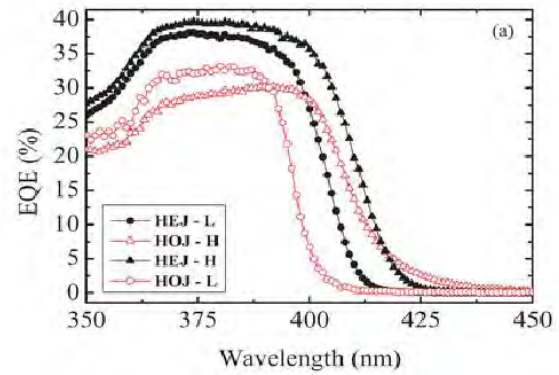


Fig 1.4.2. variation of quantum efficiency with wavelength (ref [25])

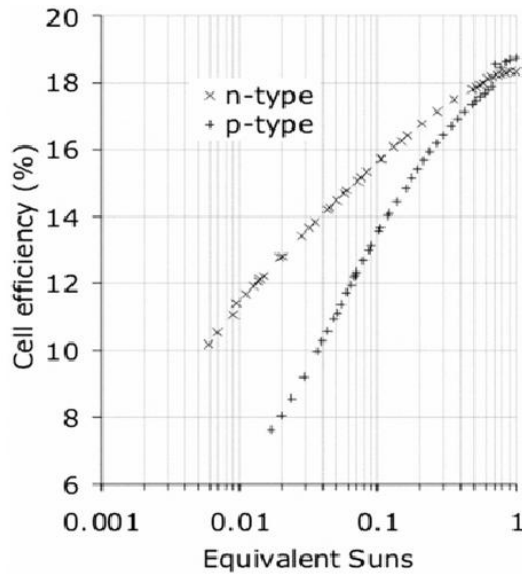


Fig 1.4.3. Variation of cell efficiency (ref[23])

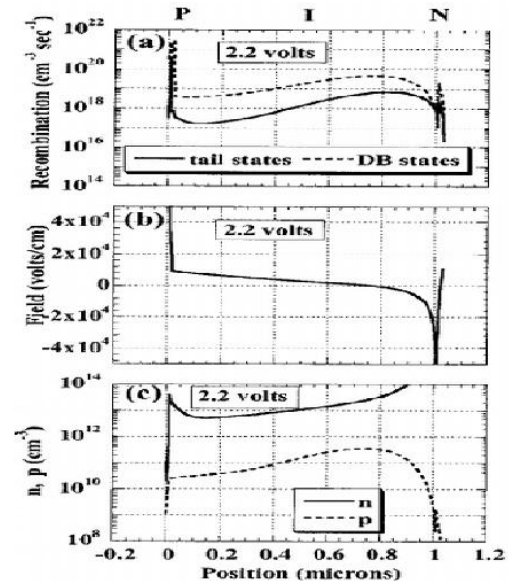


Fig 1.4.4. Variation of recombination, field and concentration with position(ref[18])

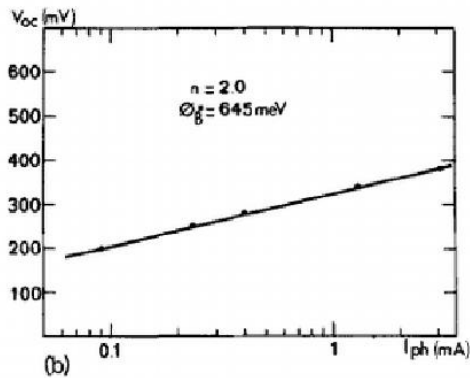


Fig 1.4.5. Variation of open circuit voltage with photon current (ref[14])

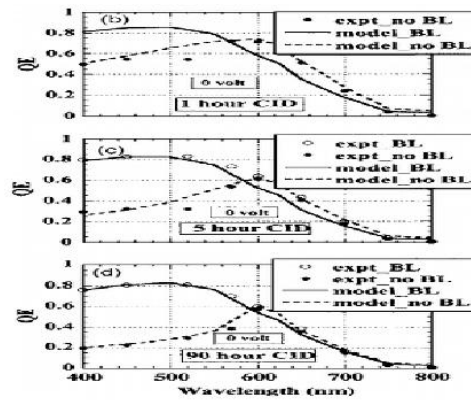


Fig 1.4.6. Variation of quantum efficiency with wavelength (ref[17])

Figure 1.4. Different plots from Literature Review

1.5 Objective of the Work

The objective of this thesis is to find out a mathematical expression for open circuit voltage defined for all levels of injection:

- i) Effect of using different combinations of metal-semiconductors
- ii) Effect of surface recombination velocity
- iii) Effect of thickness of semiconductor layer

It is inclined to study the various combinations of metal-semiconductors in this regard to find out for which combination a desired characteristic open circuit voltage can be achieved. Effect of surface recombination velocity, effect of doping and effect of semiconductor thickness are studied hereby and suitable V_{oc} characteristic for all level is explored.

The possible outcome would be finding out a suitable range of doping density, metal-semiconductor combination and semiconductor thickness to ensure to tract down the best possible solution of V_{oc} for not only specific low/ high level injection but also for all levels.

1.6 Scope of the work

Drift and diffusion components of both majority and minority carrier current densities will be used with the help of continuity equation for carriers. Applying techniques of integration on Electric field present in depletion and neutral region, a general mathematical expression of

open circuit voltage (V_{oc}) will be obtained. Excess minority carrier (hole) charge expression will be evaluated by using proper boundary conditions. In this regard, second order non linear differential equation will be solved. The general mathematical expression at first will be found for all levels of injections. Then the special cases of low level and high level injection will be studied and compared with previous works of low and high level injection to prove the authenticity. In this case proper estimations like expanding mathematical terms will be used to tract the previous result in the cases of low and high level injections. Then the variation of open circuit voltage (V_{oc}) will be studied for various combinations of metal-semiconductors, doping densities and thickness of semiconductor layers to find out the best possible range of operation in this regard. All these kinds of simulation works will be done by using MATLAB.

1.7 Conclusions

In this chapter at first the structure of Schottky Barrier Diode has been studied. Later on the operation of Solar cells has been discussed and the advantages of using SB solar cells have been mentioned. Open circuit voltage plays an important role as an important parameter in analytical modeling of SB solar cell and in this regard some lights have been implied on the objective and scope of our present work. Some of the literature works on this case has been highlighted in this section.

In chapter 2, the mathematical derivation for finding out analytical model of open circuit voltage for all levels of injections for SB Solar cell has been studied. The analytical expression for low and high levels of injections has been derived out by utilizing proper conditions and the previous findings has been traced out in this case. Using transport equations, continuity equations and solution of second order non linear differential equations help to ultimately find out the analytical model of Open circuit voltage. Excess minority carrier charge will be expressed by utilizing proper boundary conditions.

In chapter 3, with the help of mathematical derivations done in previous chapter, different characteristics plots of open circuit voltage for different doping concentrations, thickness, metal work functions, effective surface recombination velocities have been studied. The results will be obtained for low, high and intermediate levels of injections and some of the results will be compared with previous findings.

In chapter 4, the entire work will be presented in a nutshell and optimum performance of the SB Solar cell for the open circuit voltage will be attributed for different doping densities, thickness and effective surface recombination velocities.

CHAPTER 2

MATHEMATICAL DERIVATIONS

2.1 Introduction

In chapter 1, basic structures of Schottky Barrier Diode and operation of SB Solar cell have been studied. In determining efficiency of the Solar cell, Open circuit voltage plays an important role. Open circuit voltage has been defined in that chapter. Besides, Advantages of SB Solar Cell have been described briefly. Some of the past works on developing new ways of improvement of efficiency of Solar Cell have been introduced.

In this chapter, through analytical modeling of SB Solar Cell, mathematical expression for open circuit voltage will be obtained for all levels of injection. This mathematical expression will be evaluated for both low level and high level of injections later on. There have been some of the previous works concentrating on only low and high level injection condition. In this chapter, The generalized mathematical modeling will help us to track the previous findings in general and will help to find ways of determining open circuit voltage characteristics for the intermediate levels.

To understand the open circuit voltage characteristics (V_{oc}) under low and high level of injection, few works have been done previously [8-10]. A unique mathematical solution for the open circuit voltage (V_{oc}) characteristics under all levels of injection is necessary for understanding efficiency under any amount of illumination. Using different combinations of metal-semiconductors and thickness of semiconductor layer can result in different characteristic plots under different ranges of illumination.

Effect of changing doping concentrations, effect of using different combinations of metal-semiconductors, effect of surface recombination velocity and effect of thickness of semiconductor layer are studied.

It is important to study the various combinations of metal-semiconductors in this regard to find out for which combination a desired characteristic open circuit voltage can be achieved. Effect of surface recombination velocity, effect of doping and effect of semiconductor thickness are studied hereby and suitable Open circuit voltage characteristic for all level is explored.

The possible outcome would be finding out a suitable range of doping density, metal-semiconductor combination and semiconductor thickness to ensure to track down the best possible solution of Open circuit voltage for not only specific low/ high level injection but also for all levels.

2.2 Mathematical modeling of open circuit voltage for all levels of injection

The energy band diagram of metal/n-type Schottky barrier (SB) Solar cell is shown in the figure 2.1. Here Schottky contact forms at $x=0$ and ohmic contact forms at $x=L$. A depletion region of width W is formed near Schottky contact.

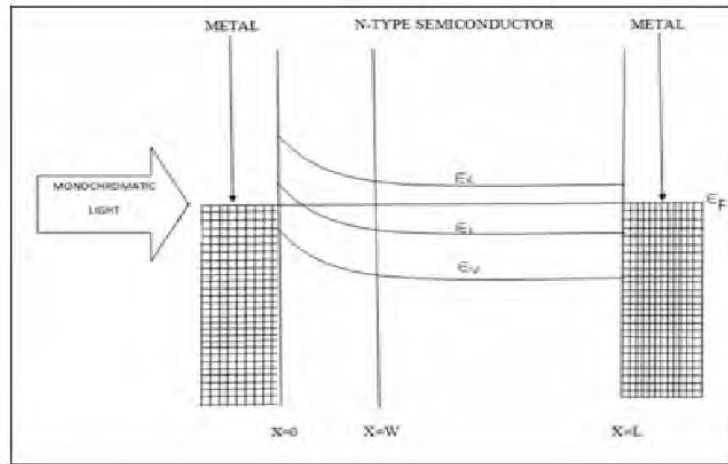


Figure 2.1. Energy Band Diagram of a Metal/n-type Semiconductor Schottky Barrier Solar Cell

The one dimensional structure of a SB Solar Cell is shown in figure 2.2.

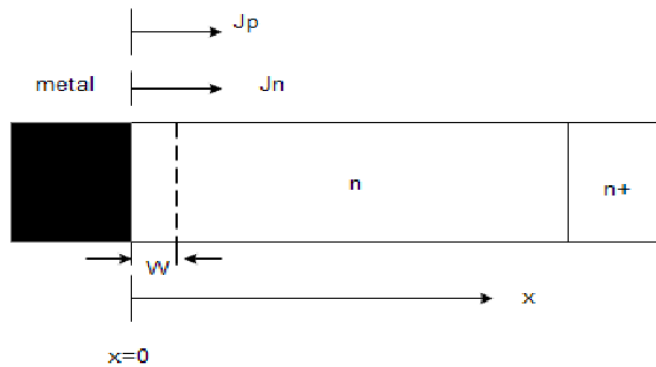


Figure 2.2. One dimensional structure of SB Solar Cell

The open circuit voltage (V_{oc}) under illumination of monochromatic light at the interface of metal and n-type semiconductor Schottky barrier Solar cell is considered for the metal. So, the boundary condition is that the total current density J_T , which is the combination of drift and diffusion current component of electrons and holes flowing in the cell must be zero.

Here, $J_T = J_n + J_p$ (2.1)

Where,

J_n = majority carrier current density

J_p = minority carrier current density

The fundamental one dimensional transport equations assuming the origin of the axis at the metal semiconductor contact, are given by the following equations:

$$J_n = qn\mu_n E + qD_n \frac{dn}{dx} \quad (2.2)$$

$$J_p = qp\mu_p E - qD_p \frac{dp}{dx} \quad (2.3)$$

Where, n = majority carrier electron concentration in n type semiconductor region in cm^{-3}

p = minority carrier hole concentration in n type semiconductor region in cm^{-3}

μ_n = electron mobility in $\text{cm}^2 \text{V}^{-1} \text{s}^{-1}$

μ_p = hole mobility in $\text{cm}^2 \text{V}^{-1} \text{s}^{-1}$

E = electric field in drift region in Vcm^{-1}

D_n = diffusion coefficient of electron in $\text{cm}^2 \text{s}^{-1}$

D_p = diffusion coefficient of hole in $\text{cm}^2 \text{s}^{-1}$

The diffusion coefficients from the Einstein relation are given as,

$$D_n = \frac{KT}{q} \mu_n \quad \text{for electrons} \quad (2.4)$$

$$D_p = \frac{KT}{q} \mu_p \quad \text{for holes} \quad (2.5)$$

Where $\frac{KT}{q}$ is called as thermal voltage V_T , K is the Boltzmann constant and T is the temperature in Kelvin.

For Open Circuit Voltage, $J_T = 0$;

Using $J_T = 0$ and from equation (2.1), (2.2) & (2.3) it can be shown as,

$$qn\mu_n E + qD_n \frac{dn}{dx} + qp\mu_p E - qD_p \frac{dp}{dx} = 0 \quad (2.6)$$

The open circuit voltage (V_{OC}) is expressed as,

$$V_{OC}=V(X=L)-V(X=0)$$

$$= [V(L)-V(W)]+[V(W)-V(0)] \quad (2.7)$$

The potential difference $[V(W)-V(0)]$ represents developed voltage within depletion region where as $[V(L)-V(W)]$ corresponds to that in the neutral region.

The Open circuit voltage will be evaluated in two different regions as

- i) Depletion region
- ii) Neutral region

Open circuit voltage of those two regions will be added to give the final mathematical expression of Open Circuit Voltage of SB Solar Cell for all levels of injections. Afterwards the necessary constants will be calculated and the result will be evaluated for special case of low level and high level of injection.

2.2.1 Open circuit potential in depletion region($0 \leq X \leq W$)

Within the depletion region, there exists built in electric field(E_b) due to donor densities and electric field (E_g) due to generation of electron-hole pairs under monochromatic light illumination. So, the total electric field(E) is represented as,

$$E=E_b(X)+E_g(X) \quad (2.8)$$

The carrier densities at non-equilibrium can be expressed as,

$$n=n_0(x)+\Delta n(x) \quad (2.9)$$

$$p=p_0(x)+\Delta p(x) \quad (2.10)$$

here, Δn is excess electron concentration and Δp is the excess hole concentration. n_0 is thermal equilibrium electron concentration and p_0 is the thermal equilibrium hole concentration.

From using equation (2.8), (2.9) and (2.10) to substitute parameters into equation (2.6), we can obtain,

$$q(n_0+\Delta n(x))\mu_n E_g(x)+q(p_0+\Delta p(x))\mu_p E_g(x)+q\Delta n(x)\mu_n E_b(x)+q\Delta p(x)\mu_p E_b(x)$$

$$+ qD_n \frac{d\Delta n(x)}{dx} - qD_p \frac{d\Delta p(x)}{dx} = 0 \quad (2.11)$$

Further simplification of equation (2.11) gives $E_g(x)$ as,

$$E_g(x) = \frac{D_p \frac{d\Delta p(x)}{dx} - D_n \frac{d\Delta n(x)}{dx}}{(n_0 + \Delta n(x))\mu_n + (p_0 + \Delta p(x))\mu_p} - \frac{(\Delta n(x)\mu_n + \Delta p(x)\mu_p)E_b(x)}{(n_0 + \Delta n(x))\mu_n + (p_0 + \Delta p(x))\mu_p} \quad (2.12)$$

In equation (2.12) both excess electron and hole concentrations are present. To make future calculation more tractable, Continuity equation has been used. Continuity equation helps to find out relation between both majority and minority carrier concentrations and lifetimes.

The continuity equations for electrons and holes are given as,

$$-\frac{1}{q} \frac{dJ_p}{dx} + G(x) - \frac{\Delta p}{\tau_p} = 0 \quad (2.13)$$

$$-\frac{1}{q} \frac{dJ_n}{dx} + G(x) - \frac{\Delta n}{\tau_n} = 0 \quad (2.14)$$

In equation (2.13) and (2.14) $G(x)$ is the generation rate of electron-hole pairs, τ_n is the lifetime of electron and τ_p is the lifetime of holes.

In the steady state J_T must be constant everywhere, and so as a result $\frac{dJ_T}{dx} = 0$.

Using equation (2.13) and (2.14) the corresponding relationship between excess carrier concentration and lifetime can be found as,

$$\frac{\Delta n}{\tau_n} = \frac{\Delta p}{\tau_p} \quad (2.15)$$

Performing integration of equation (2.12) within depletion region, Open circuit potential can be shown as,

$$\begin{aligned} V(W) - V(0) &= -\int_0^W E_g(x) dx \\ &= -\int_0^W \frac{D_p \frac{d\Delta p(x)}{dx} - D_n \frac{d\Delta n(x)}{dx}}{(n_0 + \Delta n(x))\mu_n + (p_0 + \Delta p(x))\mu_p} dx + \int_0^W \frac{(\Delta n(x)\mu_n + \Delta p(x)\mu_p)E_b(x)}{(n_0 + \Delta n(x))\mu_n + (p_0 + \Delta p(x))\mu_p} dx \end{aligned} \quad (2.16)$$

Now considering $-\int_0^W \frac{D_p \frac{d\Delta p(x)}{dx} - D_n \frac{d\Delta n(x)}{dx}}{(n_0 + \Delta n(x))\mu_n + (p_0 + \Delta p(x))\mu_p} dx$ as the first part and $\int_0^W \frac{(\Delta n(x)\mu_n + \Delta p(x)\mu_p)E_b(x)}{(n_0 + \Delta n(x))\mu_n + (p_0 + \Delta p(x))\mu_p} dx$ as the second part, the required integration can be performed to obtain desired mathematical expression of V_{oc} in depletion region.

After performing integration of the first part of equation (2.16), result of integration can be obtained as,

$$-\int_0^W \frac{D_p \frac{d\Delta p(x)}{dx} - D_n \frac{d\Delta n(x)}{dx}}{(n_0 + \Delta n(x))\mu_n + (p_0 + \Delta p(x))\mu_p} dx = \left(\frac{-D_p + D_n \frac{\tau_n}{\tau_p}}{\mu_p + \frac{\tau_n}{\tau_p} \mu_n} \right) \left[\ln \left(\frac{\Delta p(W) + \frac{n_0 \mu_n + p_0 \mu_p}{\mu_p + \frac{\tau_n}{\tau_p}}}{\Delta p(0) + \frac{n_0 \mu_n + p_0 \mu_p}{\mu_p + \frac{\tau_n}{\tau_p}}} \right) \right] \quad (2.17)$$

After performing integration of the second part of equation (2.16), result of integration can be obtained as,

$$\int_0^W \frac{(\Delta n(x)\mu_n + \Delta p(x)\mu_p)E_b(x)}{(n_0 + \Delta n(x))\mu_n + (p_0 + \Delta p(x))\mu_p} dx = -\phi_s \quad (2.18)$$

Where ϕ_s =surface potential= $\frac{1}{2} \frac{qN_d W^2}{\epsilon_s}$

Here, w is the depletion width of n type semiconductor region, ϵ_s is the dielectric permittivity of the semiconductor and N_d is the doping concentration.

Variation of surface potential (ϕ_s) with excess hole carrier concentration (Δp) is shown in the following figure:

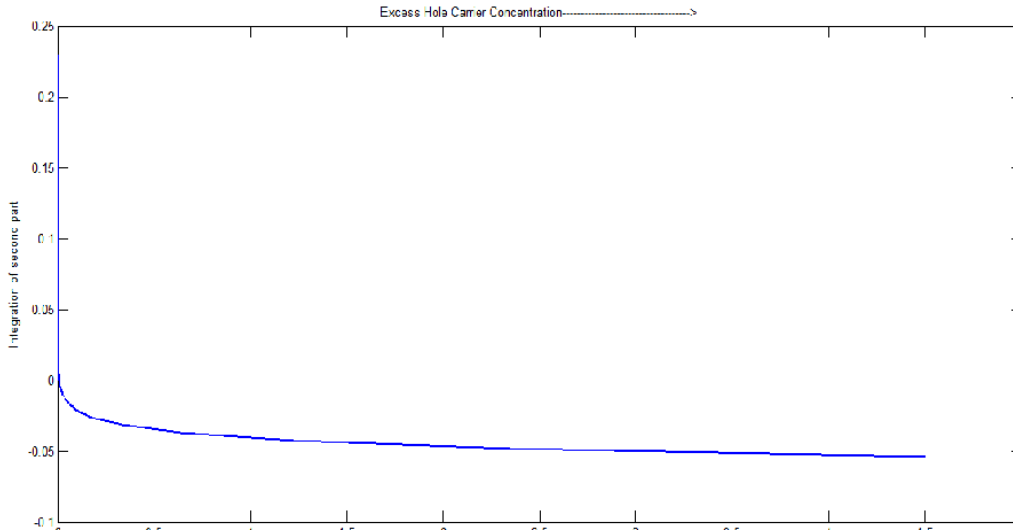


Figure 2.3. Variation of surface potential with excess hole carrier concentration

Using the equations (2.17) and (2.18) in equation (2.16), the general expression of open circuit voltage in depletion region can be easily found as,

$$V(W)-V(0)=\left(\frac{-D_p+D_n\frac{\tau_n}{\tau_p}}{\mu_p+\frac{\tau_n}{\tau_p}\mu_n}\right)\left[\ln\left(\frac{\Delta p(W)+\frac{n_0\mu_n+p_0\mu_p}{\mu_p+\frac{\mu_n\tau_n}{\tau_p}}}{\Delta p(0)+\frac{n_0\mu_n+p_0\mu_p}{\mu_p+\frac{\mu_n\tau_n}{\tau_p}}}\right)\right]-\phi_s \quad (2.19)$$

2.2.2 Open circuit potential in neutral region($W \leq X \leq L$)

In neutral region, only the electric field $E_g(x)$ associated with generation of electron-hole pairs with monochromatic light illumination exists.

Therefore in the neutral region the following relationships among parameters can be considered,

$$E=E_g(x) \quad (2.20)$$

$$n=N_d+\Delta n(x) \quad (2.21)$$

$$p = \frac{n_i^2}{N_d} + \Delta p(x) \quad (2.22)$$

Here, n_i is intrinsic carrier concentration in cm^{-3} .

Using equation (2.20), (2.21) and (2.22) into equation (2.6) after further calculations generated electric field in neutral region $E_g(x)$ can be expressed as,

$$E_g(x) = \frac{D_p - D_n \frac{\tau_n}{\tau_p}}{(N_d + \Delta n(x))\mu_n + \left(\frac{n_i^2}{N_d} + \Delta p\right)\mu_p} \frac{d\Delta p(x)}{dx} \quad (2.23)$$

The variation of excess hole carrier concentration Δp across the length of the semiconductor L is shown in the following figure:

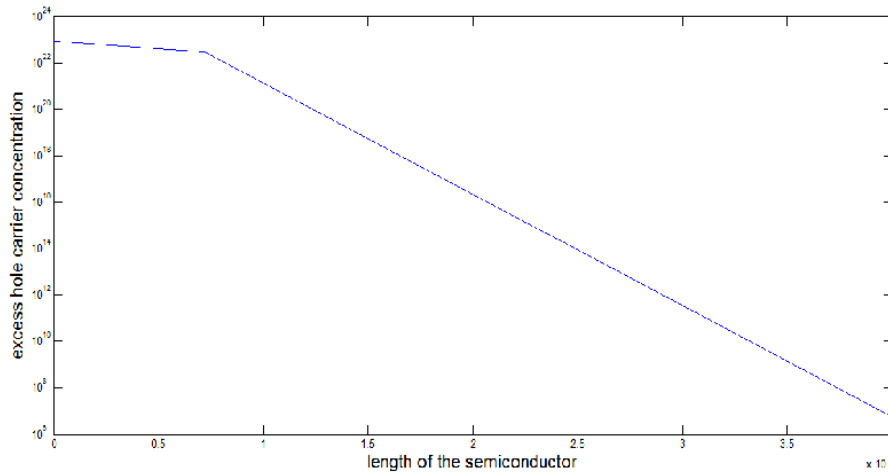


Figure 2.4. Variation of Excess hole carrier concentration with length of the semiconductor

After performing integration of equation (2.23) within neutral region, open circuit potential can be shown as,

$$V(L) - V(W) = - \int_W^L E_g(x) dx$$

$$= \left(\frac{D_n \frac{\tau_n}{\tau_p} - D_p}{\mu_p + \mu_n \frac{\tau_n}{\tau_p}} \right) \ln \left[\frac{\Delta p(L) + \frac{N_d \mu_n + \frac{n_i^2}{N_d} \mu_p}{\mu_p + \mu_n \frac{\tau_n}{\tau_p}}}{\Delta p(W) + \frac{N_d \mu_n + \frac{n_i^2}{N_d} \mu_p}{\mu_p + \mu_n \frac{\tau_n}{\tau_p}}} \right] \quad (2.24)$$

2.2.3 Open Circuit Voltage in SB Solar Cell

From equation (2.19), the mathematical expression of open circuit voltage for depletion region is obtained. From equation (2.24), the mathematical expression of open circuit voltage for neutral region is obtained.

By using equation (2.7), which indicates that the open circuit voltage of these two areas needs to be added to obtain Open circuit voltage in SB Solar Cell, it can be shown as,

$$V_{OC} = \left(\frac{-D_p + D_n \frac{\tau_n}{\tau_p}}{\mu_p + \frac{\tau_n}{\tau_p} \mu_n} \right) \left[\ln \left(\frac{\Delta p(W) + \frac{n_0 \mu_n + p_0 \mu_p}{\mu_p + \frac{\mu_n \tau_n}{\tau_p}}}{\Delta p(0) + \frac{n_0 \mu_n + p_0 \mu_p}{\mu_p + \frac{\mu_n \tau_n}{\tau_p}}} \right) \right] - \phi_s + \left(\frac{D_n \frac{\tau_n}{\tau_p} - D_p}{\mu_p + \mu_n \frac{\tau_n}{\tau_p}} \right) \ln \left[\frac{\Delta p(L) + \frac{N_d \mu_n + \frac{n_i^2}{N_d} \mu_p}{\mu_p + \mu_n \frac{\tau_n}{\tau_p}}}{\Delta p(W) + \frac{N_d \mu_n + \frac{n_i^2}{N_d} \mu_p}{\mu_p + \mu_n \frac{\tau_n}{\tau_p}}} \right] \quad (2.25)$$

This equation (2.25) is valid for all levels of injection of SB Solar Cell.

2.2.4 Mathematical expression of Open Circuit Voltage (V_{OC}) for the special case of High level injection

The assumptions for high level injections are:

For $0 \leq x \leq w$ $n_0, p_0 \ll \Delta n, \Delta p$

For $w \leq x \leq L$ $\Delta n, \Delta p \gg N_d \gg \frac{n_i^2}{N_d}$

Using these two assumptions in equation (2.25), Open circuit voltage for high level of injection can be obtained as,

$$V_{OC(\text{high})} = \left(\frac{-D_p + D_n \frac{\tau_n}{\tau_p}}{\mu_p + \frac{\tau_n}{\tau_p} \mu_n} \right) \ln \left(\frac{\Delta p(w)}{\Delta p(0)} \right) - \phi_s + \left(\frac{D_n \frac{\tau_n}{\tau_p} - D_p}{\mu_p + \mu_n \frac{\tau_n}{\tau_p}} \right) \ln \left(\frac{\Delta p(L)}{\Delta p(W)} \right) \quad (2.26)$$

2.2.5 Mathematical expression of Open Circuit Voltage (V_{OC}) for the special case of Low level injection

The assumptions for low level injections are:

For $0 \leq x \leq w$ $n_0, p_0 \ll \Delta n, \Delta p$

For $w \leq x \leq L$ $\Delta n, \Delta p \ll N_d \gg \frac{n_i^2}{N_d}$

Using these two assumptions in equation (2.25), Open circuit voltage for high level of injection can be obtained as,

$$V_{OC(\text{low})} = \left(\frac{-D_p + D_n \frac{\tau_n}{\tau_p}}{\mu_p + \mu_n \frac{\tau_n}{\tau_p}} \right) \ln \left(\frac{\Delta P(W)}{\Delta P(0)} \right) - \phi_s + \left(\frac{D_n \frac{\tau_n}{\tau_p} - D_p}{\mu_p + \mu_n \frac{\tau_n}{\tau_p}} \right) \ln \left[\frac{\Delta p(L) + \frac{N_d \mu_n + \frac{n_i^2}{N_d} \mu_p}{\mu_p + \mu_n \frac{\tau_n}{\tau_p}}}{\Delta p(W) + \frac{N_d \mu_n + \frac{n_i^2}{N_d} \mu_p}{\mu_p + \mu_n \frac{\tau_n}{\tau_p}}} \right] \quad (2.27)$$

To simplify equation (2.27), the parameters inside logarithmic term needs to be simplified.

$$\text{Let, } \frac{N_d \mu_n + \frac{n_i^2}{N_d} \mu_p}{\mu_p + \mu_n \frac{\tau_n}{\tau_p}} = r$$

Where, r is constant.

Then equation (2.27) can be written as,

$$V_{OC(\text{low})} = \left(\frac{D_n \frac{\tau_n}{\tau_p} - D_p}{\mu_p + \mu_n \frac{\tau_n}{\tau_p}} \right) \ln \left[\frac{\Delta p(L) + \frac{N_d \mu_n + \frac{n_i^2}{N_d} \mu_p}{\mu_p + \mu_n \frac{\tau_n}{\tau_p}}}{\Delta p(W) + \frac{N_d \mu_n + \frac{n_i^2}{N_d} \mu_p}{\mu_p + \mu_n \frac{\tau_n}{\tau_p}}} \right] = \left(\frac{D_n \frac{\tau_n}{\tau_p} - D_p}{\mu_p + \mu_n \frac{\tau_n}{\tau_p}} \right) \ln \left[\frac{\Delta P(L) + r}{\Delta P(W) + r} \right] \quad (2.28)$$

Expanding the logarithmic term of equation (2.28) using the following formula,

$$\ln(1+x) = x - \frac{x^2}{2} + \frac{x^3}{3} - \frac{x^4}{4} + \dots$$

$$\text{It can be written as, } \ln \left[\frac{\Delta P(L) + r}{\Delta P(W) + r} \right] \approx \frac{\Delta P(L) - \Delta P(W)}{\Delta P(W) + r}$$

Using further simplification techniques, it can be found that,

$$\left(\frac{D_n \tau_n - D_p}{\mu_p + \mu_n \frac{\tau_n}{\tau_p}}\right) \ln \left[\frac{\Delta p(L) + \frac{N_d \mu_n + \frac{n_i^2}{N_d} \mu_p}{\mu_p + \mu_n \frac{\tau_n}{\tau_p}}}{\Delta p(W) + \frac{N_d \mu_n + \frac{n_i^2}{N_d} \mu_p}{\mu_p + \mu_n \frac{\tau_n}{\tau_p}}} \right] = \frac{D_n \tau_n - D_p}{N_d \mu_n} (\Delta P(L) - \Delta P(W)) \quad (2.29)$$

Now using equation (2.29) in equation (2.27) the mathematical expression of open circuit voltage for Low level of injection can be expressed as,

$$V_{OC\text{low}} = \left(\frac{-D_p + D_n \frac{\tau_n}{\tau_p}}{\mu_p + \frac{\tau_n}{\tau_p} \mu_n}\right) \ln \left(\frac{\Delta P(W)}{\Delta P(0)}\right) - \phi_s + \frac{D_n \tau_n - D_p}{N_d \mu_n} (\Delta P(L) - \Delta P(W)) \quad (2.30)$$

2.2.6 Summary of mathematical expressions of open circuit voltage of SB Solar cell for different levels of injections

The mathematical expressions obtained for all level, low level and high level injections can be represented in the following table:

Level of injection	Expression of open circuit voltage V_{OC}
all	$V_{OC} = \left(\frac{-D_p + D_n \frac{\tau_n}{\tau_p}}{\mu_p + \frac{\tau_n}{\tau_p} \mu_n}\right) \left[\ln \left(\frac{\Delta p(W) + \frac{n_0 \mu_n + p_0 \mu_p}{\mu_p + \frac{\mu_n \tau_n}{\tau_p}}}{\Delta p(0) + \frac{n_0 \mu_n + p_0 \mu_p}{\mu_p + \frac{\mu_n \tau_n}{\tau_p}}} \right) \right] - \phi_s + \left(\frac{D_n \tau_n - D_p}{\mu_p + \mu_n \frac{\tau_n}{\tau_p}}\right) \ln \left[\frac{\Delta p(L) + \frac{N_d \mu_n + \frac{n_i^2}{N_d} \mu_p}{\mu_p + \mu_n \frac{\tau_n}{\tau_p}}}{\Delta p(W) + \frac{N_d \mu_n + \frac{n_i^2}{N_d} \mu_p}{\mu_p + \mu_n \frac{\tau_n}{\tau_p}}} \right]$
high	$V_{OC(\text{high})} = \left(\frac{-D_p + D_n \frac{\tau_n}{\tau_p}}{\mu_p + \frac{\tau_n}{\tau_p} \mu_n}\right) \ln \left(\frac{\Delta P(W)}{\Delta P(0)}\right) - \phi_s + \left(\frac{D_n \tau_n - D_p}{\mu_p + \mu_n \frac{\tau_n}{\tau_p}}\right) \ln \left(\frac{\Delta P(L)}{\Delta P(W)}\right)$
low	$V_{OC(\text{low})} = \left(\frac{-D_p + D_n \frac{\tau_n}{\tau_p}}{\mu_p + \frac{\tau_n}{\tau_p} \mu_n}\right) \ln \left(\frac{\Delta P(W)}{\Delta P(0)}\right) - \phi_s + \frac{D_n \tau_n - D_p}{N_d \mu_n} (\Delta P(L) - \Delta P(W))$

Table 2.1. Summary of mathematical expressions of Open Circuit Voltage of SB Solar cell under different levels of injection

2.2.7 Determination of excess minority carrier concentrations in depletion and neutral region

The mathematical expressions for Open Circuit Voltage of SB Solar Cells are represented for different levels of injections in tabular form in section 2.2.6.

But the excess carrier hole concentrations $\Delta p(0)$, $\Delta p(L)$ and $\Delta p(W)$ are not determined in those mathematical representations.

In this section, the excess hole concentrations in different regions will be determined.

In steady state condition, the continuity equation for holes can be written as,

$$-\frac{1}{q} \frac{dJ_p}{dx} + G(x) - \frac{\Delta p}{\tau_p} = 0$$

Where, $G(x) = \phi \{1 - R(\lambda) - a(\lambda)\} f(\lambda) \alpha e^{-\alpha x}$

If $\phi' = \phi \{1 - R(\lambda) - a(\lambda)\} f(\lambda)$

$$\text{Then the continuity equation can be written as, } -\frac{1}{q} \frac{dJ_p}{dx} + \phi' \alpha e^{-\alpha x} - \frac{\Delta p}{\tau_p} = 0 \quad (2.31)$$

Here, $R(\lambda)$ is the reflection coefficient, $a(\lambda)$ is absorbance of thin metallic layer and $f(\lambda)$ is the probability that a photon will produce an electron hole pair. Φ indicates flux of photon striking the interface and ϕ' represents wavelength dependent pre factor.

DEPLETION REGION

In depletion region,

$$J_n = qn\mu_n E + qD_n \frac{dn}{dx}$$

$$J_p = qp\mu_p E - qD_p \frac{dp}{dx}$$

Then, using $J_T = J_n + J_p = 0$; the expression of electric field can be expressed as,

$$E = \frac{D_p \tau_p - D_n \tau_n}{(\mu_p \tau_p + \mu_n \tau_n) \Delta P} \frac{d\Delta p}{dx}$$

$$= \frac{A}{\Delta P} \frac{d\Delta P}{dx}$$

Where, constant, $A = \frac{D_p \tau_p - D_n \tau_n}{\mu_p \tau_p + \mu_n \tau_n}$

Then, by differentiating J_p it can be written as,

$$\frac{dJ_p}{dx} = (q\mu_p A - qD_p) \frac{d^2 \Delta p}{dx^2} \quad (2.32)$$

Using the relationship of equation (2.32) into equation (2.31), a second order non linear differential equation is found as,

$$\frac{d^2 \Delta P}{dx^2} - \frac{\Delta P}{D_p' \tau_p} = -\frac{\phi'}{D_p} \alpha e^{-\alpha x} \quad (2.33)$$

Solving this second order differential equation of equation (2.33) through ordinary differential equation solution method, a mathematical solution will be found for excess hole carrier concentration in depletion region. The mathematical solution of excess hole carrier concentration can be written as,

$$\Delta P(x) = C_1 e^{\frac{x}{L_p'}} + C_2 e^{-\frac{x}{L_p'}} - Q_1 e^{-\alpha x} \quad (2.34)$$

Here, L_p' is the diffusion length of minority carrier hole. Relation between L_p' , D_p and τ_p can be expressed as,

$$L_p' = \sqrt{D_p \tau_p}$$

In equation (2.35), A constant Q_1 is used. This constant can be represented as,

$$\text{constant, } Q_1 = \frac{\phi' \alpha \tau_p}{\alpha^2 L_p'^2 - 1}$$

Now excess hole concentrations can be evaluated in two boundary points of depletion region namely at $x=0$ and at $x=W$.

Excess hole concentration at point $x=0$ can be evaluated with help of equation (2.34) as,

$$\Delta P(0) = C_1 + C_2 - Q_1 \quad (2.35)$$

Similarly, Excess hole concentration at point $x=W$ can be evaluated with help of equation (2.34) as,

$$\Delta P(W) = C_1 e^{\frac{W}{L_p'}} + C_2 e^{-\frac{W}{L_p'}} - Q_1 e^{-\alpha W} \quad (2.36)$$

In equation (2.35) and (2.36), two unknown constants C_1 and C_2 are present. These two unknown constants will be evaluated later on.

NEUTRAL REGION

In neutral region,

By ignoring drift current the mathematical expression of hole current can be approximated as,

$$J_p \approx -q D_p \frac{d\Delta p}{dx}$$

Then, by differentiating J_p it can be written as,

$$\frac{dJ_p}{dx} = (-qD_p) \frac{d^2 \Delta p}{dx^2} \quad (2.37)$$

Using the relationship of equation (2.37) into equation (2.31), a second order non linear differential equation is found as,

$$\frac{d^2 \Delta P}{dx^2} - \frac{\Delta P}{D_p \tau_p} = \frac{\phi'}{D_p} \alpha e^{-\alpha x} \quad (2.38)$$

Solving this second order differential equation of equation (2.38) through ordinary differential equation solution method, a mathematical solution will be found for excess hole carrier concentration in neutral region. The mathematical solution of excess hole carrier concentration can be written as,

$$\Delta P(x) = C_3 e^{\frac{x}{L_p}} + C_4 e^{-\frac{x}{L_p}} - Q_2 e^{-\alpha x} \quad (2.39)$$

Here, L_p is the diffusion length of minority carrier hole. Relation between L_p , D_p and τ_p can be expressed as,

$$L_p = \sqrt{D_p \tau_p}$$

In equation (2.39), A constant Q_2 is used. This constant can be represented as,

$$Q_2 = \frac{\phi' \alpha \tau_p}{\alpha^2 L_p^2 - 1}$$

Now excess hole concentrations can be evaluated at $x=L$ of neutral region.

Excess hole concentration at point $x=L$ can be evaluated with help of equation (2.39) as,

$$\Delta P(L) = C_3 e^{\frac{L}{L_p}} + C_4 e^{-\frac{L}{L_p}} - Q_2 e^{-\alpha L} \quad (2.40)$$

In equation (2.40) two unknown constants C_3 and C_4 are present. These two unknown constants will be evaluated in next section.

2.2.8 Evaluation of unknown constants C_1, C_2, C_3 & C_4 Using proper boundary conditions

The constants of integrations C_1, C_2, C_3 & C_4 are to be evaluated by applying the boundary conditions at $x=0$, $x=W$ and $x=L$.

The boundary conditions are:

$$\Delta P(W)_{(\text{depletion region})} = \Delta P(W)_{(\text{neutral region})} \quad (2.41)$$

$$\frac{d\Delta p}{dx} \Big|_{(x=W(\text{Depletion region}))} = \frac{d\Delta p}{dx} \Big|_{(x=W(\text{neutral region}))} \quad (2.42)$$

$$D_p \frac{d\Delta p}{dx} \Big|_{x=0} = S_p \Delta p(0) \quad (2.43)$$

$$D_p \frac{d\Delta p}{dx} \Big|_{x=L} = S_p \Delta p(L) \quad (2.44)$$

Here, S_p is the effective surface recombination velocity.

Using boundary condition of equation (2.41) into equation (2.34) and (2.39),

$$C_1 e^{\frac{w}{L_p}} + C_2 e^{-\frac{w}{L_p}} - Q_1 e^{-\alpha w} = C_3 e^{\frac{w}{L_p}} + C_4 e^{-\frac{w}{L_p}} - Q_2 e^{-\alpha w} \quad (2.45)$$

Using boundary condition of equation (2.42), with help of equation (2.34) and (2.39) it can be written as,

$$C_1 e^{\frac{w}{L_p}} - C_2 e^{-\frac{w}{L_p}} + \alpha Q_1 L_p' e^{-\alpha w} = \frac{L_p'}{L_p} C_3 e^{\frac{w}{L_p}} - \frac{L_p'}{L_p} C_4 e^{-\frac{w}{L_p}} + \alpha L_p' Q_2 e^{-\alpha w} \quad (2.46)$$

Using equation (2.45) and (2.46), C_1 and C_2 can be expressed as function of unknown quantities C_3 and C_4 . These constants C_1 and C_2 can be expressed as,

$$C_1 = \frac{C_3 e^{\frac{w}{L_p}} \left(1 + \frac{L_p'}{L_p}\right) + C_4 e^{-\frac{w}{L_p}} \left(1 - \frac{L_p'}{L_p}\right) + (Q_2 - Q_1)(\alpha L_p' - 1) e^{-\alpha w}}{2 e^{\frac{w}{L_p}}} \quad (2.47)$$

$$C_2 = \frac{C_3 e^{\frac{w}{L_p}} \left(1 - \frac{L_p'}{L_p}\right) + C_4 e^{-\frac{w}{L_p}} \left(1 + \frac{L_p'}{L_p}\right) - (Q_2 - Q_1)(\alpha L_p' + 1) e^{-\alpha w}}{2 e^{-\frac{w}{L_p}}} \quad (2.48)$$

Using equation (2.43) into equation (2.35) and (2.36), A new equation can be obtained as,

$$C_1 \left(\frac{D_p'}{L_p} - S_p\right) + C_2 \left(-\frac{D_p'}{L_p} - S_p\right) = -Q_1 (\alpha D_p' + S_p) \quad (2.49)$$

Now putting the expressions obtained for C_1 and C_2 from equation (2.47) and (2.48) into equation (2.49), it can be obtained as,

$$C_3 e^{\frac{w}{L_p}} (X) + C_4 e^{-\frac{w}{L_p}} (Y) = -S_p Q_1 - D_p' Q_1 \alpha - \frac{b_1}{2} e^{-W(\alpha + \frac{1}{L_p})} \left[\frac{D_p'}{L_p} - S_p \right] (\alpha L_p' - 1) + \frac{b_1}{2} e^{-W(\alpha - \frac{1}{L_p})} \left[-\frac{D_p'}{L_p} - S_p \right] (\alpha L_p' + 1) \quad (2.50)$$

In equation (2.50) to remove representational complexity, we have used two constants X and Y to reduce complexity of representations.

Here,

$$X = \frac{\left(\frac{D_p'}{L_p} - S_p\right) \left(1 + \frac{L_p'}{L_p}\right)}{2 e^{\frac{w}{L_p}}} + \frac{\left(-\frac{D_p'}{L_p} - S_p\right) \left(1 - \frac{L_p'}{L_p}\right)}{2 e^{-\frac{w}{L_p}}}$$

$$\text{and } Y = \frac{\left(\frac{D_p'}{L_p} - S_p\right)\left(1 - \frac{L_p'}{L_p}\right)}{2e^{\frac{W}{L_p}}} + \frac{\left(-\frac{D_p'}{L_p} - S_p\right)\left(1 + \frac{L_p'}{L_p}\right)}{2e^{-\frac{W}{L_p}}}$$

Using equation (2.44) into equation (2.40) A new equation can be obtained as,

$$C_3\left(\frac{D_p}{L_p} - S_p\right)e^{\frac{L}{L_p}} + C_4\left(-\frac{D_p}{L_p} - S_p\right)e^{-\frac{L}{L_p}} = -Q_2(\alpha D_p + S_p)e^{-\alpha L} \quad (2.51)$$

After solving equations (2.50) and (2.51), the solution for C_3 and C_4 can be easily found out.

After obtaining expressions of unknown constants C_3 and C_4 in terms of known parameters, then by putting C_3 and C_4 into equation (2.47) and (2.48), C_1 and C_2 can easily be represented as functions of known parameters.

As all the unknown constants C_1 , C_2 , C_3 and C_4 are now expressed as function of known parameters, equation (2.35), (2.36) and (2.40) will help to find out mathematical expressions of excess charges as $\Delta P(0)$, $\Delta P(L)$ and $\Delta P(W)$.

After determination of excess charge concentrations in depletion and neutral region, the expression of Open circuit voltage from equation (2.25), (2.26) and (2.30) can be determined as functions of known parameters.

2.3 Mathematical expression of Open Circuit Voltage

Low injection

In this section, the assumptions will be made from the very beginning of the work and equation (2.26) will be tried to be tracked down to verify the Mathematical expression of open circuit voltage obtained previously.

Using equation (2.16), it can be rewritten as,

$$\begin{aligned} V(W) - V(0) &= -\int_0^W E_g(x) dx \\ &= -\int_0^W \frac{D_p \frac{d\Delta p(x)}{dx} - D_n \frac{d\Delta n(x)}{dx}}{(n_0 + \Delta n(x))\mu_n + (p_0 + \Delta p(x))\mu_p} dx + \int_0^W \frac{(\Delta n(x)\mu_n + \Delta p(x)\mu_p)E_b(x)}{(n_0 + \Delta n(x))\mu_n + (p_0 + \Delta p(x))\mu_p} dx \end{aligned}$$

Using strong illumination condition and considering the assumption of low level injection

$$n_0(x), p_0(x) \ll \Delta n(x), \Delta p(x)$$

Open circuit voltage in depletion region for low level injection can be evaluated after performing necessary integrations as,

$$V(W)-V(0)=-\frac{(D_p-D_n\frac{\tau_n}{\tau_p})}{(\frac{\tau_n}{\tau_p}\mu_n+\mu_p)} \ln\left\{\frac{\Delta p(W)}{\Delta p(0)}\right\}-\phi_s \quad (2.52)$$

Where, $\phi_s = \frac{1}{2} \frac{qN_d W^2}{\epsilon_s}$.

For determining open circuit voltage in neutral region the following assumption can be used.

$$\Delta n, \Delta p \ll N_d \gg \frac{n_i^2}{N_d}$$

Then equation (2.23) can be modified as,

$$E_g(x) = \frac{D_p - D_n \frac{\tau_n}{\tau_p}}{N_d \mu_n} \frac{d\Delta p}{dx} \quad (2.53)$$

By performing integration of equation (2.53) in neutral region, the open circuit voltage for low level of injection in neutral region can be obtained as,

$$V(L)-V(W) = -\left(\frac{D_p - D_n \frac{\tau_n}{\tau_p}}{N_d \mu_n}\right) [\Delta p(L) - \Delta p(W)] \quad (2.54)$$

By adding equation (2.52) and (2.54), An expression of open circuit voltage for low level of injection can be found and the result tracks down equation (2.26).

High level injection

In this section, the assumptions will be made from the very beginning of the work and equation (2.30) will be tried to be tracked down to verify the Mathematical expression of open circuit voltage for high level injection obtained previously.

Using equation (2.16), it can be rewritten as,

$$\begin{aligned} V(W)-V(0) &= -\int_0^W E_g(x) dx \\ &= -\int_0^W \frac{D_p \frac{d\Delta p(x)}{dx} - D_n \frac{d\Delta n(x)}{dx}}{(n_0 + \Delta n(x))\mu_n + (p_0 + \Delta p(x))\mu_p} dx + \int_0^W \frac{(\Delta n(x)\mu_n + \Delta p(x)\mu_p) E_b(x)}{(n_0 + \Delta n(x))\mu_n + (p_0 + \Delta p(x))\mu_p} dx \end{aligned}$$

Using strong illumination condition and considering the assumption of high level injection

$$n_0(x), p_0(x) \ll \Delta n(x), \Delta p(x)$$

Open circuit voltage in depletion region for high level injection can be evaluated after performing necessary integrations as,

$$V(W)-V(0) = -\frac{(D_p - D_n \frac{\tau_n}{\tau_p})}{(\frac{\tau_n}{\tau_p}\mu_n + \mu_p)} \ln\left\{\frac{\Delta p(W)}{\Delta p(0)}\right\} - \phi_s \quad (2.55)$$

Where, $\phi_s = \frac{1}{2} \frac{qN_d W^2}{\epsilon_s}$.

For determining open circuit voltage in neutral region the following assumption can be used.

$$\Delta n, \Delta p \gg N_d \gg \frac{n_i^2}{N_d}$$

Then equation (2.23) can be modified as,

$$E_g(x) = - \frac{D_p - D_n \frac{\tau_n}{\tau_p}}{\Delta p (\mu_p + \mu_n \frac{\tau_n}{\tau_p})} \frac{d\Delta p}{dx} \quad (2.56)$$

By performing integration of equation (2.56) in neutral region, the open circuit voltage for high level of injection in neutral region can be obtained as,

$$V(L) - V(W) = - \left(\frac{-D_p + D_n \frac{\tau_n}{\tau_p}}{(\mu_p + \mu_n \frac{\tau_n}{\tau_p})} \right) \ln \left\{ \frac{\Delta p(L)}{\Delta p(W)} \right\} \quad (2.57)$$

By adding equation (2.55) and (2.57), An expression of open circuit voltage for low level of injection can be found and the result tracks down equation (2.30).

As the mathematical expressions of open circuit voltage for the special case of low and high level injection are tracked down in sections 2.3 and 2.4, the determination of excess charge concentrations and unknown constants will follow the same path of process followed in section 2.2.8.

2.4 Conclusions

In this chapter, Analytical modeling of open circuit voltage of SB Solar Cell for all levels of injection has been performed. Mathematical expression of open circuit voltage for all level of injection has been obtained. In the mathematical expression excess hole carrier concentrations at different regions are solved by solving second order non linear differential equations. Later, Unknown constants of excess hole concentrations are evaluated by applying proper boundary conditions. The Open circuit voltage expression is also obtained for special case of low and high levels of injections from the main mathematical representation by applying necessary assumptions. In the end, the mathematical expression of low and high level of injection are verified by using the necessary assumptions from very beginning of modeling and tracking down the mathematical expressions obtained previously by general expression.

In the next chapter, the variation of Open circuit voltage will be explored as function of various parameters like doping concentrations, effective surface recombination velocity, length of the semiconductor region, metal work functions under different levels of injection. The necessary plots and discussions will try to explain the findings.

Chapter 3

RESULTS AND DISCUSSIONS

3.1 Introduction

In the previous chapter, mathematical expression for analytical modeling of Open circuit voltage of Schottky barrier (SB) Solar cell for all levels of injection has been obtained.

In this chapter, the characteristic plots of open circuit voltage for various combination of metal-semiconductor have been obtained. Different parameters like doping density, metal work function, effective surface recombination velocity, length of Semiconductors have been varied around practical ranges to study the open voltage circuit characteristics of SB Solar Cell.

3.2 Open Circuit Voltage as a function of doping concentrations for various metal-semiconductor combinations of SB Solar Cell

Here, Different Characteristic Plots have been obtained for a range of Doping concentrations ($10^{14} \text{ cm}^{-3} \leq N_d \leq 10^{17} \text{ cm}^{-3}$). Different metals are also used to obtain different V_{oc} plots in this doping range. The photon flux is considered to be $\phi = 2 \times 10^{17} \text{ cm}^{-2} \text{ s}^{-1}$ for all the cases discussed here and surface recombination velocity (S_{eff}) of 200 cm/s is considered. Absorption coefficient at $\lambda = 550 \text{ nm}$ is considered as 10^4 cm^{-1} .

In this section Si is used as semiconductor and various metals like Sn, W, Cu, Rh, Pd are used.

Metals	Work function in eV
Sn	4.42
W	4.55
Cu	4.65
Rh	4.98
Pd	5.12

Table 3.1. Work function of different metals

The Electron affinity of n-Si is 4.05eV and room temperature band gap is 1.12eV.

3.2.1 Effect of doping concentrations on Open Circuit Voltage for all levels of injection (metal- n Si Semiconductor)

Variation of open circuit voltage (V_{OC}) as a function of doping concentration (N_d) for five different metals is plotted in Figure 3.1.

Figure 3.1 shows that V_{oc} increases with N_d . For a given N_d , V_{oc} increases with metal work function. As N_d increases, the depletion region width decreases. As a result electric field becomes stronger in that region. So with the increase of electric field it becomes easier for photo generated holes to drift from n-type semiconductor to metal side and electrons from metal to n-type semiconductor side. As a result of increasing pile up of photo generated electrons and holes in those two regions of metal and semiconductor adjacent to depletion layer, V_{OC} increases with increasing doping concentrations.

Mathematically this phenomenon can be explained as the following equation:

$$V_{oc} = \phi_B + \ln(J_{sc}/A * T^2) \quad (3.1)$$

With increase of N_d , depletion width decreases and as a result the value of short circuit current (J_{SC}) increases. With increase of J_{SC} , V_{oc} increases.

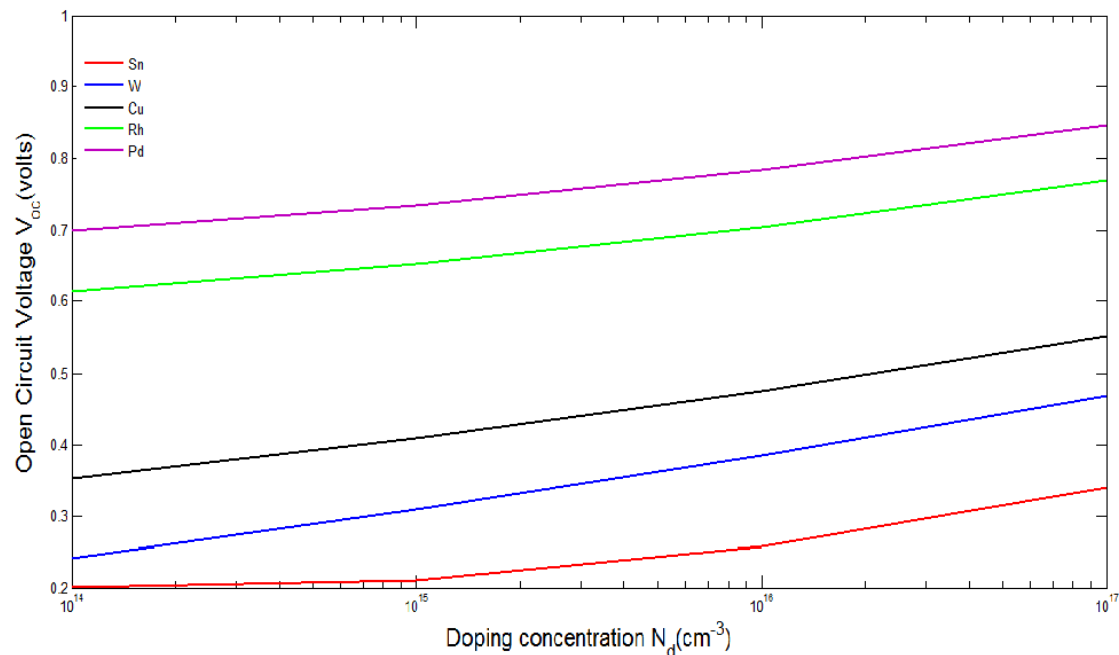


Figure 3.1. Variation of Open Circuit Voltage with doping concentration for different metal-n Si combinations for all levels of injection

Changing metals according to metal work function also affect V_{OC} . With increase of metal work function, V_{OC} increases. The reason is that increase of metal work function means increase of barrier height. But the holes move from n-Si to metal and electrons move from metal to n-Si. Due to their opposite direction of movement actually barrier works as sink for electrons and holes. So it has become easier for photo generated electrons and holes to accumulate at opposite sides and increase V_{OC} .

3.2.2 Effect of doping concentrations on Open Circuit Voltage for low level of injection (metal-n Si Semiconductor)

In the following figure 3.2, the variation of open circuit voltage (V_{OC}) is obtained as a function of doping concentration (N_d). Here Si is used as Semiconductor and Sn, W, Cu, Rh, Pd are used as metals. We have considered low level of injection in this regard.

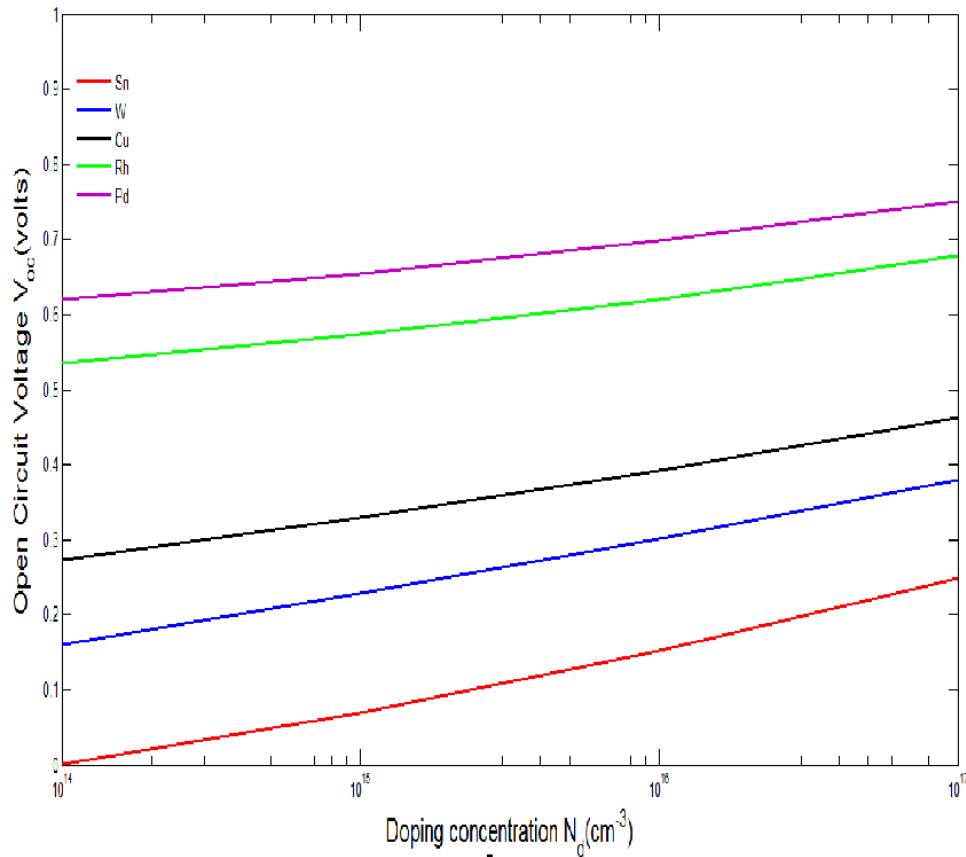


Figure 3.2. Variation of Open Circuit Voltage with doping concentration for different metal-n Si combinations for low level of injection

Due to low level of injections the rate of photo generated excess electron and hole concentrations are considered very much lower than doping concentration (N_d). As a result of lower rate of generation of electron-hole pairs, V_{OC} will certainly be of lower value compared to all level injection discussed in section 3.2.1. But the value of V_{OC} will increase with increasing N_d and increasing metal work function. As it has been previously explained in section 3.2.1 that increased doping makes higher electric field and accumulation of charge becomes much greater and so V_{OC} increases. Increased metal work function means higher height of sink for electrons and holes and accumulation becomes greater and V_{OC} increases.

3.2.3 Effect of doping concentrations on Open Circuit Voltage for high level of injection (metal-n Si Semiconductor)

In the following figure 3.3, variation of open circuit voltage (V_{OC}) is obtained as a function of doping concentration (N_d). Here Si is used as Semiconductor and Sn, W, Cu, Rh, Pd are used as metals. We have considered high level of injection in this regard.

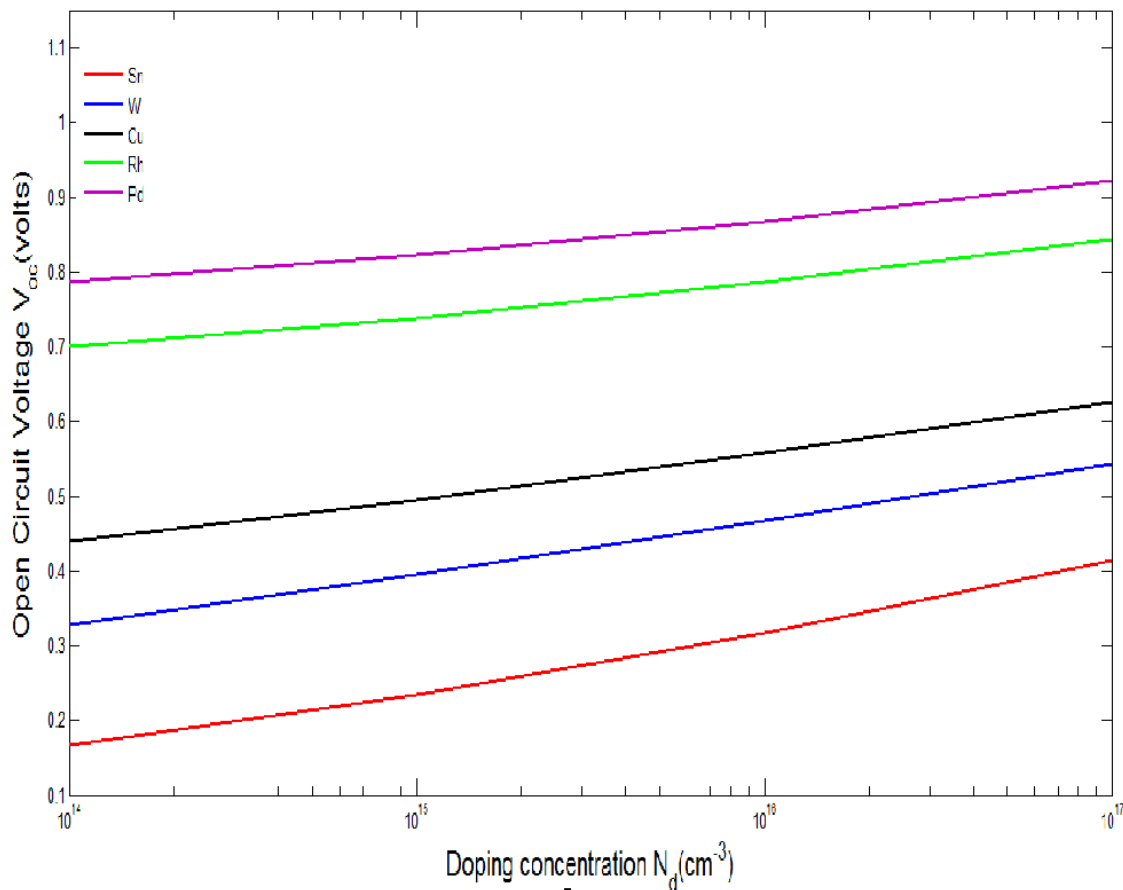


Figure 3.3. Variation of Open Circuit Voltage with doping concentration for different metal-n Si combinations for high level of injection

Due to high level of injections the rate of photo generated excess electron and hole concentrations are considered very much higher than doping concentration (N_d). As a result of higher rate of generation of electron-hole pairs, V_{OC} will certainly be of higher value compared to all level and low level injection. But the value of V_{OC} will increase with increasing N_d and increasing metal work function. As it has been previously explained in section 3.2.1 that increased N_d makes higher electric field and accumulation of charge becomes much greater and so V_{OC} increases. Increased metal work function means higher height of sink for electrons and holes and accumulation becomes greater and V_{OC} increases.

3.2.4 Effect of doping concentrations on Open Circuit Voltage for all levels of injection (metal-n GaAs Semiconductor)

The main difference between the previous case of n-Si semiconductor (discussed in section 3.2.1, 3.2.2 and 3.2.3) is that in this case of using n-GaAs as semiconductor layer, the value of Electron affinity and bandgap changes. In this case of n-GaAs, the value of Electron affinity is 4.07eV and bandgap is 1.42eV.

In the following figure 3.4, variation of open circuit voltage (V_{OC}) is obtained as a function of doping concentration (N_d). Here GaAs is used as Semiconductor and Sn, W, Cu, Rh, Pd are used as metals. We have considered all level of injection in this regard.

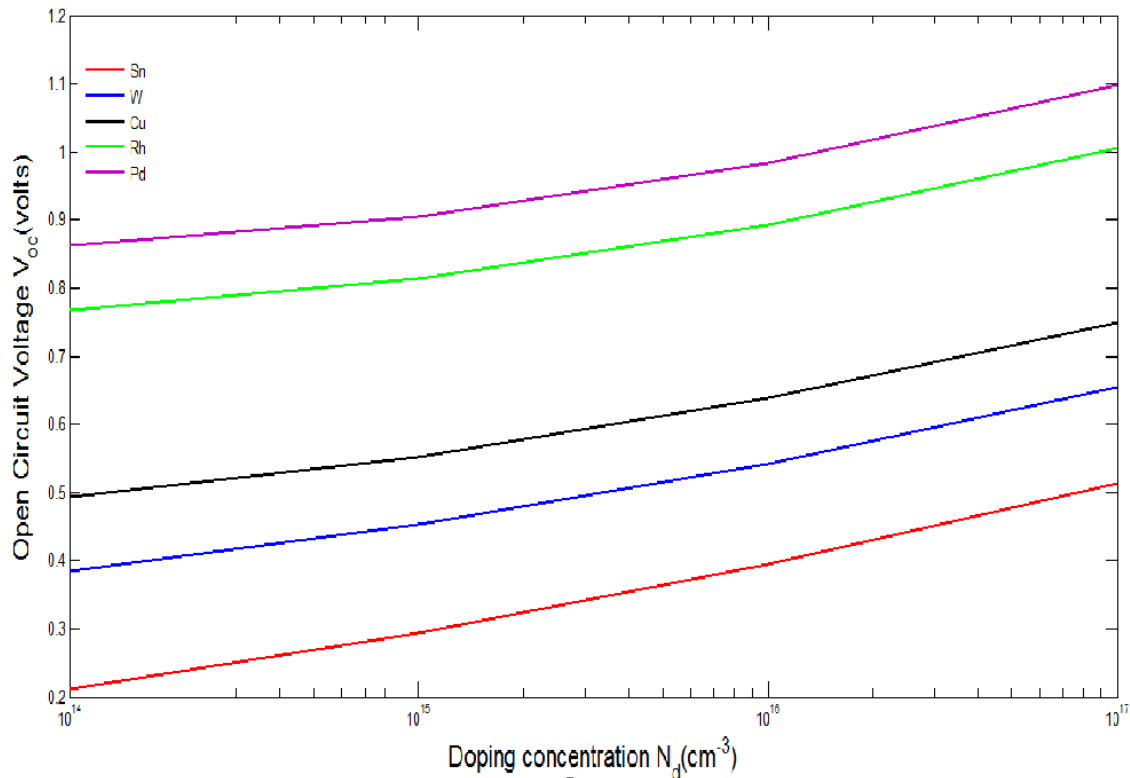


Figure 3.4. Variation of Open Circuit Voltage with doping concentration for different metal-n GaAs combinations for all levels of injection

In this figure, V_{OC} is greater compared with previous case of n-Si metal SB Solar Cell. While using n-GaAs as semiconductor, increase of electron affinity and increase of bandgap leads to increased V_{OC} . Decrease in effective density of states in conduction and valence band leads to decrease of energy gap between conduction band and Fermi level. As a result, although Schottky barrier decreases due to increased electron affinity, built in potential barrier increases because of lower gap between conduction band and Fermi level. But the barrier basically acts as sink due to reverse movement of carriers, as a result V_{OC} increases.

As it has been previously explained in section 3.2.1 that increased doping makes higher electric field and accumulation of charge becomes much greater and so V_{OC} increases. Increased metal work function means higher height of sink for electrons and holes and accumulation becomes greater and V_{OC} increases.

3.2.5 Effect of doping concentrations on Open Circuit Voltage for low level of injection (n-GaAs Semiconductor)

In the following figure 3.5, variation of open circuit voltage is obtained as a function of doping concentration. Here GaAs is used as Semiconductor and Sn, W, Cu, Rh, Pd are used as metals. We have considered low level of injection in this regard.

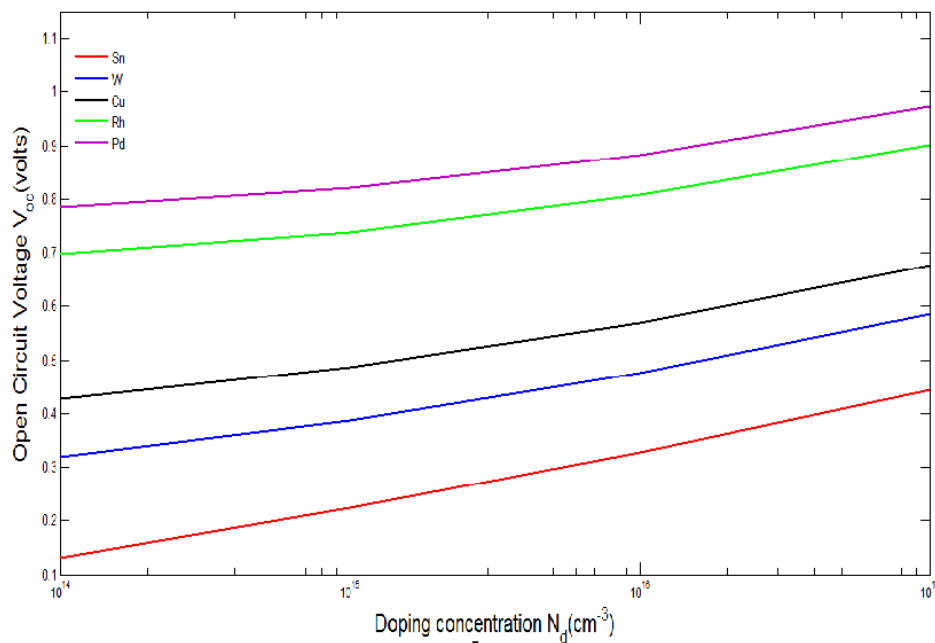


Figure 3.5. Variation of Open Circuit Voltage with doping concentration for different metal-n GaAs combinations for low level of injection

Due to low level of injections the rate of photo generated excess electron and hole concentrations are considered very much lower than doping concentration (N_d). As a result of lower rate of generation of electron-hole pairs, V_{OC} will certainly be of lower value compared to all level injection. But the value of V_{OC} will increase with increasing doping concentration and increasing metal work function. Using n-GaAs as semiconductor in this case, increase of electron affinity and increase of bandgap leads to increased V_{OC} than compared with figure 3.2. As it has been previously explained in section 3.2.1 that increased doping makes higher electric field and accumulation of charge becomes much greater and so V_{OC} increases. Increased metal work function means higher height of sink for electrons and holes and accumulation becomes greater and V_{OC} increases.

3.2.6 Effect of Doping concentrations on Open Circuit Voltage for high level of injection (n-GaAs Semiconductor)

In the following figure 3.6, variation of open circuit voltage is obtained as a function of doping concentration. Here GaAs is used as Semiconductor and Sn, W, Cu, Rh, Pd are used as metals. We have considered high level of injection in this regard.

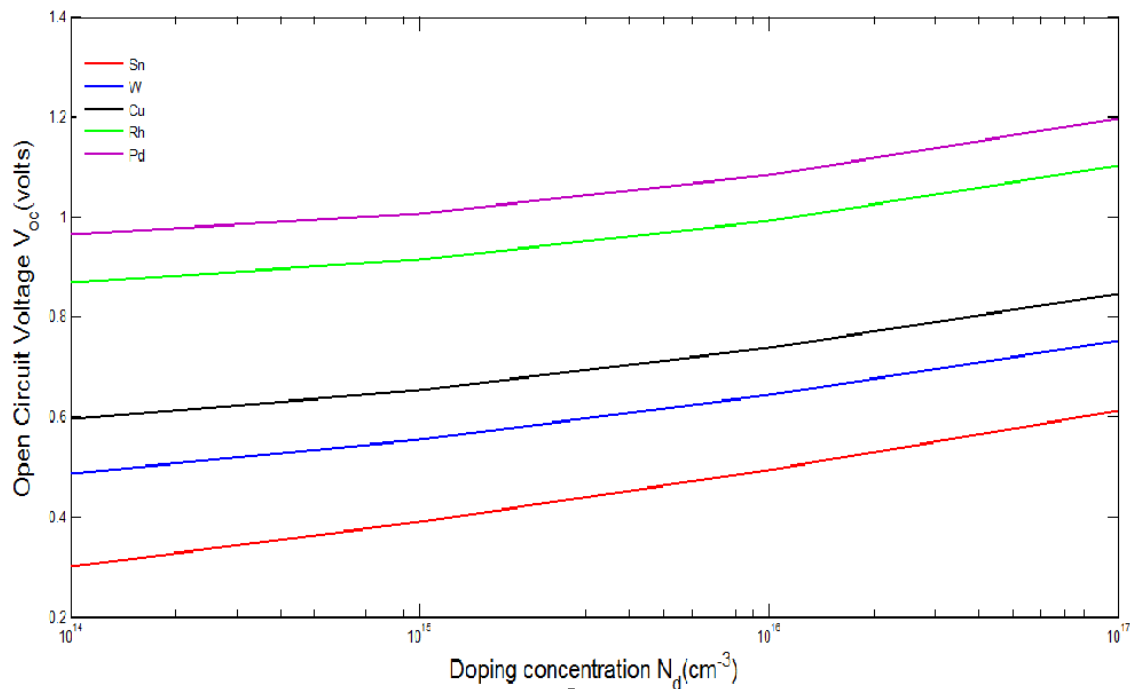


Figure 3.6. Variation of Open Circuit Voltage with doping concentration for different metal-n GaAs combinations for high level of injection

Due to high level of injections the rate of photo generated excess electrons and holes are considered very much higher than doping concentration. As a result of higher rate of generation of electron-hole pairs, V_{OC} will certainly be of higher value compared to all level and low level injection. But the value of V_{OC} will increase with increasing doping concentration and increasing metal work function. As it has been previously explained in section 3.2.1 that increased doping makes higher electric field and accumulation of charge becomes much greater and so V_{OC} increases. Increased metal work function means higher height of sink for electrons and holes and accumulation becomes greater and V_{OC} increases.

3.3 Effect of metal work function at the metal-semiconductor interface on Open circuit voltage for different levels of injections

In the following figures 3.7-3.8, we have compared all, low and high levels of injections at metal-n Si interface and metal- GaAs interface for different metal work functions. In these cases, we have considered doping concentration $N_d=10^{14}\text{cm}^{-3}$ and the photon flux is considered to be $\phi=2\times 10^{17}\text{cm}^{-2}\text{s}^{-1}$ for all the cases discussed here and recombination velocity of 200 cm/s is considered. Absorption coefficient at $\lambda=550\text{nm}$ is considered as 10^4cm^{-1} .

3.3.1 Effect of metal work function at the metal-n-Si semiconductor interface on Open circuit voltage for different levels of injections

In the following figure 3.7, we have compared all, low and high levels of injections at metal-n Si interface for different metal work functions.

In this figure 3.7, all, low and high level of injection is compared with variation of metal work function. With increase of metal work function, V_{OC} increases. The reason is that increase of metal work function means increase of barrier height. But the holes move from n-Si to metal and electrons move from metal to n-Si. Due to their direction of movement actually the barrier acts as sink for electrons and holes. As a result it has become easier for photo generated electrons and holes to accumulate at opposite sides and increase V_{OC} . In the case of low level injection, due to lower carrier concentration of photo generated electron hole pairs compared to doping density, V_{OC} decreases as there is less accumulation of electron hole pairs. On the other hand in case of high level of injection due to increased concentration of photo generated electron hole pairs compared to doping, V_{OC} increases than all and low level of injection.

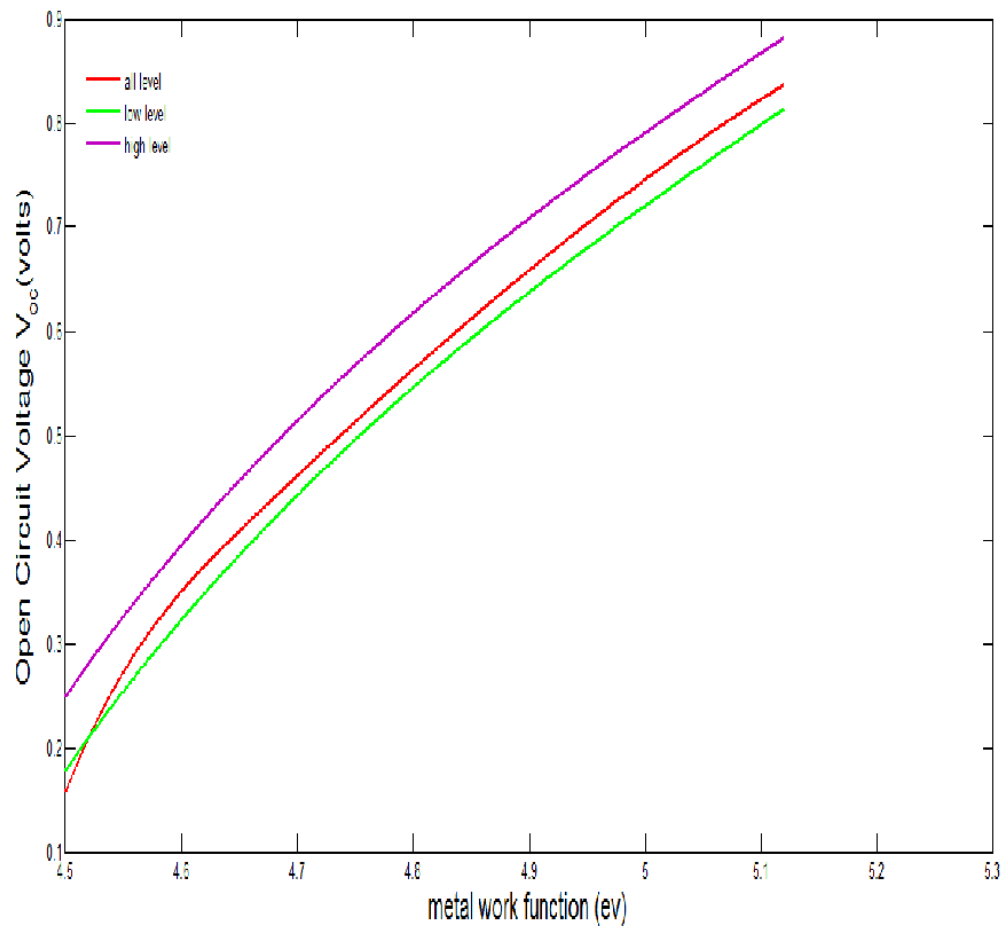


Figure 3.7. Effect of different levels of injections on Open circuit voltage for various metal work functions for different metal-n Si SB Solar Cell

3.3.2 Effect of metal work function at the metal-n-GaAs semiconductor interface on Open circuit voltage for different levels of injections

In the following figure 3.8, we have compared all, low and high levels of injections at metal-n GaAs interface for different metal work functions.

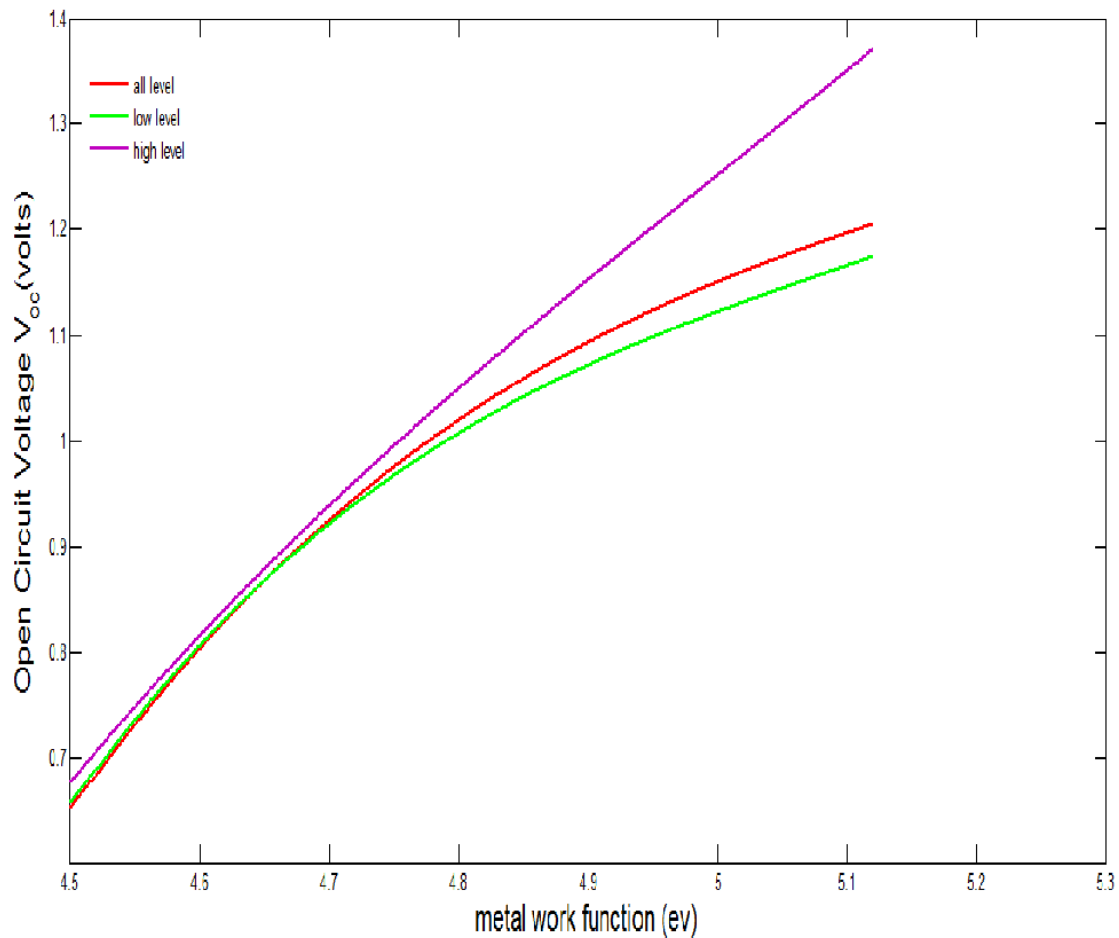


Figure 3.8. Effect of different levels of injections on Open circuit voltage for various metal work functions for different metal-n GaAs SB Solar Cell

In this figure, all, low and high level of injection is compared with variation of metal work function. The values obtained for V_{OC} for this case of using n-GaAs as semiconductor, increase in comparison with the previous case of using n-Si semiconductor. , increase of electron affinity and increase of bandgap leads to increased V_{OC} . Decrease in effective density of states in conduction and valence band leads to decrease of energy gap between conduction band and Fermi level. As a result, although Schottky barrier decreases due to increased electron affinity, built in potential barrier increases because of lower gap between conduction band and Fermi level. But the barrier basically acts as sink due to reverse movement of carriers, as a result V_{OC} increases.

3.4 Effect of surface recombination velocity on open circuit voltage for SB Solar Cell

In the following figures 3.9-3.11, we will compare all, low and high levels of injections at metal-n Si interface for a range of effective surface recombination velocity (S_{eff}). In these cases, we have considered doping concentration $N_d=10^{14} \text{cm}^{-3}$ and the photon flux is considered to be $\phi^i=2 \times 10^{17} \text{cm}^{-2}\text{s}^{-1}$ for all the cases discussed here. Absorption coefficient at $\lambda=550 \text{nm}$ is considered as 10^4cm^{-1} .

Due to increase of effective surface recombination velocity, the rate of recombination will increase. As a result the photo generated electron-hole pairs will recombine and so the amount of short circuit current will decrease. The decrease of the short circuit current will lead to the decrease of open circuit voltage according to the following formula:

$$V_{oc} = \phi_B + \ln(J_{sc}/A * T^2)$$

3.4.1 Effect of surface recombination velocity on open circuit voltage for metal-n Si combinations considering all levels of injection

Here in figure 3.9, Open circuit voltage characteristic is obtained for different metal-n Si combinations with increase of effective surface recombination velocity, the value of open circuit voltage decreases slightly. Here all level of injection is considered.

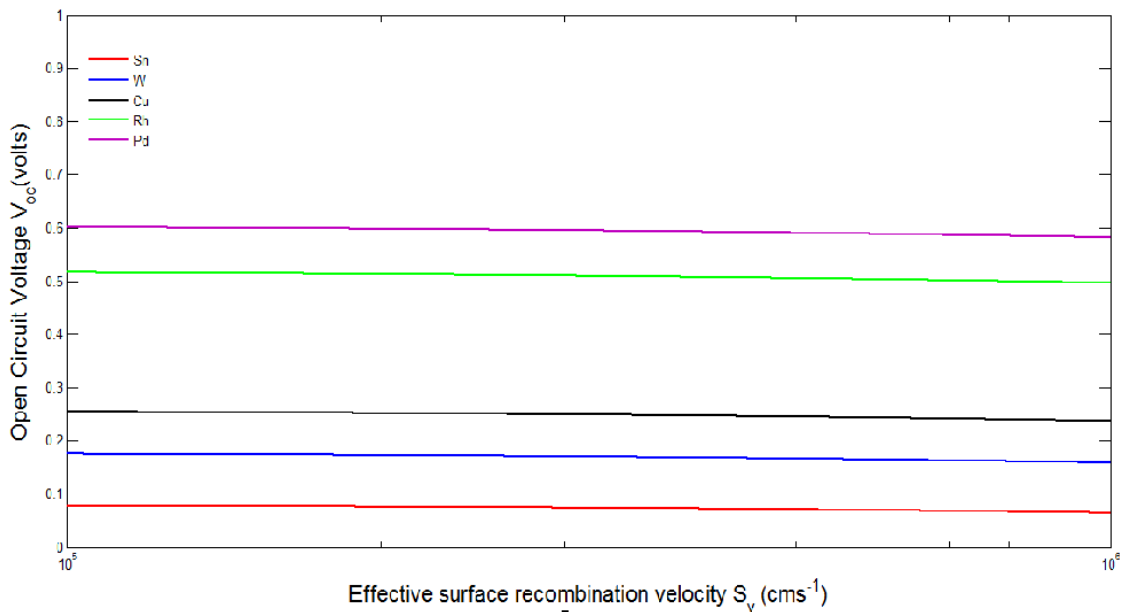


Figure 3.9. Open circuit voltage characteristics with variation of effective surface recombination velocity for all levels of injections for metal-n Si Solar cell

Increase in effective surface recombination velocity leads to increased rate of recombination of electron-hole pairs. As a result, the amount of short circuit current will decrease. According to the equation (3.1), Open circuit voltage V_{OC} will decrease. Here, V_{OC} decreases slightly as dependency is weak. The reason of weak dependency is that the mathematical terms represent effective surface recombination inside logarithmic term.

3.4.2 Effect of surface recombination velocity on Open circuit voltage for metal-n Si combinations considering low level of injection

Here in figure 3.10, Open circuit voltage characteristic is obtained for different metal-n Si combinations with increase of effective surface recombination velocity, the value of open circuit voltage decreases slightly. We have considered low level of injection in this regard.

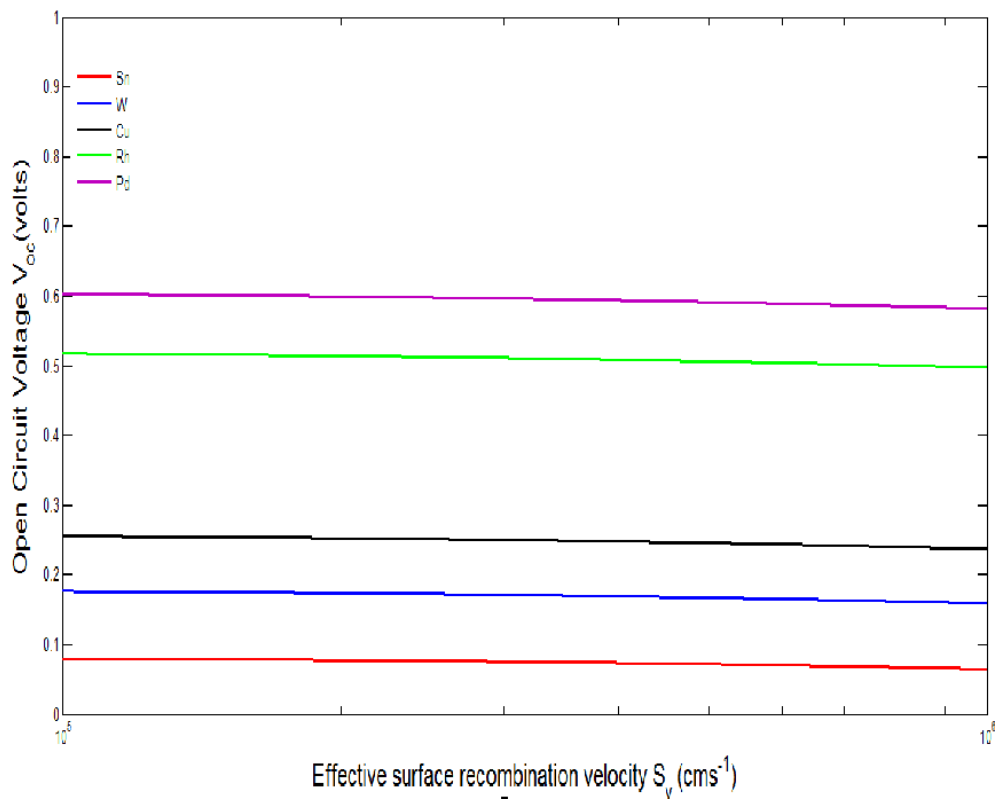


Figure 3.10. Open circuit voltage characteristics with variation of effective surface recombination velocity for low level of injection for metal-n Si Solar cell

In this case of low level of injection, excess charge concentration is negligible compared with doping concentration. In the expansion of mathematical terms for low level of injection, both excess charge carrier terms are present like the mathematical expression of all level injection. As a result, the result for variation of effective surface recombination velocity is tractable with previous result of figure 3.9.

3.4.3 Effect of surface recombination velocity on open circuit voltage for metal-n Si combinations considering high level of injection

Here in figure 3.11, Open circuit voltage characteristic is obtained for different metal-n Si combinations with increase of effective surface recombination velocity, the value of open circuit voltage increases slightly. We have considered high level of injection in this regard.

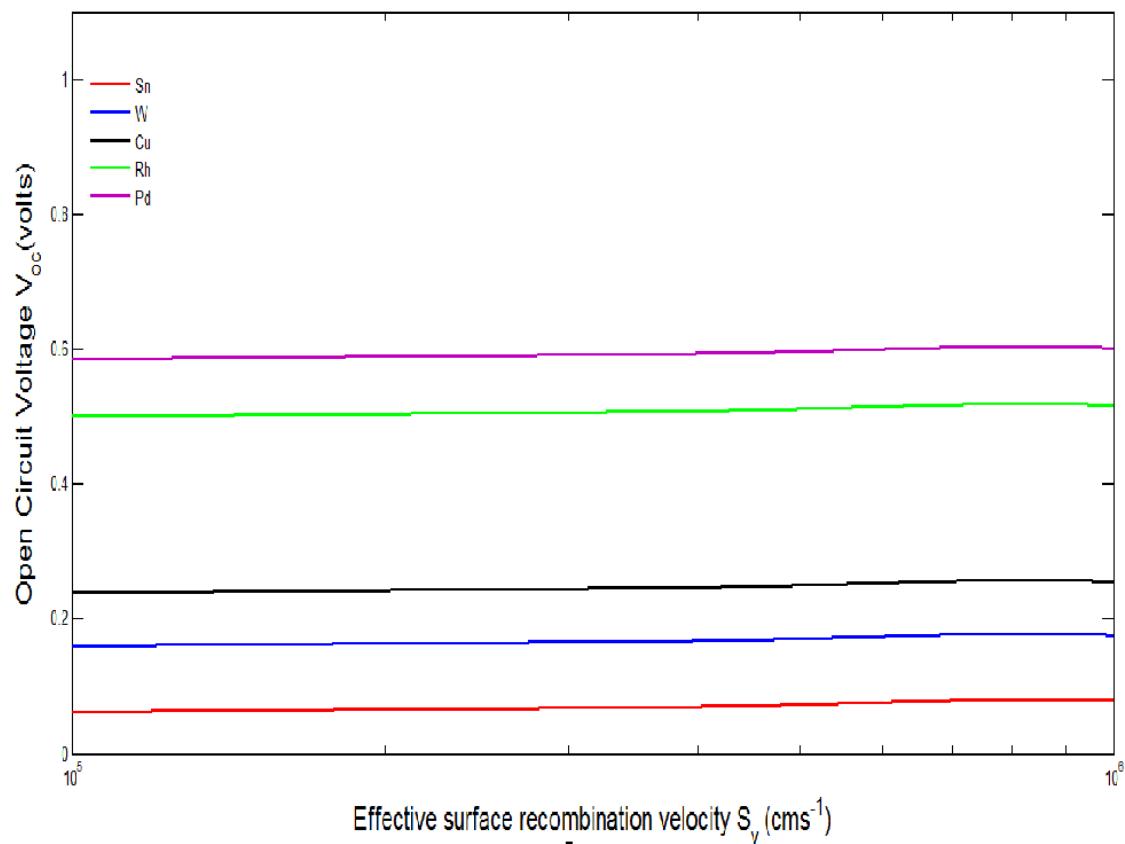


Figure 3.11. Open circuit voltage characteristics with variation of effective surface recombination velocity for high level of injection for metal-n Si Solar cell

In this case of high level of injection, excess charge concentration is negligible compared with doping concentration. In the expansion of mathematical terms for high level of injection, both excess charge carrier terms are present like the mathematical expression of all level and low level of injection. As a result, the result for variation of effective surface recombination velocity is tractable with previous result of figure 3.9-3.10.

3.5 Effect of the semiconductor thickness on Open circuit voltage

In the following figures 3.12-3.15, we have compared all, low and high levels of injections at metal-n Si interface over a range of semiconductor thickness for different metal work functions. In these cases, we have considered doping concentration $N_d=10^{14}\text{cm}^{-3}$ and the photon flux is considered to be $\phi=2\times 10^{17}\text{cm}^{-2}\text{s}^{-1}$ for all the cases discussed here and recombination velocity of 200 cm/s is considered. Absorption coefficient at $\lambda=550\text{nm}$ is considered as 10^4cm^{-1} .

3.5.1 Effect of the semiconductor thickness on Open circuit voltage considering all levels of injections for metal n-Si semiconductor SB Solar Cell

In the following figure 3.12, Different metal-n Si semiconductor SB Solar cell open circuit voltage characteristic have been studied considering all levels of injection.

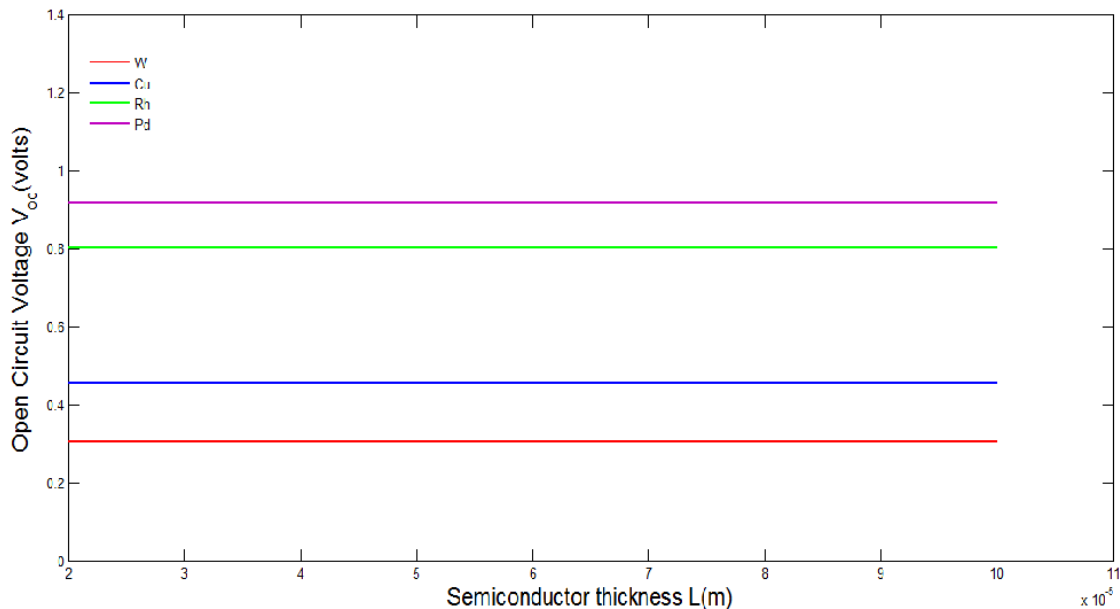


Figure 3.12. Effect of semiconductor thickness on Open circuit voltage for all levels of injections for different metal-n Si Solar cell

In this case of all level of injection, thickness of the semiconductor layer does not cause any change in open circuit voltage. The reason is that increase in length does not imply any significant change in photo generated electron hole pairs. Only the excess charge concentration in neutral end point depends exponentially on length but its contribution is negligible and as a result V_{OC} does not vary with L .

With increase of metal work function, V_{OC} increases but remains constant over L . increase in metal work function makes the height of sink for electrons and holes higher and as a result short circuit current density increases and so V_{OC} increases according to equation(3.1).

3.5.2 Effect of the semiconductor thickness on Open circuit voltage considering low level of injection for metal n-Si semiconductor SB Solar Cell

Here, in figure 3.13, effect of semiconductor thickness is taken into account by considering low level injection.

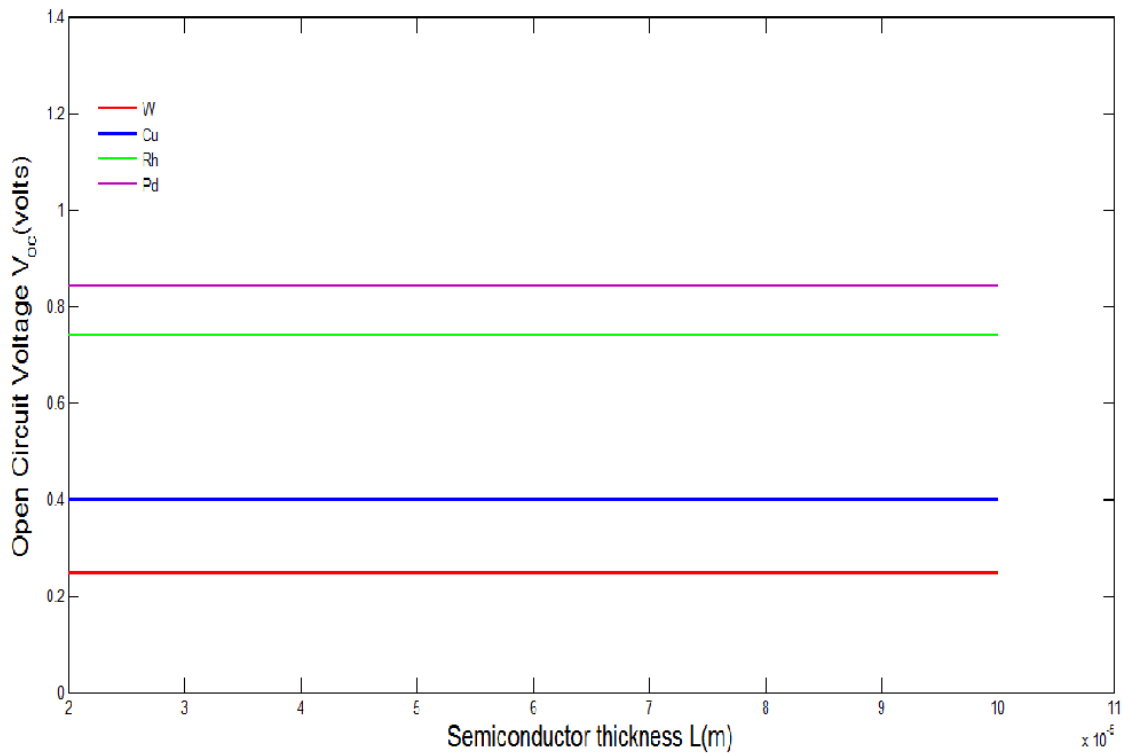


Figure 3.13. Effect of semiconductor thickness on Open circuit voltage for low level of injection for different metal-n Si Solar cell

In this case of low level of injection, presence of excess charge concentration in neutral end point is tractable with the mathematical equation for all level of injection. As a result like previous case of all level injection the contribution of excess carrier concentration is negligible because of exponential dependency on length and as a result there is no variation with L .

3.5.3 Effect of the semiconductor thickness on Open circuit voltage considering high level of injection for metal n-Si semiconductor SB Solar Cell

Here, in figure 3.14, it has been observed that open circuit voltage increases slightly with increase of length.

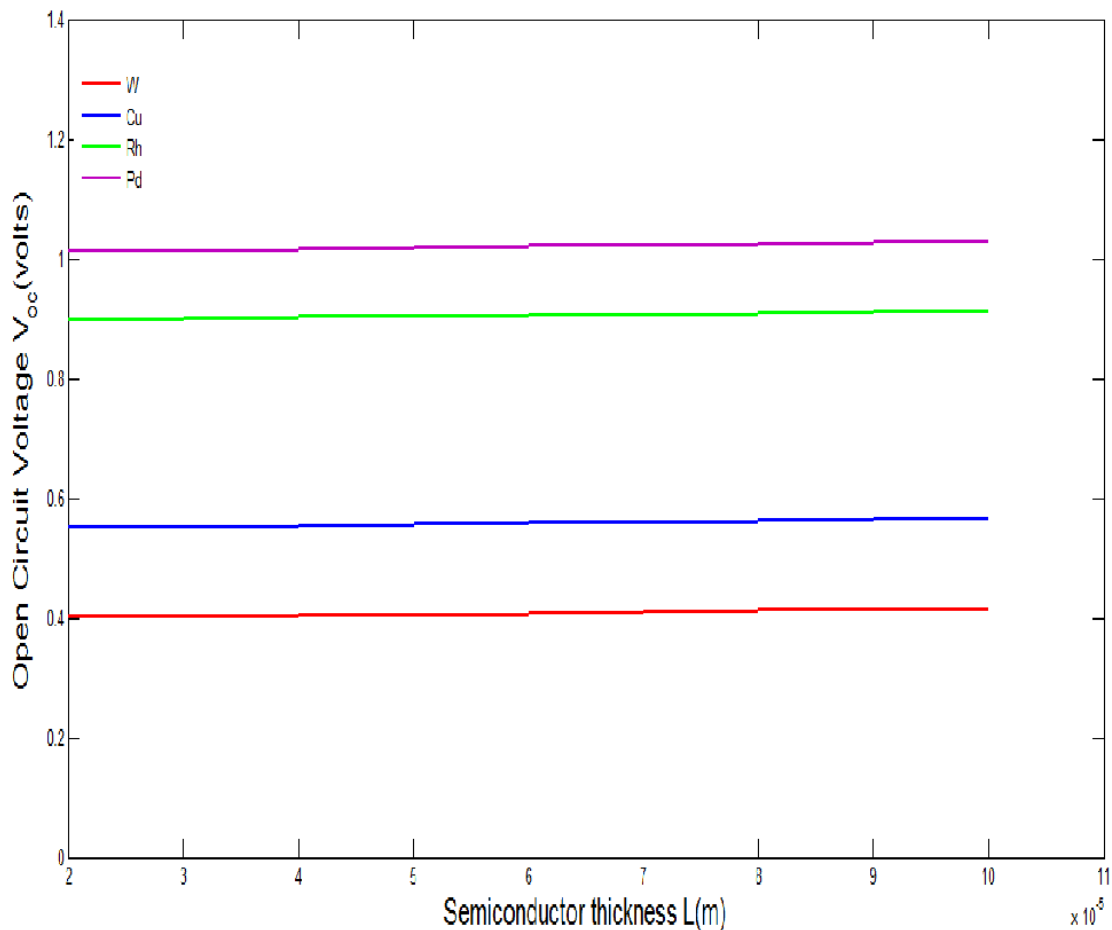


Figure 3.14. Effect of semiconductor thickness on Open circuit voltage for high level of injection for different metal-n Si Solar cell

In the case of high level of injection, slight increase of open circuit voltage V_{OC} is visible with increase over length. In this case, excess charge carrier concentration is considered very much higher than doping concentration and as a result of exponential dependency on length L , slight increase in V_{OC} is observable.

3.5.4 Comparison of low level and high level of injection by studying the effect of thickness on Open circuit voltage for metal-n Si SB Solar cell

In the following figure 3.15, low level and high level of injection have been considered for W-Si and Cu-Si SB Solar Cell.

The comparison shows the gradually increasing characteristic plot of open circuit voltage in the case of high level injection and literally constant open circuit voltage characteristic for low level of injection.

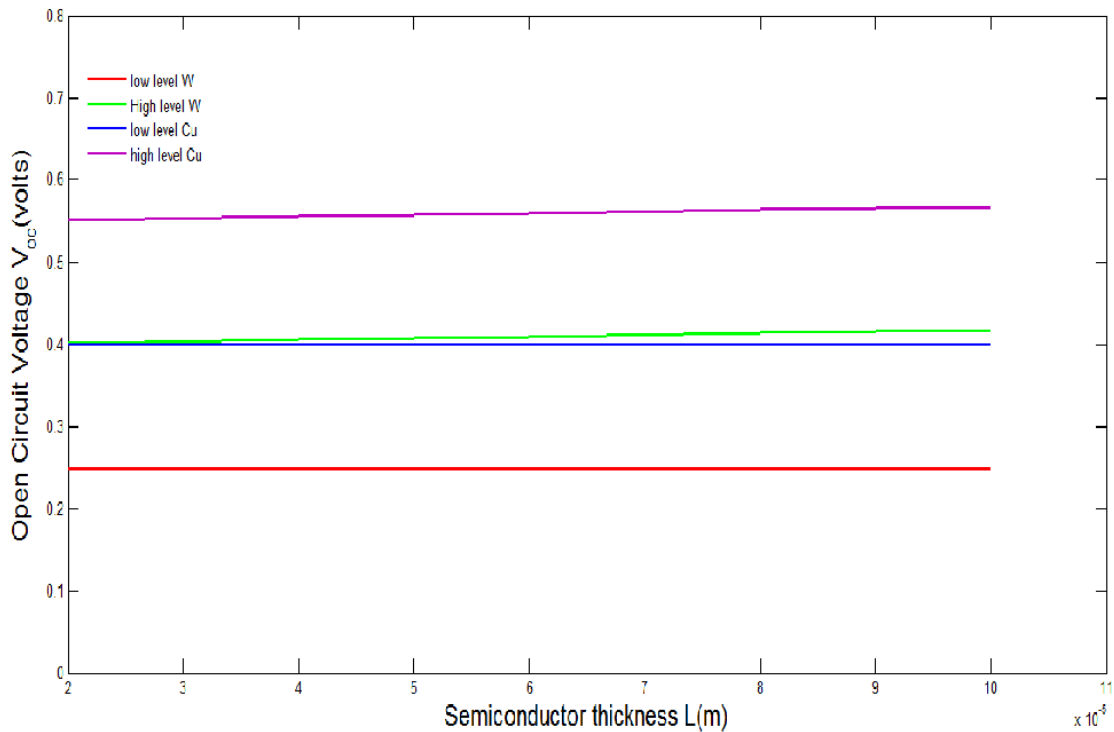


Figure 3.15. Comparison of Open circuit voltage variation on Semiconductor thickness for both low level and high level injection

3.5.5 Effect of the semiconductor thickness on Open circuit voltage considering all levels of injections for metal n-GaAs semiconductor SB Solar Cell

In the following figure 3.16 , Different metal-n GaAs semiconductor SB Solar cell open circuit voltage characteristic have been studied considering all levels of injection.

Because of changing of semiconductor from Si to GaAs; the increased value of bandgap and electron affinity ultimately leads to increased value of open circuit voltage in this case compared with the case of using Si as Semiconductor.

Thickness of the semiconductor layer does not cause any change in open circuit voltage. Only the excess charge concentration in neutral end point depends exponentially on length but its contribution is negligible and as a result V_{OC} does not vary with L .

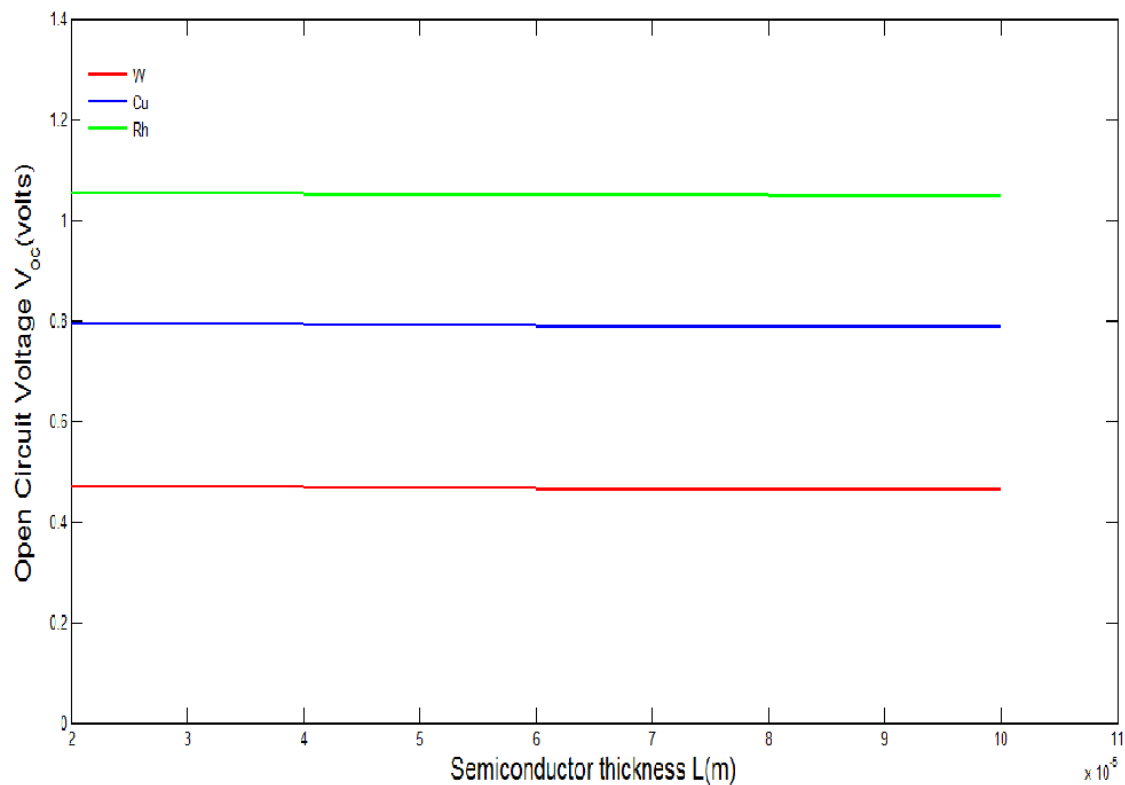


Figure 3.16. Effect of semiconductor thickness on Open circuit voltage for all levels of injections for different metal-n GaAs Solar cell

3.5.6 Effect of the semiconductor thickness on Open circuit voltage considering low level of injection for metal n-GaAs semiconductor SB Solar Cell

In the following figure 3.17, the variation of Open circuit voltage with thickness of GaAs Layer has been observed for low level of injection.

In this case of low level of injection, presence of excess charge concentration in neutral end point is tractable with the mathematical equation for all level of injection. As a result like previous case of all level injection the contribution of excess carrier concentration is negligible because of exponential dependency on length and as a result there is no variation with L .

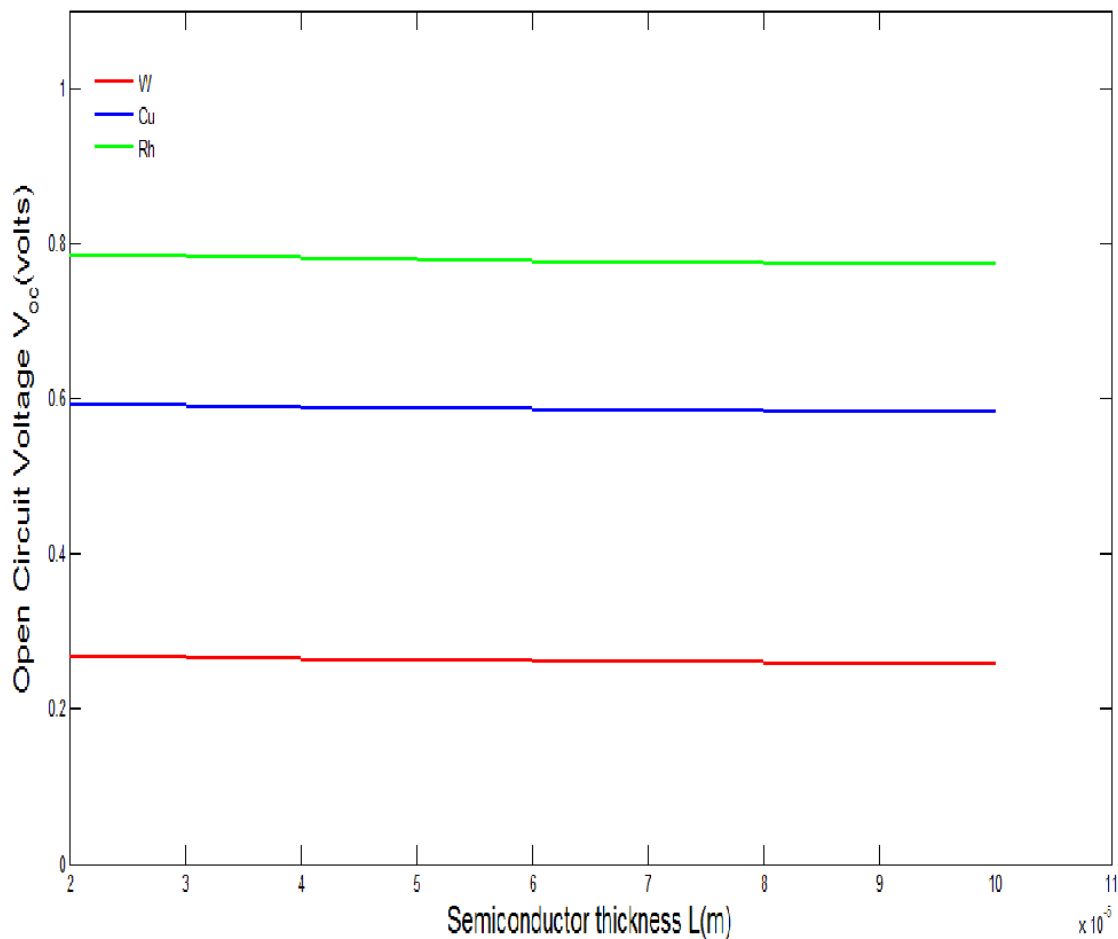


Figure 3.17. Effect of semiconductor thickness on Open circuit voltage for low level injection for different metal-n GaAs Solar cell

3.5.7 Effect of the semiconductor thickness on Open circuit voltage considering high level of injection for metal n-GaAs semiconductor SB Solar Cell

In the following figure 3.18, the variation of Open circuit voltage with thickness of GaAs Layer has been observed for high level of injection.

In the case of high level of injection, slight increase of open circuit voltage V_{OC} is visible with increase over length. In this case, excess charge carrier concentration is considered very much higher than doping concentration and as a result of exponential dependency on length L , slight increase in V_{OC} is observable.

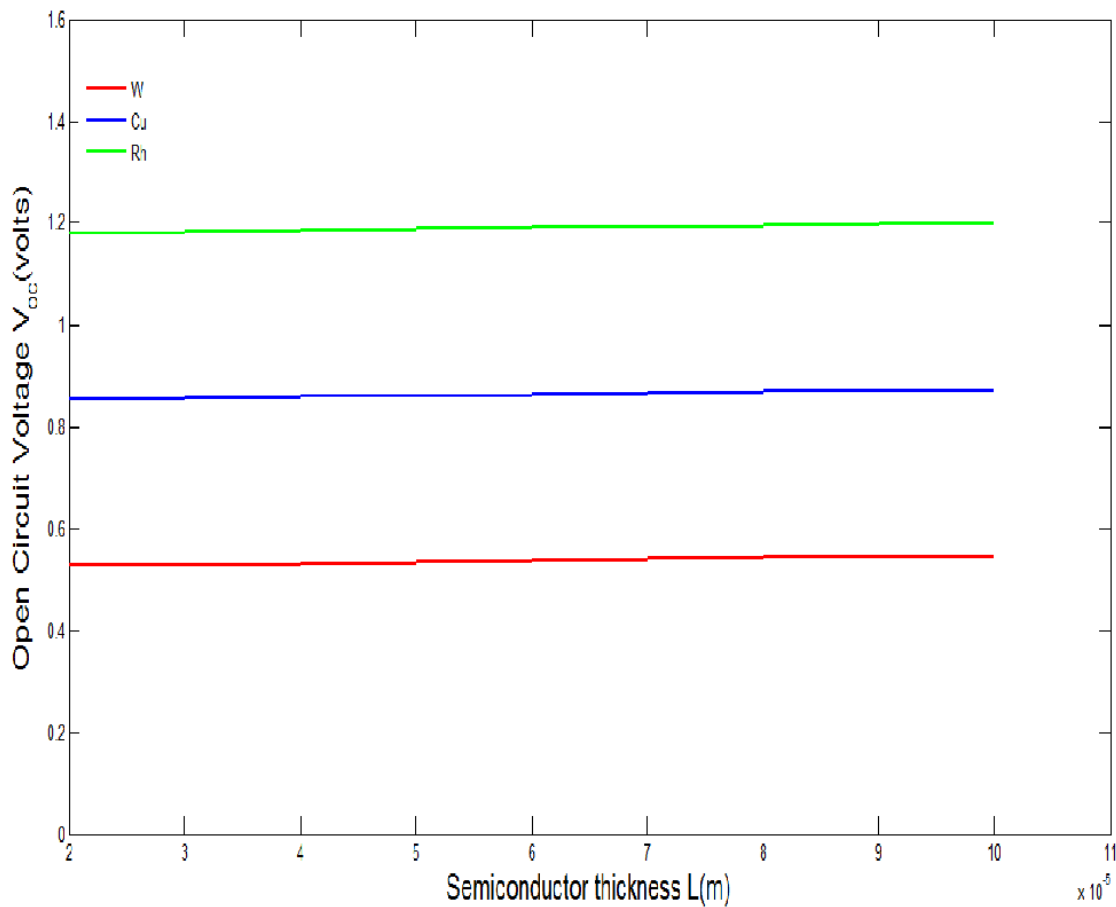


Figure 3.18. Effect of semiconductor thickness on Open circuit voltage for high level injection for different metal-n GaAs Solar cell

3.5.8 Comparison of low level and high level of injection by studying the effect of thickness on Open circuit voltage for metal-n GaAs SB Solar cell

In the following figure 3.19, low level and high level of injection have been considered for W-GaAs and Cu-GaAs SB Solar Cell.

The comparison shows the gradually increasing characteristic plot of open circuit voltage in the case of high level injection and literally constant open circuit voltage characteristic for low level of injection. The values of open circuit voltage are higher compared with figure 3.15. Using n-GaAs as semiconductor, increase of electron affinity and increase of bandgap leads to increased V_{OC} .

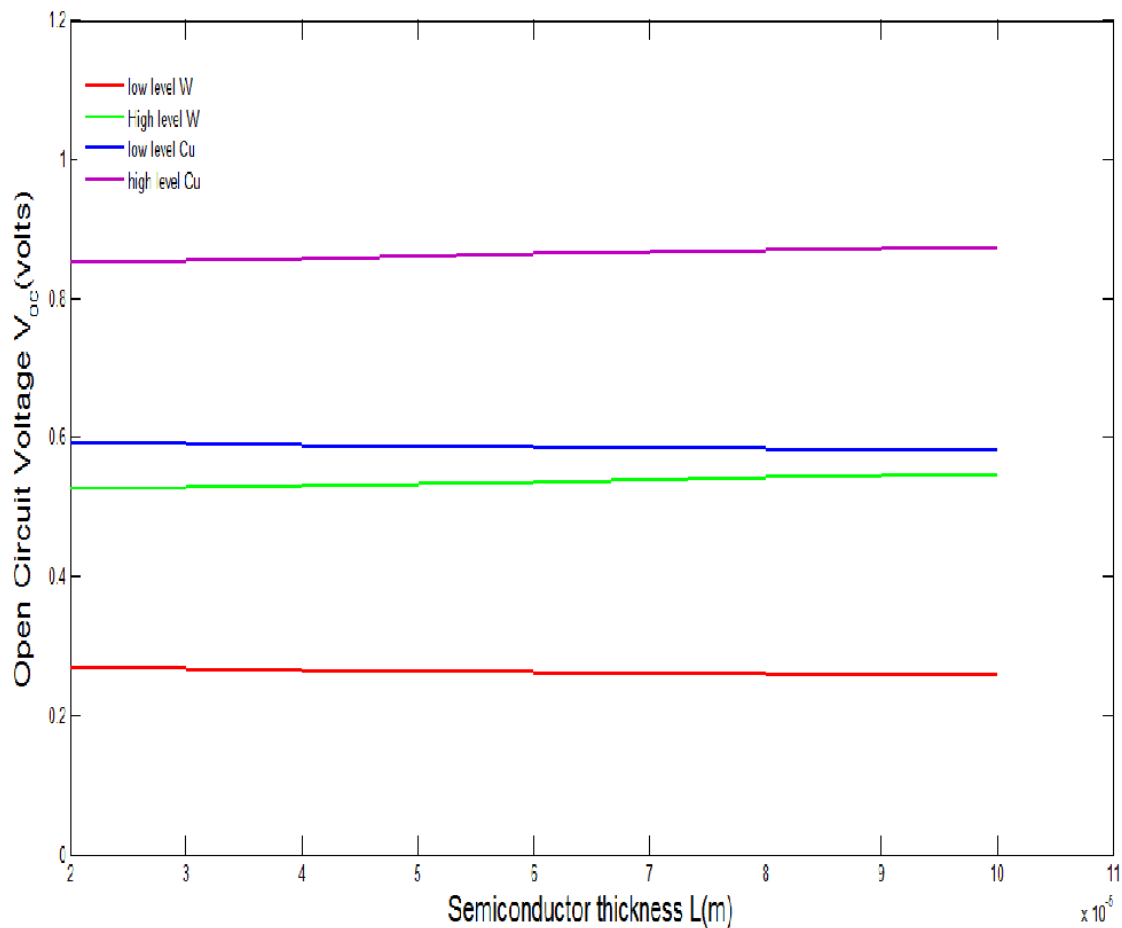


Figure 3.19. Open circuit voltage variation on Semiconductor thickness for both low level and high level injection for metal-n GaAs SB Solar Cell

3.6 Variation of Open circuit voltage with metal work functions for various doping concentrations (N_d) under different levels of injection

Here, Different Characteristic Plots have been obtained for various Doping concentrations ($10^{15}\text{cm}^{-3} \leq N_d \leq 10^{17}\text{cm}^{-3}$) over a range of metal work function. The photon flux is considered to be $\phi = 2 \times 10^{17} \text{cm}^{-2}\text{s}^{-1}$ for all the cases discussed here and surface recombination velocity (S_{eff}) of 200 cm/s is considered. Absorption coefficient at $\lambda = 550\text{nm}$ is considered as 10^4cm^{-1} .

In the following figures 3.20, 3.21 and 3.22, the variation of open circuit voltage is observed for general, low and high levels of injection.

3.6.1 Variation of Open circuit voltage with metal work functions for various doping concentrations (N_d) under all levels of injection of metal-n Si SB Solar Cell

In the following figure 3.20, the variation of open circuit voltage is obtained as a function of metal work function for various doping concentrations under all levels of injection.

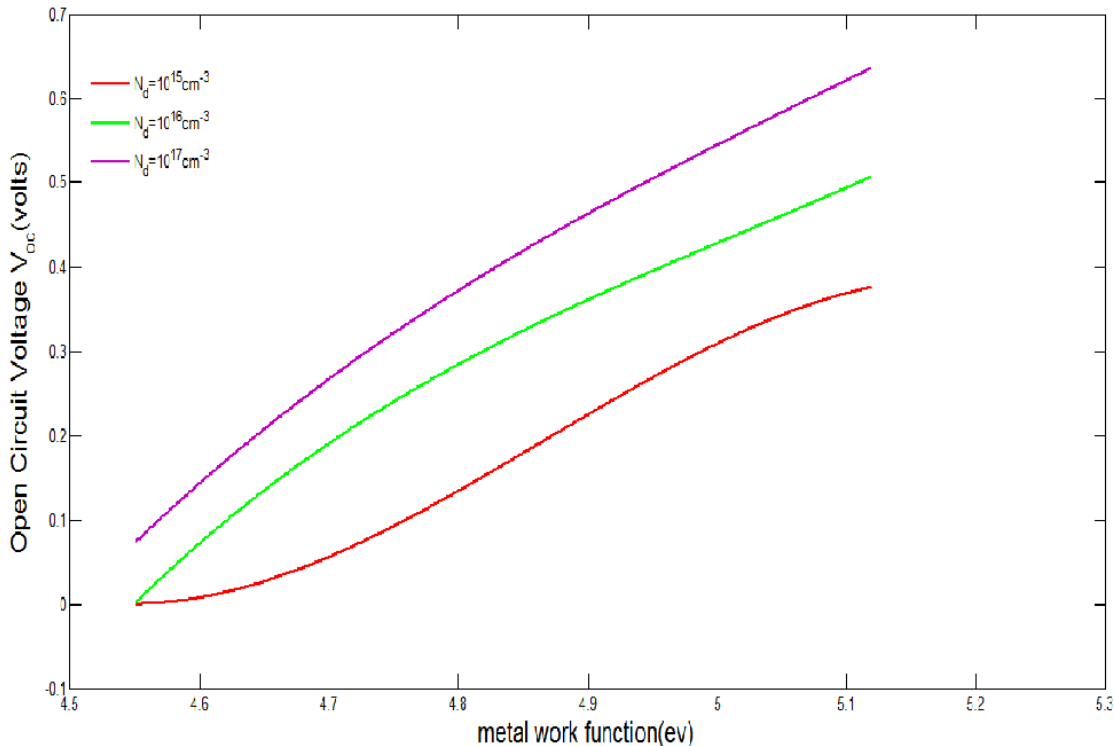


Figure 3.20. Variation of Open circuit voltage with metal work functions for various doping concentrations for different metal-n Si SB Solar cells for all levels of injection

In this figure, Changing metals according to metal work function affect V_{OC} . With increase of metal work function, V_{OC} increases. The reason is that increase of metal work function means increase of barrier height. But the holes move from n-Si to metal and electrons move from metal to n-Si. Due to their direction of movement actually the barrier acts as sink for electrons and holes. As a result it has become easier for photo generated electrons and holes to accumulate at opposite sides and increase V_{OC} .

Open circuit voltage increases with the increase of doping. Due to increase of doping, depletion region width decreases. So the electric field increases in the depletion region. As a result, more photo generated holes cross from n-Si semiconductor to metal side. Also photo generated electrons cross from metal to n-Si semiconductor easily. Accumulation of electron and hole pairs increase and as a result V_{OC} increases.

3.6.2 Variation of Open circuit voltage with metal work functions for various doping concentrations (N_d) under low level of injection of metal-n Si SB Solar Cell

In the following figure 3.21, the variation of open circuit voltage is obtained as a function of metal work function for various doping concentrations under low level of injection.

Due to low level of injections the rate of photo generated excess electrons and holes are considered very much lower than doping concentration. As a result of lower rate of generation of electron-hole pairs, V_{OC} will certainly be of lower value compared to all level injection. But the value of V_{OC} will increase with increasing doping concentration and increasing metal work function. As it has been previously explained in section 3.2.1 that increased doping makes higher electric field and accumulation of charge becomes much greater and so V_{OC} increases. Increased metal work function means higher height of sink for electrons and holes and accumulation becomes greater and V_{OC} increases.

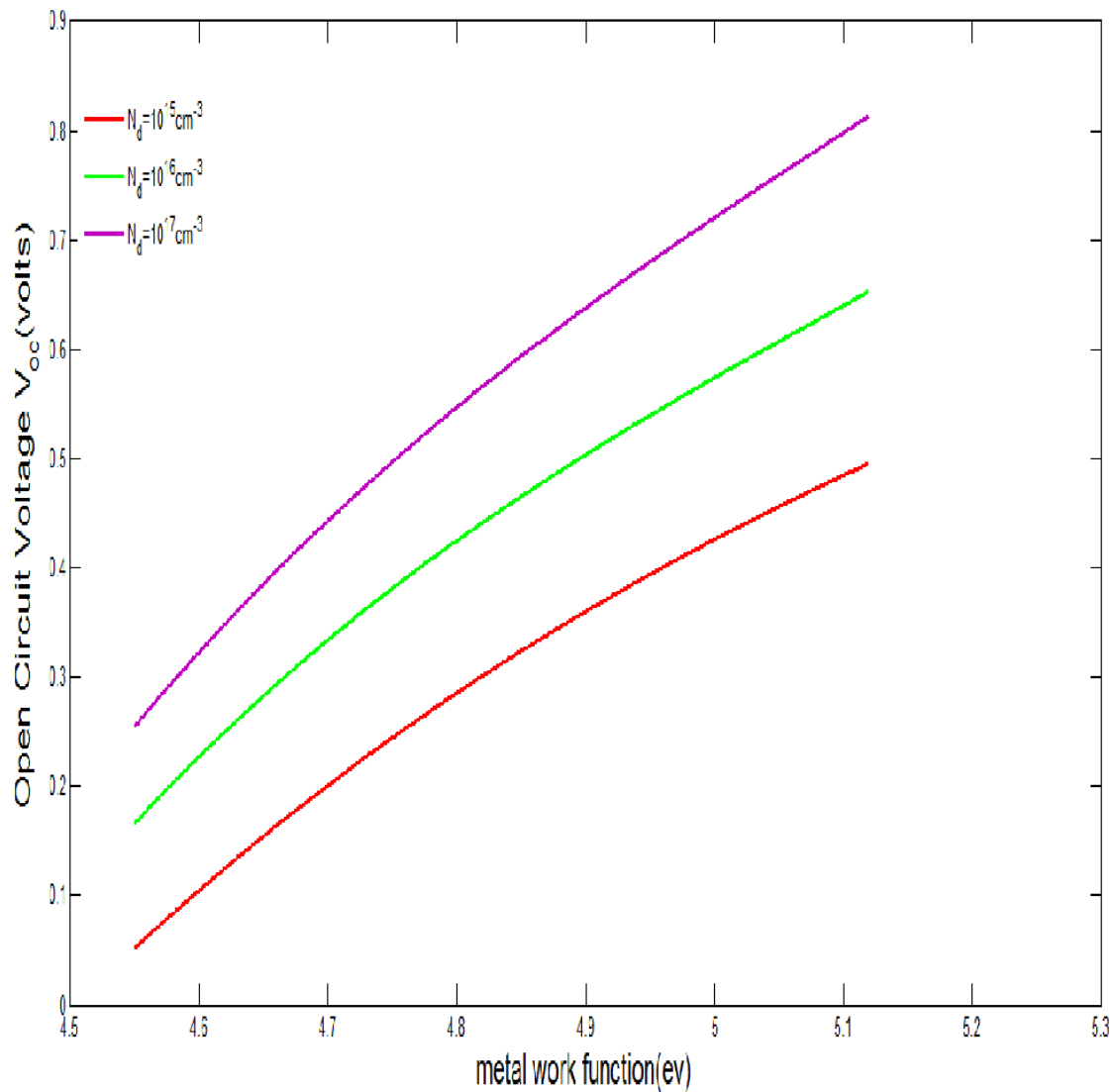


Figure 3.21. Variation of Open circuit voltage with metal work functions for various doping concentrations for different metal-n Si SB Solar cells for low level of injections

3.6.3 Variation of Open circuit voltage with metal work functions for various doping concentrations (N_d) under high level of injection of metal-n Si SB Solar Cell

In the following figure 3.22, the variation of open circuit voltage is obtained as a function of metal work function for various doping concentrations under high level of injection.

Due to high level of injections the rate of photo generated excess electrons and holes are considered very much higher than doping concentration. As a result of higher rate of generation of electron-hole pairs, V_{OC} will certainly be of higher value compared to all level and low level injection. But the value of V_{OC} will increase with increasing doping concentration and increasing metal work function. As it has been previously explained in section 3.2.1 that increased doping makes higher electric field and accumulation of charge becomes much greater and so V_{OC} increases. Increased metal work function means higher height of sink for electrons and holes and accumulation becomes greater and V_{OC} increases.

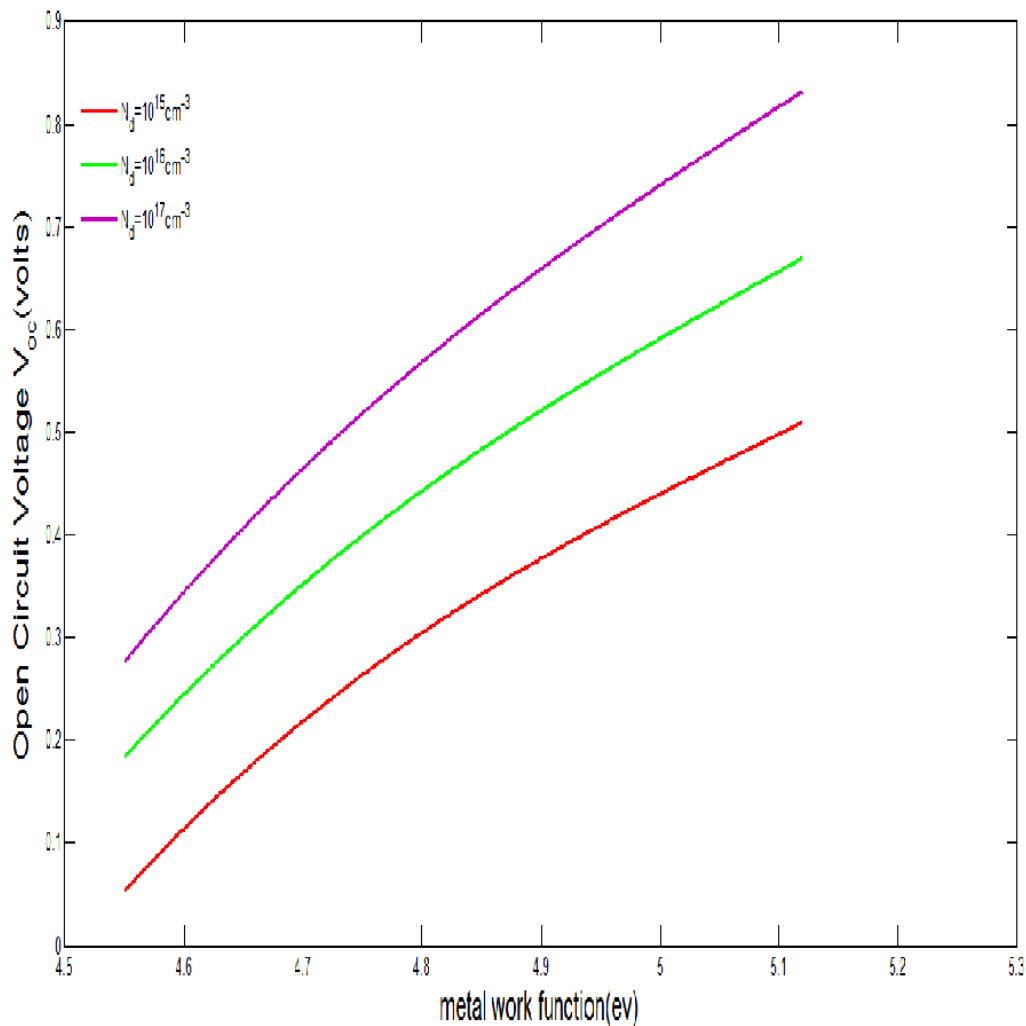


Figure 3.22. Variation of Open circuit voltage with metal work functions for various doping concentrations for different metal-n Si SB Solar cells for high level of injections

3.7. Variation of Open circuit voltage with thickness of semiconductor for various doping concentrations (N_d)

Here, Different Characteristic Plots have been obtained for various Doping concentrations ($10^{15} \text{ cm}^{-3} \leq N_d \leq 10^{17} \text{ cm}^{-3}$) over a range of semiconductor thickness L . The photon flux is considered to be $\phi' = 2 \times 10^{17} \text{ cm}^{-2} \text{ s}^{-1}$ for all the cases discussed here and surface recombination velocity (S_{eff}) of 200 cm/s is considered. Absorption coefficient at $\lambda = 550 \text{ nm}$ is considered as 10^4 cm^{-1} .

In the following figures 3.23, 3.24 and 3.25, the variation of open circuit voltage is observed for general, low and high levels of injection.

3.7.1 Variation of Open circuit voltage with thickness of semiconductor for various doping concentrations (N_d) for all levels of injection

The following figure 3.23 is obtained for Open circuit voltage under all levels of injection for various doping concentrations.

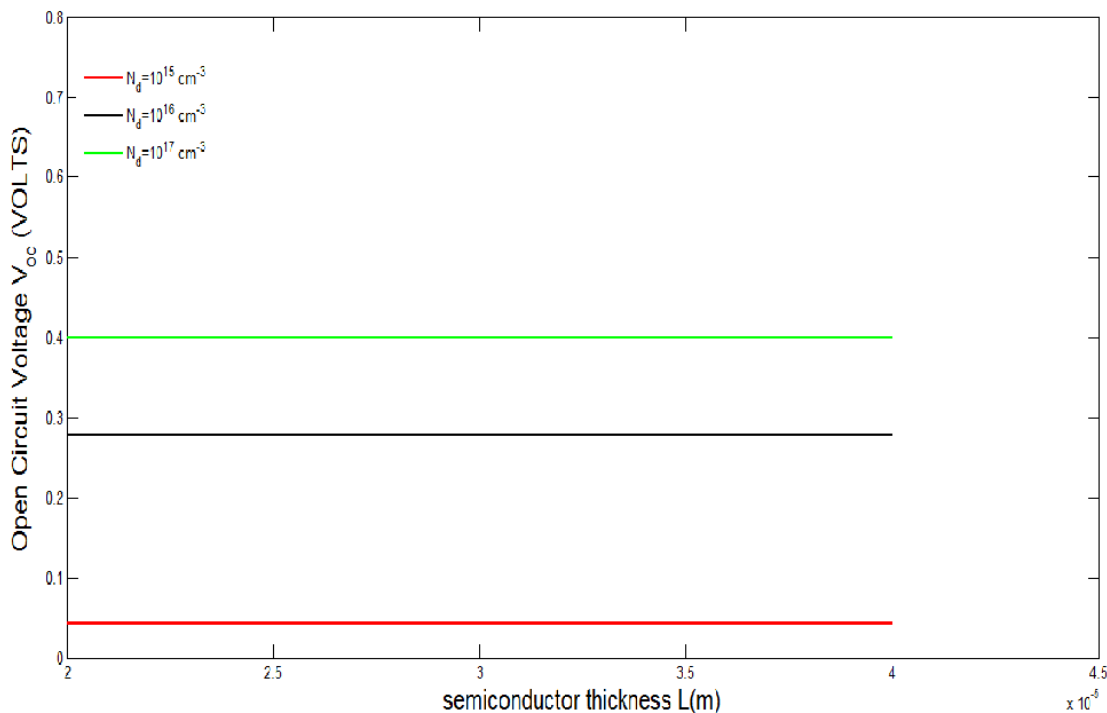


Figure 3.23. Open circuit voltage as a function of Si semiconductor thickness for various doping concentrations under all levels of injection

In this case of all level of injection, thickness of the semiconductor layer does not cause any change in open circuit voltage. The reason is that increase in length does not imply any significant change in photo generated electron hole pairs. Only the excess charge concentration in neutral end point depends exponentially on length but its contribution is negligible and as a result V_{OC} does not vary with L .

With the increase of doping, depletion region width decreases. Electric field becomes stronger as a result and amount of short circuit current increases. As a result according to equation (3.1), V_{OC} increases.

3.7.2 Variation of Open circuit voltage with thickness of semiconductor for various doping concentrations (N_d) for low level of injection

The following figure 3.24 is obtained for Open circuit voltage by considering low level of injection for various doping concentrations.

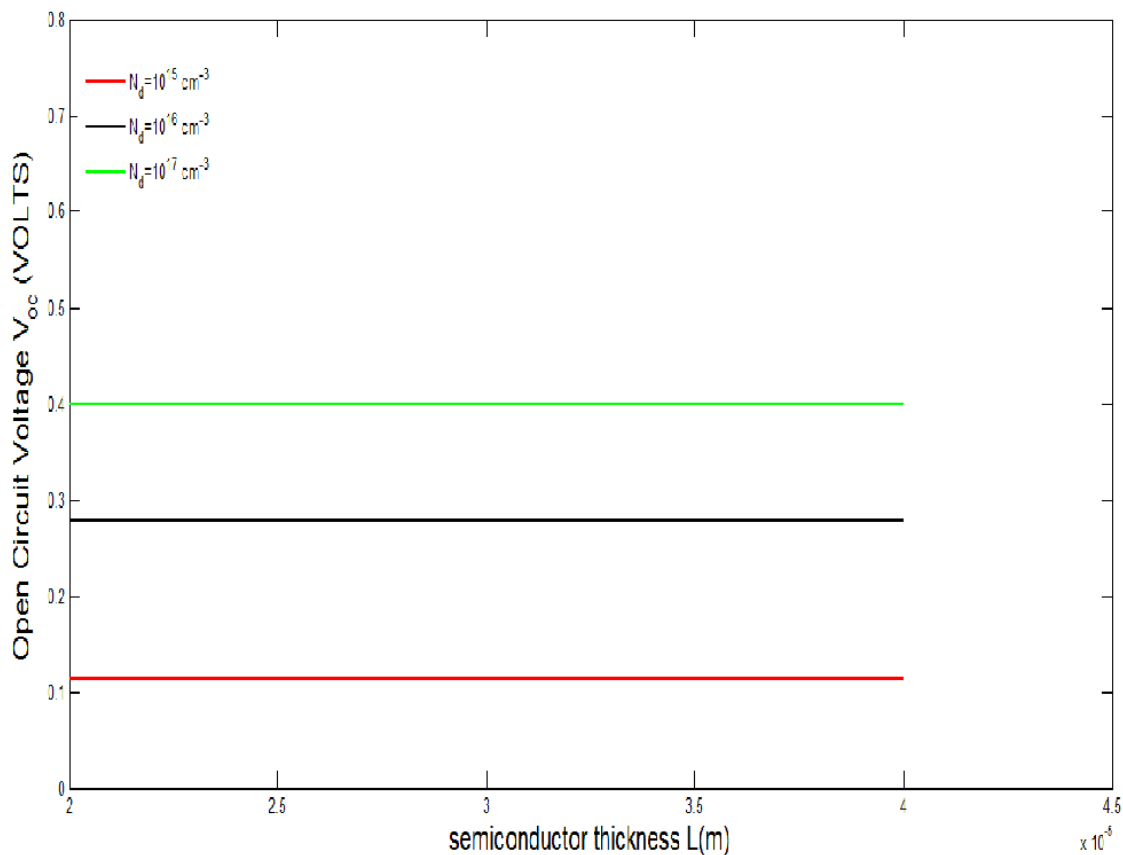


Figure 3.24. Open circuit voltage as a function of Si semiconductor thickness for various doping concentrations under low level of injection

In this case of low level of injection, presence of excess charge concentration in neutral end point is tractable with the mathematical equation for all level of injection. As a result like previous case of all level injection the contribution of excess carrier concentration is negligible because of exponential dependency on length and as a result there is no variation with L .

The increase of doping concentration implies increase in V_{OC} due to increase in electric field. V_{OC} is lower than the case of all level of injection as excess charge carrier concentration is negligible compared with doping concentration and due to less amount of excess charge carrier V_{OC} is lower.

3.7.3 Variation of Open circuit voltage with thickness of semiconductor for various doping concentrations (N_d) for high level of injection

The following figure 3.25 is obtained for Open circuit voltage by considering high level of injection for various doping concentrations.

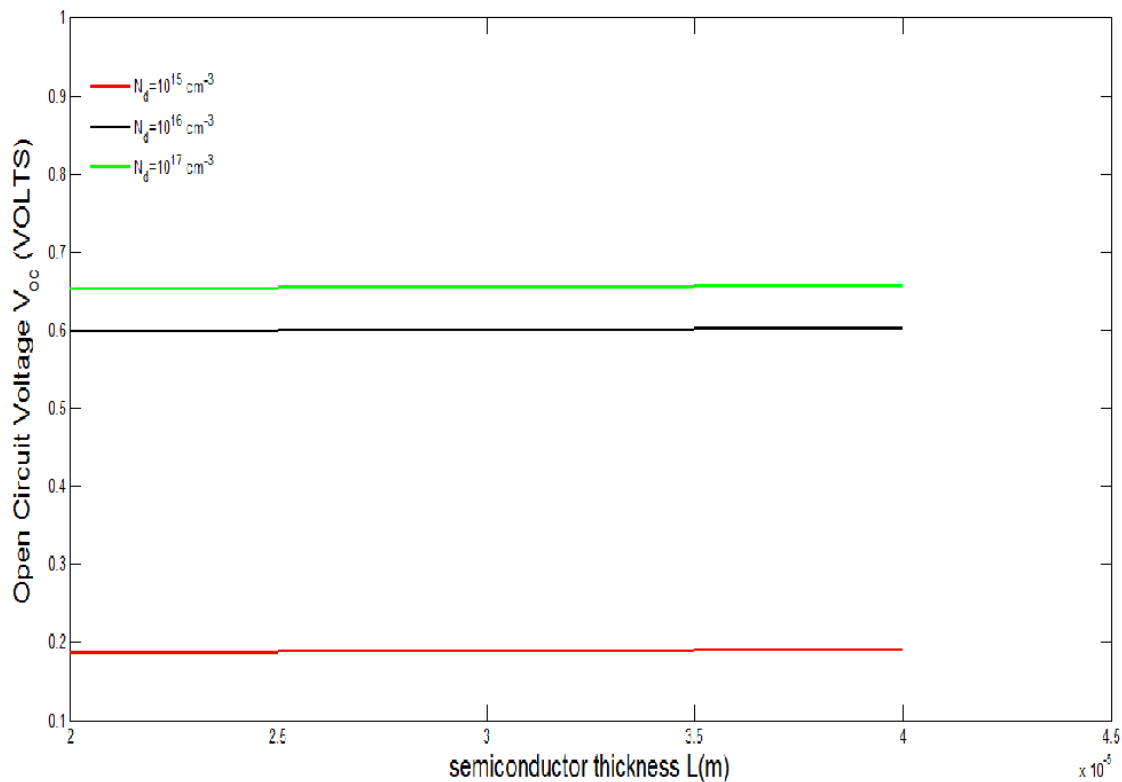


Figure 3.25. Open circuit voltage as a function of Si semiconductor thickness for various doping concentrations under high level of injection

In the case of high level of injection, slight increase of open circuit voltage V_{OC} is visible with increase over length. In this case, excess charge carrier concentration is considered very much higher than doping concentration and as a result of exponential dependency on length L , slight increase in V_{OC} is observable.

The increase of doping concentration implies increase in V_{OC} due to increase in electric field. V_{OC} is higher than the case of all level and low level of injection as excess charge carrier concentration is much higher compared with doping concentration and due to huge amount of excess charge carrier V_{OC} is higher than previous cases.

3.8 Open circuit voltage as a function of Semiconductor layer thickness for various ranges of effective surface recombination velocity

Here, Different Characteristic Plots have been obtained for various effective surface recombination velocities (S_{eff}) over a range of semiconductor thickness L . The photon flux is considered to be $\phi' = 2 \times 10^{17} \text{ cm}^{-2} \text{ s}^{-1}$ for all the cases discussed here and doping concentration (N_d) of 10^{14} cm^{-3} is considered. Absorption coefficient at $\lambda = 550 \text{ nm}$ is considered as 10^4 cm^{-1} .

In the following figures 3.26, 3.27 and 3.28, the variation of open circuit voltage is observed for general, low and high levels of injection.

3.8.1 Open circuit voltage as a function of Semiconductor layer thickness for various ranges of effective surface recombination velocity under all levels of injection

The following figure 3.26 shows the variation of open circuit voltage as function of thickness under all levels of injection.

In this case of all level of injection, thickness of the semiconductor layer does not cause any change in open circuit voltage. The reason is that increase in length does not imply any significant change in photo generated electron hole pairs. Only the excess charge concentration in neutral end point depends exponentially on length but its contribution is negligible and as a result V_{OC} does not vary with L .

Increase in the value of effective surface recombination velocity means increase in recombination rates of electron-hole pairs. As a result, with increase of effective surface recombination velocity, amount of short circuit current decreases and as a result V_{OC} decreases.

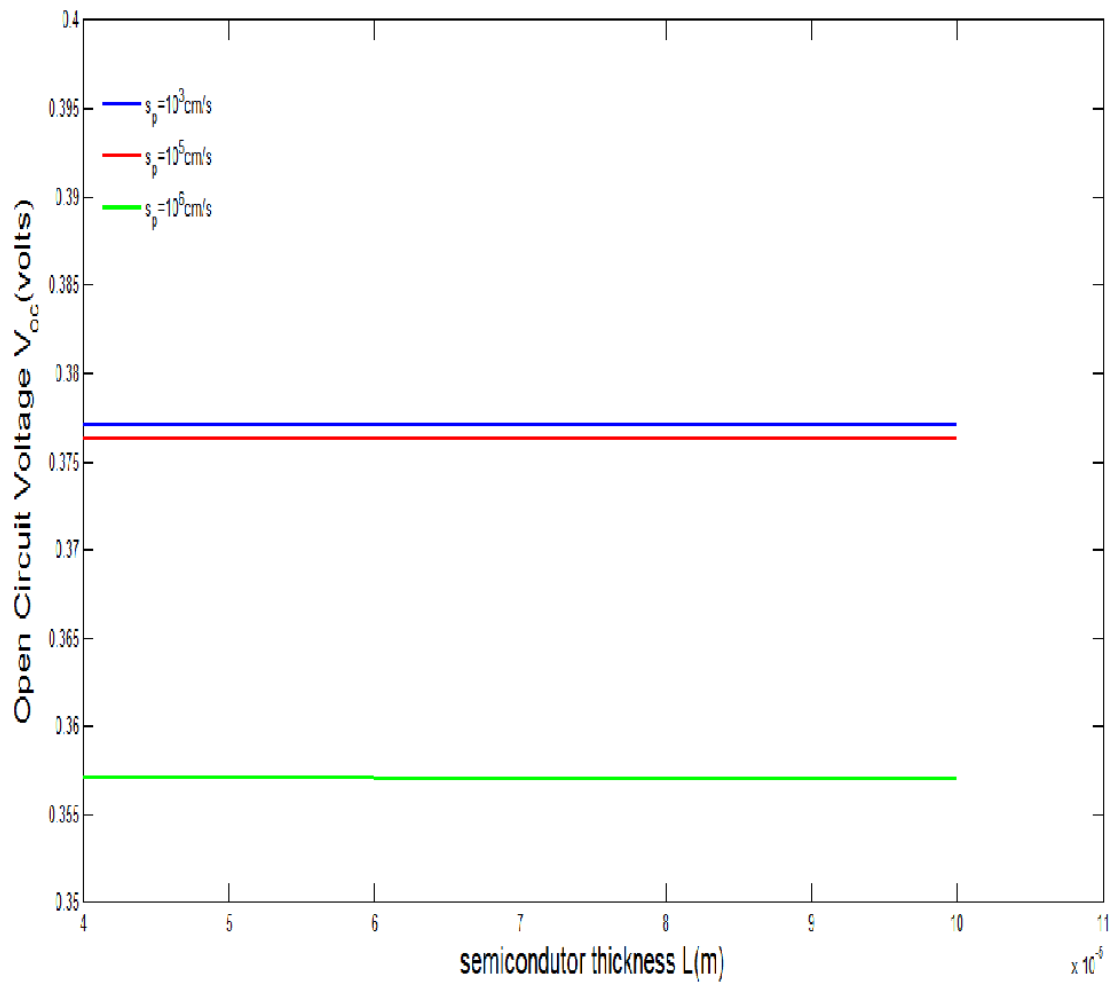


Figure 3.26. Variation of open circuit voltage as a function of semiconductor thickness for different values of effective surface recombination velocity under all levels of injection

3.8.2 Open circuit voltage as a function of Semiconductor layer thickness for various ranges of effective surface recombination velocity under low level of injection

The following figure 3.27 shows the variation of open circuit voltage under low level of injection for different values of effective surface recombination velocities.

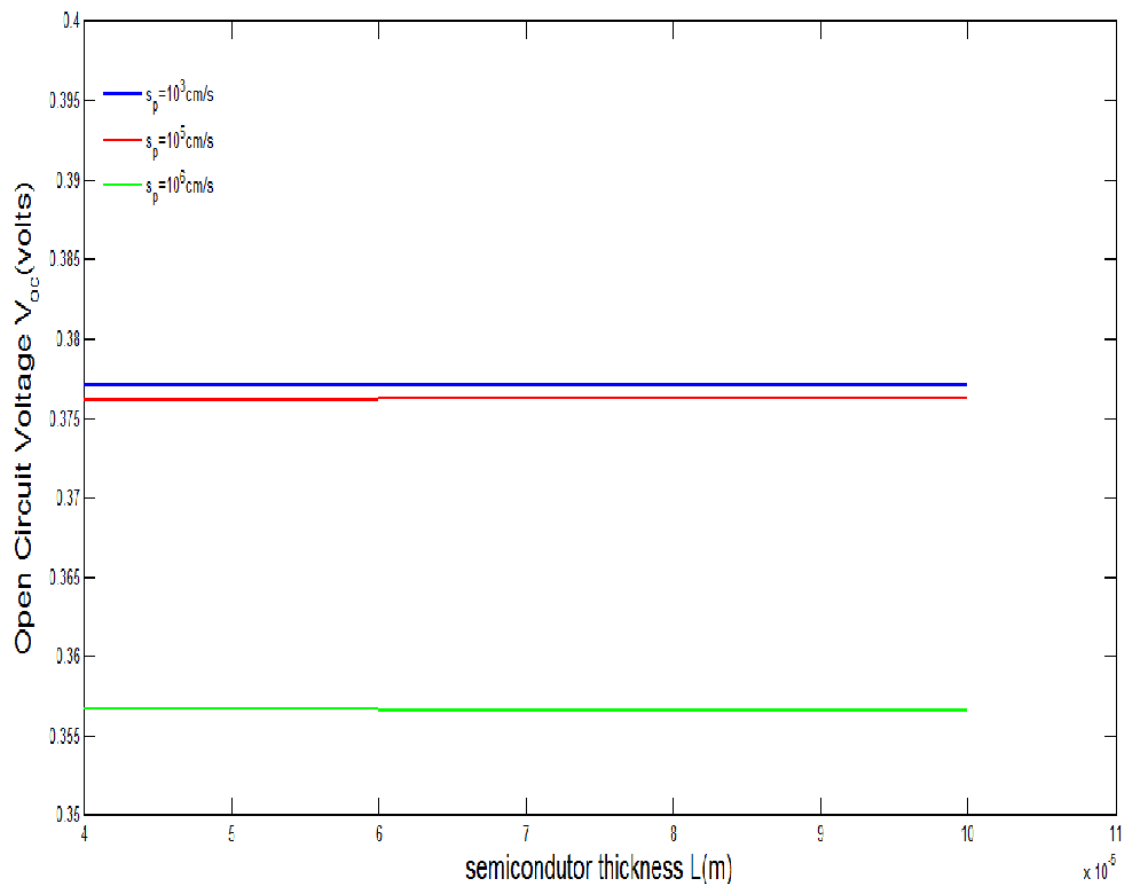


Figure 3.27. Variation of open circuit voltage as a function of semiconductor thickness for different values of effective surface recombination velocity under low level of injection

In this case of low level of injection, presence of excess charge concentration in neutral end point is tractable with the mathematical equation for all level of injection. As a result like previous case of all level injection the contribution of excess carrier concentration is negligible because of exponential dependency on length and as a result there is no variation with L .

With increase of effective surface recombination velocity, amount of short circuit current decreases and as a result V_{OC} decreases according to equation (3.1).

3.8.3 Open circuit voltage as a function of Semiconductor layer thickness for various ranges of effective surface recombination velocity under high level of injection

The following figure 3.28 shows the variation of open circuit voltage under high level of injection for different values of effective surface recombination velocities.

In this case of high level of injection, presence of excess charge concentration in neutral end point is tractable with the mathematical equation for all level and low level of injection. As a result like previous case of all level injection the contribution of excess carrier concentration is negligible because of exponential dependency on length and as a result there is slight variation with L . With increase of effective surface recombination velocity, amount of short circuit current decreases and as a result V_{OC} decreases.

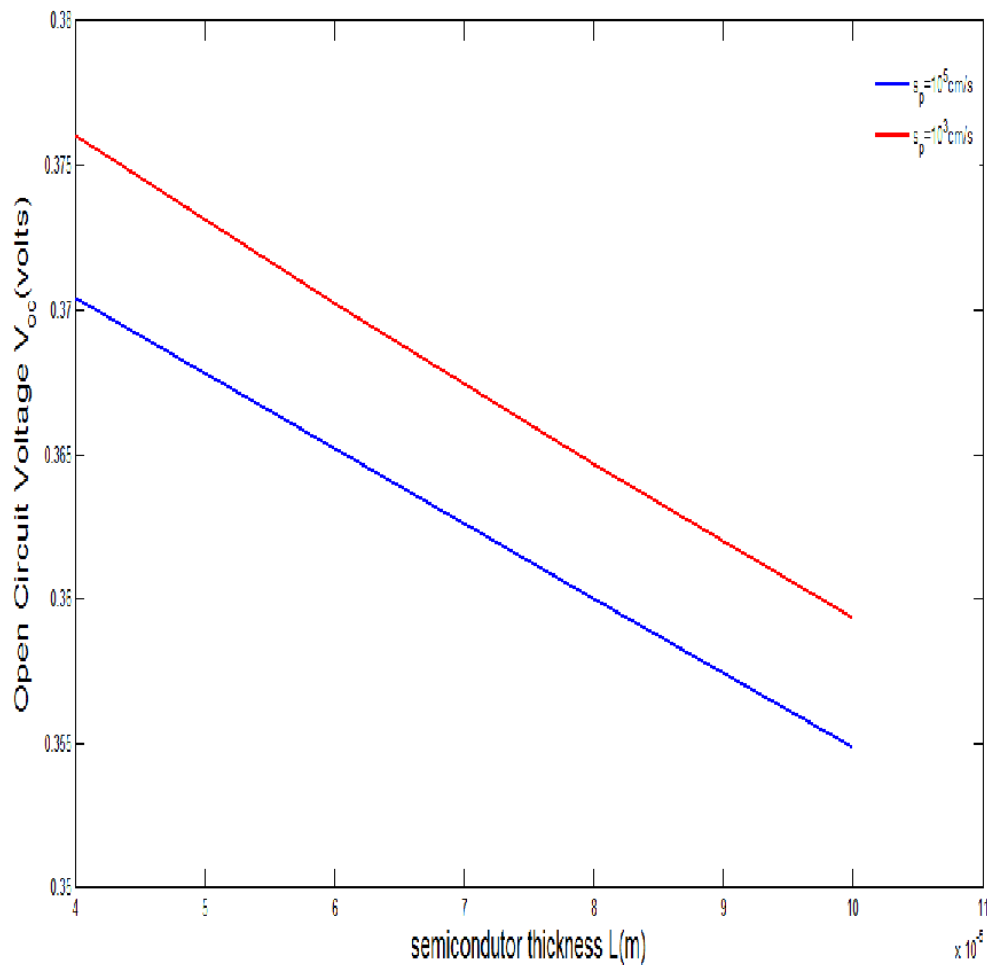


Figure 3.28. Variation of open circuit voltage as a function of semiconductor thickness for different values of effective surface recombination velocity under high level of injection

3.9 Comparison of Open circuit voltage as a function of doping concentrations for all, low and high level of injections for a metal-n Si SB Solar Cell

The following figure 3.29 compares the variation of open circuit voltage for all, low and high level of injections. Cu is considered here as the metal and Si is considered as semiconductor.

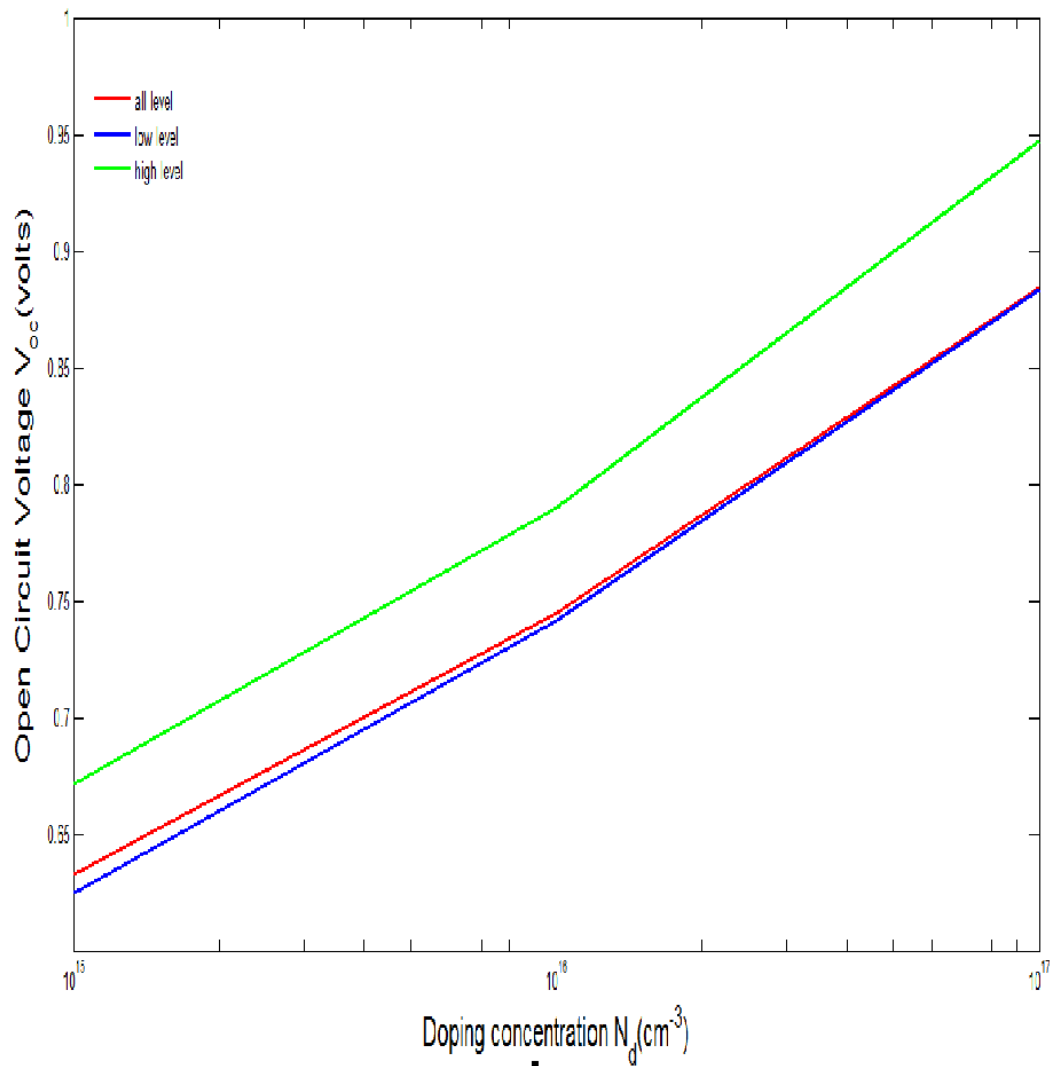


Figure 3.29. Comparison of Open circuit voltage for different levels of injection as a function of doping concentrations for metal-n Si SB Solar Cell

In this case, at initial doping concentration low level of injection is slightly lower than all level of injection, then the low and all level injection merges. High level of injection always indicates higher value than these two levels. The reason is that due to higher excess charge concentration than doping concentration at high level of injection, V_{OC} is higher than other level of injection.

On the other hand, increase of doping means decrease in depletion region and as a result increase in electric field means higher short circuit current which indicates higher rate of accumulation and as a result V_{OC} increases with doping concentration.

The following figure 3.30 compares the variation of open circuit voltage for all, low and high level of injections. Cu is considered here as the metal and GaAs is considered as semiconductor.

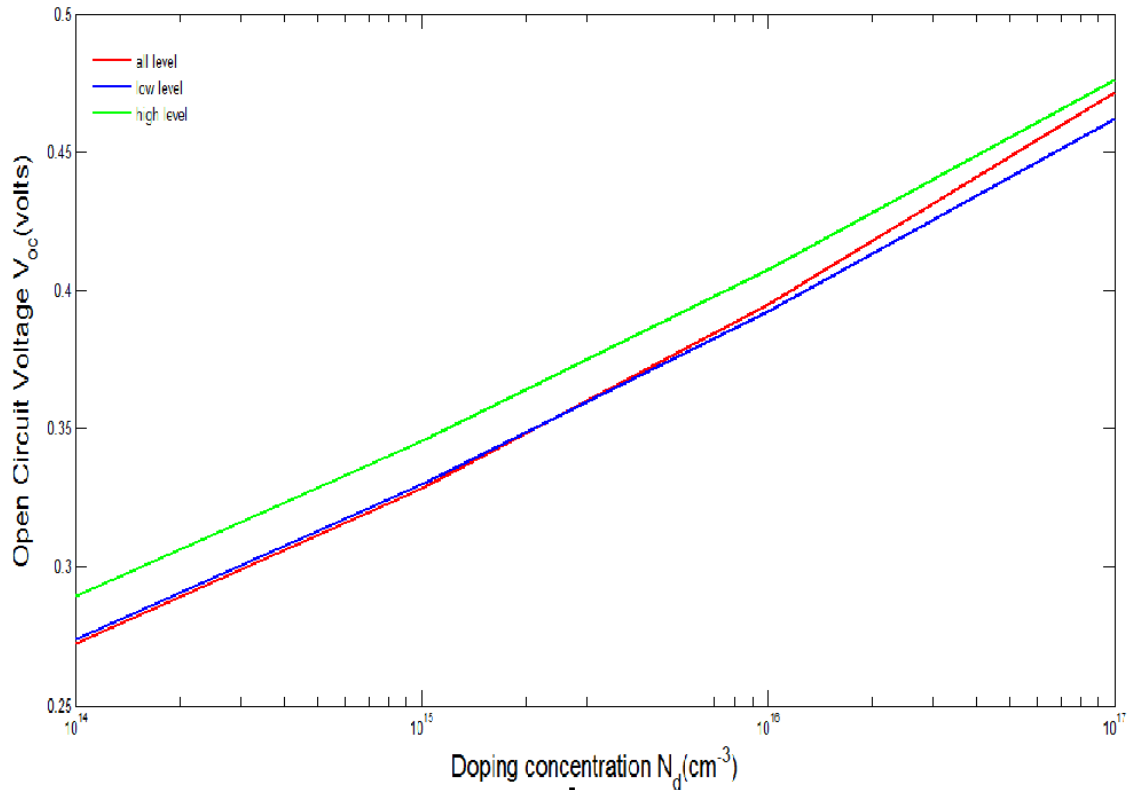


Figure 3.30. Comparison of Open circuit voltage for different levels of injection as a function of doping concentrations for metal-n GaAs SB Solar Cell

In this case, at initial doping concentration all level of injection is slightly lower than low level of injection, then the low and all level injection merges. High level of injection always indicates higher value than these two levels. The reason is that due to higher excess charge concentration than doping concentration at high level of injection, V_{OC} is higher than other level of injection. With increase of doping concentration, it has been observed from the figure that all level of injection comes closer to high level of injection for higher doping like 10^{17}cm^{-3} .

On the other hand, increase of doping means decrease in depletion region and as a result increase in electric field means higher short circuit current which indicates higher rate of accumulation and as a result V_{OC} increases with doping concentration.

3.10 Conclusions

In the previous chapter, Analytical Modeling of open circuit voltage of SB Solar Cell for all levels of injection has been performed. Mathematical Expression has been obtained for the special case of low and high level of injection.

In this chapter, different characteristic plots have been obtained for open circuit voltage considering different levels of injection for various parameters. Doping concentration has been varied over a range and variation of open circuit voltage has been obtained by using both metal- n Si and metal- n GaAs SB Solar Cell. Open circuit voltage increases with increase of doping and in case of using GaAs, higher open circuit voltage has been obtained. Then metal work function has been varied and the comparisons of Open circuit voltage characteristic plots have been made for all, low and high levels of injection. Both metal- n Si and metal- n GaAs SB Solar Cell cases have been studied. Variation of open circuit voltage as function of effective surface recombination velocity and semiconductor thickness layer has been studied. The variation is not that much visible in these cases. Open circuit voltage is also studied as function of semiconductor thickness for various ranges of effective surface recombination velocity. Comparison of Open circuit voltage as function of doping concentrations for different levels of injection has been compared for metal- n Si and metal- n GaAs SB Solar Cell.

There is no comparison made between our present work of special case of low and high level of injection and previous work on low and high level of injection. The main reason is that in the previous work only related data of metal and doping concentration is given but some of the important parameters values are not given. As a result due to lack of sufficient identical data set from previous work it is not possible to show characteristic comparison between past and present work. But the mathematical expressions of low and high level of injection of our work which has been obtained from the mathematical expression of all level of injection are identical with the previous work's mathematical expression of low and high level of injection.

CHAPTER 4

CONCLUSIONS

4.1 Summary

Open circuit Voltage and Short Circuit current density bear great importance in efficiency calculation of Solar Cell. In this work, Analytical model of Open Circuit Voltage (V_{OC}) of SB Solar Cell has been derived for all levels of injection. Mathematical analysis has been carried out separately in depletion region and neutral region. The joint analysis ultimately helps to find out the mathematical expression of V_{OC} under all levels of injection. Different integration techniques are collaborated in this case. In the analytic expression there are unknown excess charge minority carrier concentration terms in the boundary of depletion and neutral region. These unknown concentrations are evaluated by solving second order non-linear differential equation. Proper boundary conditions are evaluated to determine unknown constants to fully determine analytic model of V_{OC} under different levels of injection. For the special case of low level and high level of injection that general mathematical expression is modified accordingly making necessary assumptions. In the past, there has been no work on finding out analytical open circuit voltage model for SB Solar Cell under all levels of injection. There has been few works on considering low level and high level of injection. This current work is the first one for finding out mathematical expression of open circuit voltage under all levels of injection. As a result it has been possible to make analysis under intermediate level of injection. This is the most significant part of this work and it has carried out mathematical analysis of Open circuit voltage under low and high level of injection as special case of all level of injection. This work also helps to make comparison of previous works of low and high level injection with this one and tracking down the similar mathematical expressions of open circuit voltage helps to make judgment of the validity of this work with previous works of low and high level injection.

Different characteristic plots of V_{OC} have been obtained for different levels of injection. V_{OC} is obtained as a function of metal work function, doping concentration, effective surface recombination velocity and thickness of the semiconductor layer. The variation of V_{OC} is prominent in the case of variation of metal work function and doping concentration. Physical explanations are given briefly for different levels of injections in those cases. The effect of effective surface recombination velocity and thickness of semiconductor layers are not prominent in study of V_{OC} characteristics and the reasons are also explained. The results are obtained by using all, low and high levels of injection. Si and GaAs are used as semiconductor layers. Some comparisons are made for V_{OC} for the special case of low and high level of injection as function of metal work function. Small variation of V_{OC} as function of Thickness of semiconductor layer is also compared. Although there are no works on all level injections of solar cell, some of the literatures attribute to low and high level of injection. Comparisons are made between previous variation of V_{OC} and our present modeling of V_{OC} for all level injection.

4.2 Future course of research work

This work considers analysis of V_{OC} along single dimension. This work can be extended for the multidimensional case. This work can be also extended to calculate the efficiency of SB Solar Cell for all levels of injection. In this case, Short circuit current density characteristics are required to be studied as functions of various parameters. Later on after successful calculation of fill factor, the efficiency can be plotted and measured for various ranges of values of parameters.

REFERENCES

1. G.F. Brown, J.W. Ager III, W. Walukiewicz and J. Wu, "Solar energy materials and solar cells", ELSEVIER, pp-478-483,2010.
2. S. W. Feng, C. M. Lai, C. H. Chen, W. C. Sun and L.W. Tu, "Theoretical simulations of the effects of the indium content, thickness and defect density of the i-layer on the performance of p-i-n InGaN single homojunction solar cells", Journal of applied physics, 2010.
3. A. Yamamoto, M. R. Islam, T. T. Kang, and A. Hashimoto, "Recent advances in InN based solar cells: status and challenges in InGaN and InAlN solar cells" Physica Status Solidi C7 1309-16,2010.
4. G. F. Brown, J. W. Ager III, W. Walukiewicz and J. Wu, "Finite element simulations of compositionally graded InGaN solar cells", Sol.Energy Mater.Sol.cells 478-483, 2010.
5. K. L. Narasimhan and V.Premchandran, "Origin of the open circuit voltage in amorphous silicon Schottky barrier cells", J.Appl. Phys. 56,1984.
6. S. Rajputra, S.Vallurupalli, and V. P. Singh, "Copper Phthalocyanine based Schottky diode solar cells", J. Mater. Sci:Mater. Electron. 18,2007.
7. S. Lin, B. P. Zhang, S. W. Zeng, X. M. Cai, J. Y. Zhang, S.X. Wu, A. K. Lin and G. E. Weng, "Preparation and properties of Ni/InGaN/GaN Schottky barrier photovoltaic cells", Solid State Electron. 63 , pp-105-109,2010.
8. P. K. Dubey and V. V. Paranjape, "Open circuit voltage of a schottky barrier solar cell", J.Appl.Phys.,47,1976.
9. S. K. Behura, P. Mahala and A. Ray, "A model on the effect of injection levels over the open circuit voltage of Schottky barrier solar cells", journal of electron devices, vol 10 ,pp-471-482, 2011.
10. P. Mahala, S. K. Behura, A. S. Kushwaha, A. Ray, O. Jani and C.Dhanavantri, "A study on the 2 D simulation of Pt/InGaN/GaN/metal Schottky junction Solar cell", IOP, Semicond. Sci.Technol., 2013.
11. M. B. Prince, M.B and M. Wolf, "New developments in silicon photovoltaic devices," *Radio Engineers, Journal of the British Institution of*, vol.18, no.10, pp.583,594, October 1958.

12. D. P. Bortfeld, A. R. Gobat, N. F. Lamorte and G. W. McIver, "High-efficiency gallium-arsenide solar cells," *Electron Devices Meeting, 1961 International*, vol.7, no., pp.36,36, 1961.
13. L. Cuadra, A. Marti and L. Antonio, "Influence of the overlap between the absorption coefficients on the efficiency of the intermediate band solar cell," *Electron Devices, IEEE Transactions on*, vol.51, no.6, pp.1002,1007, June 2004.
14. W. A. Anderson and A. E. Delahoy, "Schottky barrier diodes for solar energy conversion," *Proceedings of the IEEE*, vol.60, no.11, pp.1457,1458, Nov. 1972.
15. W. A. Anderson, J. K. Kim and A.E. Delahoy, "Barrier height modification in silicon Schottky (MIS) solar cells," *Electron Devices, IEEE Transactions on*, vol.24, no.4, pp.453,457, Apr 1977.
16. C. Lanza and H. J. Hovel, "Efficiency calculations for thin-film polycrystalline semiconductor Schottky barrier solar cells," *Electron Devices, IEEE Transactions on*, vol.24, no.4, pp.392,396, Apr 1977.
17. A. N. Corpus-Mendoza, M.M. De Souza and F. U. Hamelmann, "Design of Schottky Contacts for Optimum Performance of Thin-Film Silicon Solar Cells," *Photovoltaics, IEEE Journal of*, vol.5, no.1, pp.22,27, Jan. 2015.
18. Hongyue Liu, Yeeheng Lee, T. Jamali-beh, Z. Lu, R. Collins and C.R. Wronski, "Light-induced degradation in different p-i-n and n-i Schottky barrier solar cell structures," *Photovoltaic Specialists Conference, 1996., Conference Record of the Twenty Fifth IEEE*, vol., no., pp.1125,1128, 13-17 May 1996.
19. Chunhai Ji and W.A. Anderson, "Device performance and current transport study of metal-induced grown microcrystalline Si for solar cell Applications," *Photovoltaic Specialists Conference, 2005. Conference Record of the Thirty-first IEEE*, vol., no., pp.1544,1547, 3-7 Jan. 2005.
20. P. Panayotatos and H.C. Card, "Use of VOC/JSC measurements for determination of barrier height under illumination and for fill-factor calculations in Schottky-barrier solar cells," *Solid-State and Electron Devices, IEE Proceedings I*, vol.127, no.6, pp.308,311, December 1980
21. Martin Peckerar, H. C. Lin and R.L. Kocher, "Open circuit voltage of MIS Schottky diode solar cells," *Electron Devices Meeting, 1975 International*, vol.21, no., pp.213,216, 1975.
22. J. C. Zolper and A. M. Barnett, "The effect of dislocations on the open-circuit voltage of gallium arsenide solar cells," *Electron Devices, IEEE Transactions on*, vol.37, no.2, pp.478,484, Feb 1990.

23. Gong Chun, N. Posthuma, F. Dross, Emmanuel Van Kerschaver, Flamand Giovanni, G. Beaucarne, Jef Poortmans and R.J.O.M. Hoofman, "Comparison of n- and p-type high efficiency silicon solar cell performance under low illumination conditions," *Photovoltaic Specialists Conference, 2008. PVSC '08. 33rd IEEE*, vol., no., pp.1,4, 11-16 May 2008.
24. M. A. Wolf and M. Wolf, "Characteristics and performance of silicon solar cells between low-and high-level injection—Part II: Results of the study," *Electron Devices, IEEE Transactions on*, vol.32, no.4, pp.800,806, Apr 1985.
25. Cai Xiaomei, Wang Yu, Chen Bihua, Ming-Ming Liang, Wen-Jie Liu, Jiang-Yong Zhang, Xue-Qin Lv, Lei-Ying Ying and Bao-Ping Zhang, "Investigation of InGaN p-i-n Homojunction and Heterojunction Solar Cells," *Photonics Technology Letters, IEEE*, vol.25, no.1, pp.59,62, Jan.1, 2013.